



**INSTITUTE FOR  
TROPOSPHERIC RESEARCH**  
WISSENSCHAFTSGEMEINSCHAFT  
GOTTFRIED WILHELM LEIBNIZ

# *Biennial Report*

## *1999/2000*





*Biennial Report*  
*1999 & 2000*



**INSTITUTE FOR  
TROPOSPHERIC RESEARCH**  
WISSENSCHAFTSGEMEINSCHAFT  
GOTTFRIED WILHELM LEIBNIZ



## Impressum

### **Published by**

Institute for Tropospheric Research (IfT)  
Institut für Troposphärenforschung e.V. Leipzig (IfT)

Member of the Wissenschaftsgemeinschaft Gottfried Wilhelm Leibniz (WGL)

<i>Postal address:</i>	Permoserstr. 15	<i>Phone:</i>	++49 - 341-235-2321
	04318 Leipzig	<i>Fax:</i>	++49 - 341-235-2361
	Germany	<i>E-mail:</i>	monika@tropos.de
		<i>Internet:</i>	<a href="http://www.tropos.de">http://www.tropos.de</a>

### **Editors**

Konstanze Kunze, Andrea Mehlhose, Katja Schmieder, Monika Schulze

### **Editorial Board**

*Jost Heintzenberg, Hartmut Herrmann, Eberhard Renner*

### **Technical management / DTP / Layout**

Katja Schmieder

### **Printed by**

MERKUR Druck- und Kopierzentrum GmbH  
Hauptmannstraße 4  
04109 Leipzig  
Internet: <http://www.merkurdruck.de>

### **Photo and illustration credits**

© IfT; all pages, except for pages:

**12:** *courtesy of A. Petzold, Deutsches Zentrum für Luft- und Raumfahrt (DLR)*

**53:** *Archives: Sächsisches Landesamt für Umwelt und Geologie, G.Engler  
"Kahleberg - (LSG Osterzgebirge) - 10/1996".*


**Introduction and Overview** 3

**Detailed contributions to current research projects**

- ◆ Lindenberg Aerosol Characterization Experiment 1998 (LACE98) 11
- ◆ Indian Ocean Experiment (INDOEX) 15
- ◆ Size segregated characterization of fine particulate matter in Leipzig and Melpitz 27
- ◆ Multiphase modeling and laboratory studies 34
- ◆ The micro-scale meteorological model MITRAS: An overview 42

**Short contributions to current research projects**

- ◆ Submicrometer particles in the tropopause region (CARIBIC) 49
- ◆ Temperature profiling in the troposphere using a Raman lidar 51
- ◆ National and transboundary effects of emission changes on components of precipitation in Saxon border regions (OMKAS-Project) 53
- ◆ Cloud water analysis with high pressure liquid chromatography in combination with mass spectrometry 55
- ◆ Cloud processing of mineral dust particles and the effects on cloud microphysics 57
- ◆ On the influence of large-eddy simulation (LES)-based turbulence parameters on mesoscale cloud forecast 59
- ◆ Tethered balloon measurements with MAPS-Y 62
- ◆ Particle formation and growth in the IfT laminar flow tube (IfT-LFT) 64
- ◆ The effect of subgridscale turbulence on the formation of new particles 67
- ◆ Parallelization of Chemistry-Transport Models 70
- ◆ The gas-phase reaction of OH radicals with benzene 73
- ◆ Direct investigations of OH reactions in aqueous solution 75
- ◆ Dry deposition of ammonia over grassland - micrometeorological flux gradient measurements and bidirectional flux calculations using an inferential model 78

**Appendix**

- ◆ Publications 83
- ◆ University courses 100
- ◆ Doctoral theses 102
- ◆ Master theses 103
- ◆ Guest scientists 104
- ◆ Scientific events 105
- ◆ Memberships 106
- ◆ National and international cooperation 107
- ◆ Boards 110





*Introduction &  
Overview*

---





## Introduction and Overview

In the outskirts of Leipzig, on the campus of the former Academy of Sciences, in close neighborhood of the Environmental Research Center, other research establishments and businesses you find the Institute for Tropospheric Research. It was founded in 1991 for the investigation of physical and chemical processes in the polluted troposphere (roughly the first 10 km of our atmosphere).

aerosols, and clouds important physico-chemical processes of aerosol and cloud formation and the relationships with climate and health are poorly understood. This limitation is mainly due to analytical difficulties with the very small samples and with the complex behavior of tropospheric multiphase systems, in which individual processes seldom can be distinguished. In climate research



*Fig. 1: IfT main building.*

Meanwhile a well-defined and globally unique research profile emerged with a focus on aerosols, i.e. small airborne particles and clouds. Despite their minute absolute amount aerosols and clouds are essential parts of the atmosphere because they control the budgets of energy, water and trace substances of the Earth System. The research interest in these highly disperse systems is stimulated foremost by their potential change through human activities. These system changes feed back into the anthroposphere not only through regional and global climate change but also directly through health effects of inhaled haze and fog particles. Despite strong connections between humans,

this limitation is reflected in much larger uncertainties in predicted anthropogenic aerosol and cloud effects in comparison to numbers published by the Intergovernmental Panel on Climate Change for additional greenhouse gases. Rapid advances in our understanding of tropospheric multiphase processes and an application of this process understanding to the prediction of the consequences of human impacts can only be expected from concerted approaches from several directions. Consequently, the Institute for Tropospheric Research conducts field studies in several polluted regions parallel to the development of analytical methods for aerosol and cloud research.



**Fig. 2:** Particle sampling systems during the INTERCOMP 2000 campaign at the research station Melpitz.

These tools are not only applied in field experiments but also in extensive laboratory investigations, which form a second major activity. A third and equally important approach consists of the formulation and application of numerical models that reach from process models to regional simulations of the formation, transformation and effects of tropospheric multiphase systems.

### Field experiments

The atmosphere is an aerosol, i.e. a carrier gas mixture with suspended solid and liquid particles. Field experiments elucidate the atmospheric life cycle and related processes of aerosol and cloud particles. This task is vastly more difficult than comparable trace gas studies, in which only one number has to be known for each substance at each point in time and space. Particles sizes over more than six orders of magnitude occur in atmospheric aerosols and clouds, all of which play an important role in certain processes. All condensable substances of the Earth System can be found in the aerosol and a large number of them contributes to climate and biospheric effects. As a consequence of this multidimensional system essential aerosol and cloud properties are not well-established on a global scale yet.

The uncertainty and thus the studies of the Institute for Tropospheric Research start with particle sources. The combustion of fossil and

contemporary fuels is one of the most prominent aerosol sources. However, these sources are still poorly characterised in terms of climate-relevant aerosol parameters. In collaboration with car manufacturers the institute establishes size dependent particle emission data of cars at test stands, in particular in the nanometer size range that was not covered by conventional emission studies. According to long-term measurements of the institute in a street canyon the car related emissions of particles and their precursor gases are subject to strong physical and chemical transformations even before they reach the sidewalk. These transformations will be investigated by a new mobile aerosol laboratory on a trailer behind a moving car in traffic.

Emission studies at cars are complemented by measurements at stationary combustion sources. Here the research focuses on particle properties that determine the absorption of solar radiation. Dedicated methods have been developed for the analysis of soot components, a major absorber of sun light. With aerosol measurements at welding stands finally the Institute for Tropospheric research characterises toxic industrial particle emissions. Health related aerosol studies will be expanded in the future in collaboration with the Environmental Research Center with coupled indoor and outdoor aerosol experiments and concurrent clinical investigations in the urban region of Leipzig. Even the largest highly polluted regions in the



plumes of North America, Europe, the Indian subcontinent and Eastern Asia are insufficiently characterised in terms of aerosol burdens and ensuing climate effects. Thus, the institute focused the most recent field campaigns on the European and Indian plumes. These experiments were conducted within a large framework of international collaboration.

As baseline reference an austral area near Tasmania has been studied. By means of an intercontinental commercial aircraft, the results of the regional experiments are connected through regular CARIBIC flights between Germany, the Indian Ocean and Southern Africa (cf. Fig. 3).

Process studies are conducted at suitable locations such as mountain observatories, tethered balloons and over cooling towers of large power plants.

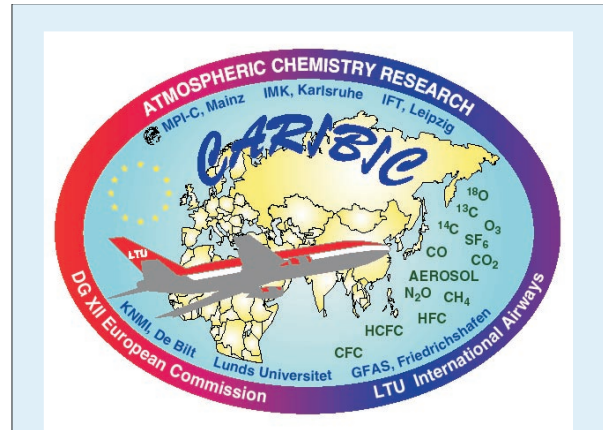


**Fig. 3:** The logo of the international project CARIBIC (Civil Aircraft for Regular Investigation of the atmosphere Based on an Instrument Container).



**Fig. 4:** Tethered balloon measurements near the coast of the North Sea.

These experiments are dedicated to particle nucleation, particle processing through clouds and the influence of anthropogenic aerosols on the optical properties of clouds.

### Modeling

For the description of complex atmospheric processes, model systems of varying dimensions and complexity are developed, tested and applied to micro to mesoscale problems. The ultimate goal is to simulate the many interactions between aerosol particles, gases and clouds in a coupled

three-dimensional meteorology-chemistry-transport model. With this model system as a toolbox scientific as well as legal tasks are addressed.

The Fifth Framework Program of the European Union states as long-term goal that no critical loads may be exceeded in the acidification and eutrophication of soils and water and for surface ozone. For the reduction of these critical loads guidelines are requested for national limits in sulfur dioxide, nitrogen oxides, ammonia and volatile organics. Already today European guidelines define limits in particulate mass concentrations below  $10 \mu\text{m}$  (PM<sub>10</sub>). It is expected that these guidelines



will be extended shortly to smaller particles (PM<sub>2.5</sub>). To meet these guidelines significant regionally different efforts will have to be undertaken in order to reduce emissions.

Models are indispensable tools in the search for efficient and cost-effective means of meeting present and future limits of gaseous and particulate air pollution. As done in the past, the Institute for Tropospheric Research will give advice to the Saxonian government on preventative air pollution measures.

The knowledge of the present emissions is a prerequisite for the development and evaluation of strategies for emission strategies directed and an improvement of air quality. As a basis for the simulation of present and future scenarios the institute developed a dynamic emission inventory for Saxony. This inventory enables us to supply emission data for natural and anthropogenic air pollutants (SO<sub>2</sub>, NO<sub>x</sub>, CO, NH<sub>3</sub>, non-methane hydrocarbons, dust, heavy metals, polychlorinated dibenzo-dioxines/-furanes. For extended investigations emissions of the greenhouse gases CO<sub>2</sub>, CH<sub>4</sub> and N<sub>2</sub>O can be supplied for numerical simulations of the transport and transformation of air pollutants over Saxony. The use of a geographical information system (GIS ArcInfo) allows a spatial resolution of emission data and a connection with political and or geographical structures including a digital road map and land use data.

### Laboratory experiments

In atmospheric research there is a continuous development of physico-chemical models for the description of the most relevant process. These models are based on process parameters, which need to be determined in physical and chemical laboratory experiments.

In the physics section of the institute laboratory experiments cover the development of a large number of methods to characterize atmospheric particles and drops, in particular their size distribution and thermodynamic properties. Complex measuring and sampling systems are being designed for the characterization of cloud drops and interstitial particles.

Spectroscopic techniques such as the Differential Optical Absorption Spectroscopy have been developed for the analysis of trace gases and aerosol particles. There is an ongoing development of the multi-wavelength aerosol LIDAR (Light Detection and Ranging) technique that includes the measurement of atmospheric state parameters such as temperature and wind. Graphitic carbon is specified and quantified with a dedicated Raman spectrometer combined with multi-wavelength absorption measurements on aerosol samples.

Process-oriented laboratory studies are being



*Fig. 5:* Measurement with the multi-wavelength aerosol LIDAR during a field campaign.

carried out jointly by the physics and chemistry sections in two main areas. The first of these activities concerns a laminar flow tube reactor in which particle formation from (SO<sub>2</sub>) and organic precursors (e.g., terpenes) is being investigated. In the second activity the transition from a moist aerosol to a cloud will be simulated in a laminar flow channel.

In the chemistry section there are several process-oriented laboratory studies. Gas phase reactions of the radicals OH and NO<sub>3</sub> are being investigated in flow reactors. These reactions are important for ozone and particle formation caused by biogenic and anthropogenic emissions of volatile hydrocarbons. The chemical identity of atmospheric particles will be characterized in reaction chambers. In a single drop experiment phase transfer parameters of trace gases and radicals are being determined for different chemical species and surfaces. Mechanisms of non-radical oxidations in the liquid phase are being studied with the stopped-flow technique and optical detectors. Experiments with radical reactions in the liquid phase form a core activity of the laboratory experiments because of their importance for processes in haze particles, fogs and clouds. For the understanding of the oxidation of organic trace gases in the tropospheric multi-phase system a large number of reactions



with the OH and NO<sub>3</sub> radicals are being studied as well as reactions of halogenated oxidants. The latter species are of interest for the emission of reactive halogen compounds from sea salt particles.



**Fig. 6:** The lft laminar flow tube reactor.

Several laboratory experiments are dedicated to the chemical characterization of atmospheric organic aerosol components. Besides the conventional combustion techniques, mass spectroscopic and chromatographic techniques coupled directly to analysis by mass spectrometry or capillary electrophoresis with different sampling and segregation techniques are being developed. The close cooperation of the physics and chemistry section has led to the development of a patented sampling method for narrow well-defined particle size ranges that is coupled directly to the mass spectroscopic analyses.



**Fig. 7:** A laser photolysis-long path laser absorption experiment for the study of nitrate radical kinetics in aqueous solution.





*Detailed*

***contributions***

*to current research projects*







## Lindenberg Aerosol Characterization Experiment 1998 (LACE 98)

Dietrich Althausen, Albert Ansmann, Wolfram Birmili, Erika Brüggemann, Bernhard Busch, Thomas Gnauk, Andreas Keil, Christian Kosziar, Detlef Müller, Dörthe Müller, Christian Neusüß, Ulla Wandinger, Manfred Wendisch, Heike Wex, Alfred Wiedensohler

The Lindenberg Aerosol Characterization Experiment 1998 (LACE 98), which was coordinated by IfT, was conducted from July 13 to August 12, 1998 about 70 km southeast of Berlin, Germany. The experiment focussed on the characterization of atmospheric particles in the tropospheric column in order to quantify radiative effects of representative summer-time aerosol distributions in central Europe and to determine uncertainties in these quantifications. The experimental design is briefly outlined. A few results are presented.

### Motivation

One of the main reasons for the large uncertainty in future-climate predictions is a non-adequate description of the global aerosol distribution in climate models. To provide the modeling community with the needed data, integrated field campaigns in key regions of the Earth have been conducted in the past years and will be performed during the next decade. Whereas the Aerosol Characterization Experiment 1 (ACE 1, Tasmania, November-December 1995) documented the chemical and physical characteristics of aerosol particles in a remote (clean) marine atmosphere, the second ACE (ACE 2, Canaries and Portugal, June-July 1997) extended these observations to the North Atlantic Ocean with emphasis on the anthropogenic perturbation of the background aerosol. The Tropospheric Aerosol Radiative Forcing Observational Experiment (TARFOX, off the east coast of the USA, July 1996) focussed on the column-integrated radiative effects by one of the world's major plumes of urban/industrial haze. In contrast, the Smoke, Clouds, and Radiation-Brazil experiment (SCAR-B, Brazil, August-September 1995) and the Indian Ocean Experiment (INDOEX, Maldives and tropical Indian Ocean, February-March 1999) concentrated on pollution emitted from less-developed regions. LACE 98 was planned to extend the efforts to the highly industrialized central European region.

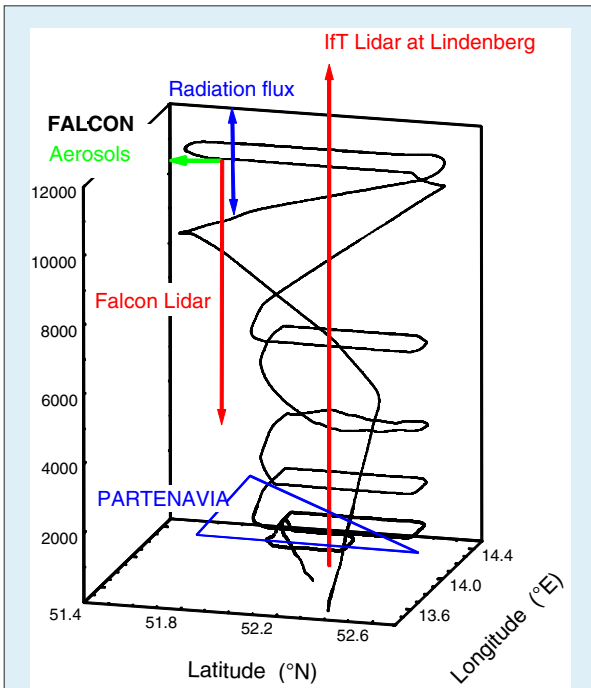
The specific tasks of LACE 98 were threefold: (a) study of the aerosol system and the interaction with the radiation field over a polluted central European site during summer, (b) quantification of the direct climatic effect of the observed, mainly anthropogenic aerosol particles, and (c) quantification of the uncertainties of the optical

properties of the particles and associated radiative effects, calculated from measured chemical composition and particle size distribution of the aerosol. To meet these three objectives, vertically resolved measurements of the aerosol radiative effects (solar irradiances) were required in conjunction with profile measurements of chemical, microphysical, and optical aerosol properties.

### Experiment

Three airplanes carrying sophisticated aerosol and radiation payloads probed the entire troposphere in a complementary and coordinated way. The observations yielded a comprehensive set of data needed for the radiative transfer calculations and for the direct comparison of these results with observations of solar irradiances. In-situ size distribution measurements covered the size range from nuclei-mode particles with diameters  $> 3$  nm to coarse-mode particles and small ice crystals up to  $20 \mu\text{m}$  in diameter. Information on the humidity growth factor of the aerosol particles was obtained by operating two different optical particle spectrometers in an overlapping size range, one instrument measuring particles at low relative humidity and another instrument measuring particles in situ. Aerosol samples for chemical analysis, for measurement of the particle size distribution, aerosol scattering and absorption coefficients, and radiative flux densities (i.e., irradiances) were taken with high vertical resolution. The surface reflectance of the inhomogeneous experimental area (grassy land, fields, forests, and lakes) was measured as a function of wavelength and solar zenith angle.

Three advanced aerosol lidars (two ground-based Raman lidars, one airborne High Spectral Resolution Lidar) were employed. In contrast to widely used simple backscatter lidars, advanced systems measure pure molecular backscatter signals and thus allow an unambiguous determination of the volume extinction coefficient of the particles under ambient conditions. The lidars measured vertical extinction profiles at up to three wavelengths simultaneously (290, 355, and 532 nm).



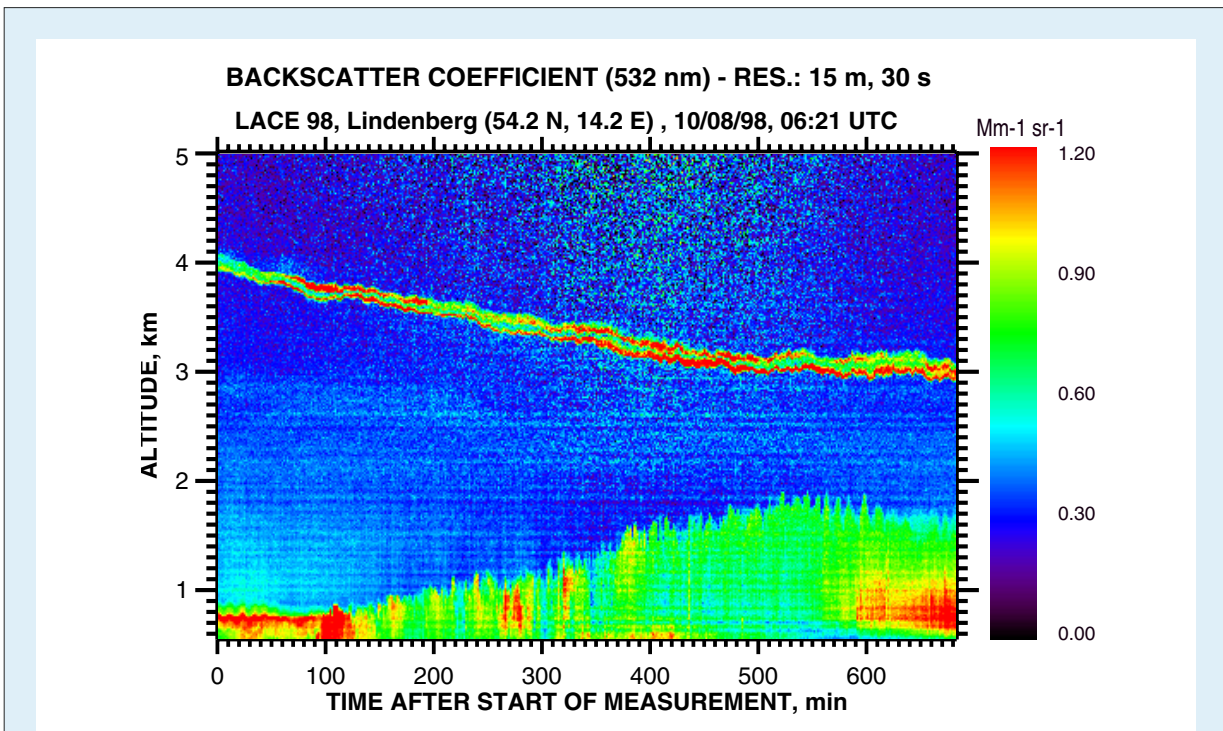
**Fig. 1:** LACE 98 flight pattern of the DLR Falcon and the IfT Partenavia. The vertical axis shows the altitude above ground in meter. Aerosols stand for the observations of microphysical and optical properties of the particles (courtesy of A. Petzold, DLR).

Fig. 1 shows a typical flight pattern of the Falcon of DLR, Oberpfaffenhofen, and the Partenavia chartered by IfT. The Partenavia flew ascents and descends including a triangular pattern at four to six height levels between 500 and 4000 m. In a

complementary way, the Falcon mainly operated in the free troposphere, flying two 60-km straight legs in north-south direction at six different height levels, one near and the other 20 km east of Lindenberg. The in-flight coordination was directed from the ground via radio operation based on actual lidar aerosol profile and radiosonde temperature and humidity observations. One of the main objectives of the third aircraft was the daytime- (i.e., solar-zenith-angle-) dependent characterization of the spectral ground reflectance over the field sites which is a crucial input parameter for radiative transfer calculations. For this purpose, the Cessna of Freie Universität Berlin flew up to four flight legs between 500 and 2500 m over the Lindenberg area.

Fig. 2 shows an example of a lidar measurement taken on August 10, 1998. On that day each aircraft performed two flights, one in the morning and one in the afternoon. The slowly descending aerosol layer in the free troposphere originated from forest fires in western Canada about ten days before.

The aircraft and lidar observations were complemented by extensive ground-based observations of particle properties and of the dependence of particle growth and scattering efficiency on relative humidity. A modified high-flow Anderson PM 10 inlet was used for the nephelometer measurements and impactor and filter sampling for mass and chemical analysis.



**Fig. 2:** Temporal development of the boundary layer and the forest-fire aerosol layer in the free troposphere on August 10, 0620-1740 UTC. Observation was made with lidar.



A low-flow Anderson PM 10 inlet was employed for particle number concentration, number size distribution, volatility, hygroscopicity, and light absorption measurements. Both inlets were mounted 10 m above ground level to avoid near-ground aerosol contaminations.

Compared to previous aerosol campaigns, LACE 98 provided a rather comprehensive chemical characterization of single particles and of particle ensembles by means of a variety of different state-of-the-art instruments and techniques. The chemical composition information was used for so-called mass closure experiments, aerosol source identifications, and the estimation of the refractive indices of the particles. Next to the number size distribution of the particles, the refractive index is the most important input parameter in the calculation of the particle optical properties.

## Results

A few results are highlighted. On the basis of the ground-based and the airborne in-situ observations, the relationship between the measured particle number size distribution, the chemical composition (complex refractive index), the humidity-dependent particle growth, and the optical properties of the particles was investigated. Volume scattering and absorption coefficients were measured with integrating three-wavelength nephelometers and Particle/Soot Absorption Photometers for dry particles. Observations with a telephotometer and horizontally and vertically pointing lidars yielded particle extinction (scattering+absorption) coefficients under ambient humidity conditions.

The measured particle volume scattering and absorption coefficients were compared with results of Mie scattering calculations based on the derived chemical and microphysical particle properties. Relative deviations between the measured and calculated values of the order of  $\pm 20\%$  were found in the case of the scattering coefficient for both ground-based and airborne sampling. Fig. 3 shows two examples of intercomparisons based on the airborne observations. A clear day (10 August 1998, cf. Fig. 2) and a polluted day (1 August 1998) are chosen.

Considerably larger discrepancies (40% to 50%) were found for the absorption coefficients. An extensive uncertainty analysis showed that better agreement is only possible if the size distribution measurement and the determination of the absorbing fraction of the aerosol are improved. Inherent sizing uncertainties in the size distribution measurement, which cannot be avoided with the currently used instrumentation, dominate the

uncertainty in the calculated volume scattering coefficient. Calculated absorption coefficients were most sensitive to uncertainties in the imaginary part of the refractive index, which strongly depends on the fraction of absorbing material in the aerosol particles. These uncertainties propagated into considerable variations in the derived single scattering albedos (scattering-to-extinction ratio). The latter quantity is a useful parameter in the description of the influence of the particles on climate.

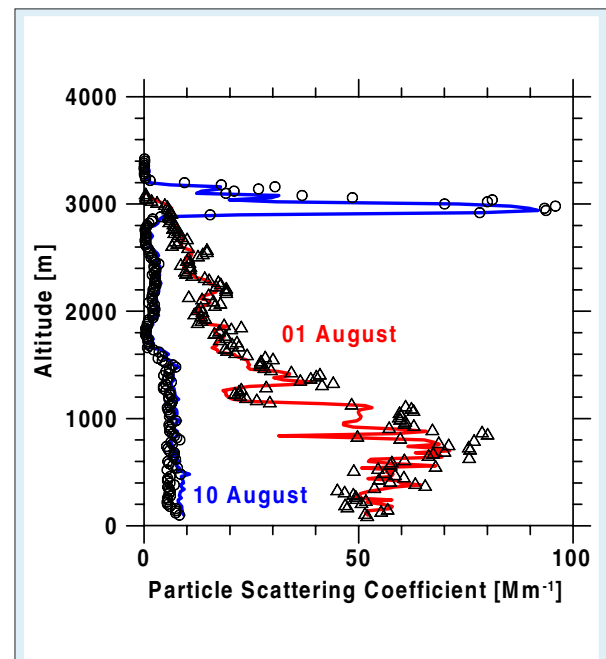


**Fig. 3:** Volume scattering coefficient at 550 nm wavelength versus altitude above ground. The circles and triangles show the measured aircraft data, the solid lines are calculated from the height-resolved information on the particle size distribution and chemical composition. The atmosphere was rather clean on August 10 and polluted on August 1. Note the aerosol peak at 3 km height on August 10 indicating the thin forest-fire aerosol layer (cf. Fig. 2).

As one of the central LACE 98 activities, the aircraft observations were compared with respective profiles of microphysical and optical properties determined from the airborne and ground-based lidar data. The agreement was always good, the deviations were less than 30%. The single scattering albedo could be estimated from the lidar and aircraft data. For the biomass-burning layer in the free troposphere (cf. Figs. 2 and 3) and the highly polluted boundary layer (cf. Fig. 3) the single scattering albedos for particles were close to 0.80 and 0.90, respectively. Albedo values around 0.8 indicate considerable absorption of solar radiation by particles, which contributes to a warming of the atmosphere. Values between 0.9 and 0.95 are typical for mixtures of soil, maritime, and anthropogenic particles over Europe. In this case,



backscattering of solar energy dominates and typically causes a cooling of the atmosphere.

On the basis of the quality-assured lidar-aircraft data, the relationship between the physical, chemical, and optical properties found in the tropospheric column and the downwelling and upwelling radiative flux densities (influenced by the particles) were investigated. The microphysical and chemical profile information was used as input parameters in radiative transfer calculations. Significant differences between the measured and calculated solar (broadband) and spectral surface insolutions were found. Because the approach was based on the well-defined and consistent input data set, it was concluded that the revealed inconsistencies are linked to fundamental problems in understanding of the solar radiative transfer in the atmosphere. The underestimation of atmospheric absorption by the model may have caused the discrepancies.

Finally, the radiative impact of the measured aerosol distributions was estimated. The radiative aerosol forcing obtained from the measurements and calculations at the top of the atmosphere

ranges from  $-4 \text{ W/m}^2$  for relatively clean conditions to  $-16 \text{ W/m}^2$  for polluted situations. As already found in previous field campaigns, anthropogenic aerosols over the highly industrialized regions of North America and Europe tend to cool the Earth/atmosphere system.

In summary, during LACE 98 several, representative cases of tropospheric aerosol distributions have successfully been characterized in terms of the chemical composition, particle size distribution, particle extinction, scattering, and absorption properties as well as of the radiative effects. The aerosol data sets can be used for a proper description of central European aerosol conditions in mesoscale and global atmospheric models.

Problems in the characterization of the radiative effects of aerosols at ambient conditions mainly arise from the uncertainties in the determined particle absorption properties and from the fact that most in-situ measurements are done under low, nonambient humidity conditions. Radiative closure studies clearly demonstrated that more work is needed in order to improve the knowledge of the radiative transfer in the atmosphere.

### Funding

- Bundesministerium für Bildung, Wissenschaft, Forschung und Technologie (BMBF)

### Cooperation

- DLR Neustrelitz
- DLR Oberpfaffenhofen
- DWD, Meteorologisches Observatorium Lindenberg
- DWD, Meteorologisches Observatorium Potsdam
- Freie Universität Berlin
- GSF München
- MPI für Chemie, Mainz
- MPI für Meteorologie, Hamburg
- Technische Universität München
- Technische Universität Darmstadt
- Universität Bremen
- Universität Frankfurt
- Universität Hohenheim
- Universität Mainz
- Universität München
- Universität Potsdam
- Universität Wien
- Universität Würzburg



## Indian Ocean Experiment (INDOEX)

Jost Heintzenberg, Alfred Wiedensohler, Dietrich Althausen, Albert Ansmann, Brigitte Gerlach, Kathleen Franke, Thomas Gnauk, Andreas Maßling, Detlef Müller, Christian Neusüß, Frank Wagner

The Institute for Tropospheric Research participated in the Indian Ocean Experiment (INDOEX) with ground-based in-situ aerosol measurements and with its unique six-wavelength aerosol lidar.

During the intensive field phase, aerosol in-situ measurements were made on the NOAA research vessel Ron Brown in cooperation with the University of Washington and the Pacific Marine Environmental Laboratory of NOAA, both in Seattle. IfT contributed number size distribution and hygroscopicity measurements, and chemical analysis of organic and elemental carbon of impactor samples. The cruise took place from 23 February to 30 March 1999 and was divided into three parts:

- leg 1: from Port Louis, Mauritius (day of year: 54), to Male, Maldives (day of year: 60);
- leg 2: from Male, Maldives (day of year: 63), in the region of the Maldives to Male, Maldives (day of year: 82);
- leg 3: from Male, Maldives (day of year: 85), in the region of the Bay of Bengal to Male, Maldives (day of year: 89).

The lidar system was stationed at the Maldives International Airport on Hulule island (4.1°N, 73.3°E). A detailed characterization of the seasonal cycle of optical and physical particle properties on a vertical scale over the Maldives was retrieved from observations in February/March, July, and October 1999, and in March 2000.

### Seasonal cycle of optical and physical particle properties over the Indian Ocean from six-wavelength lidar observations in the Maldives

The lidar (Althausen et al. 2000) provides backscatter coefficients at 355, 400, 532, 710, 800, and 1064 nm, and extinction coefficients and extinction-to-backscatter (lidar) ratios at 355 and 532 nm. An inversion scheme (Müller et al. 1999a, 1999b) processes the optical information to derive profiles of volume concentration distribution, from which respective profiles of effective radius, surface-area and volume concentration are retrieved, and complex refractive index. The single-scattering albedo at 532 nm follows from Mie-scattering calculations. The measurements were accompanied by routine observations of the particle optical depth at 18 wavelengths between 350 and 1100 nm with a sunphotometer. Routine launches of radiosondes (Vaisala RS80) provided profiles of pressure, temperature and relative humidity over the lidar site.

Fig. 1 gives an example of a two-layered particle structure. Above the convective boundary layer, which stretches to approximately 1000 m height follows an elevated particle layer between 1500 and 4000 m height. Sunphotometer observations prior to the measurement showed an optical depth of 0.53 at 530 nm. According to backtrajectory analysis, the particle layer was advected from India (Ansmann et al. 2000).

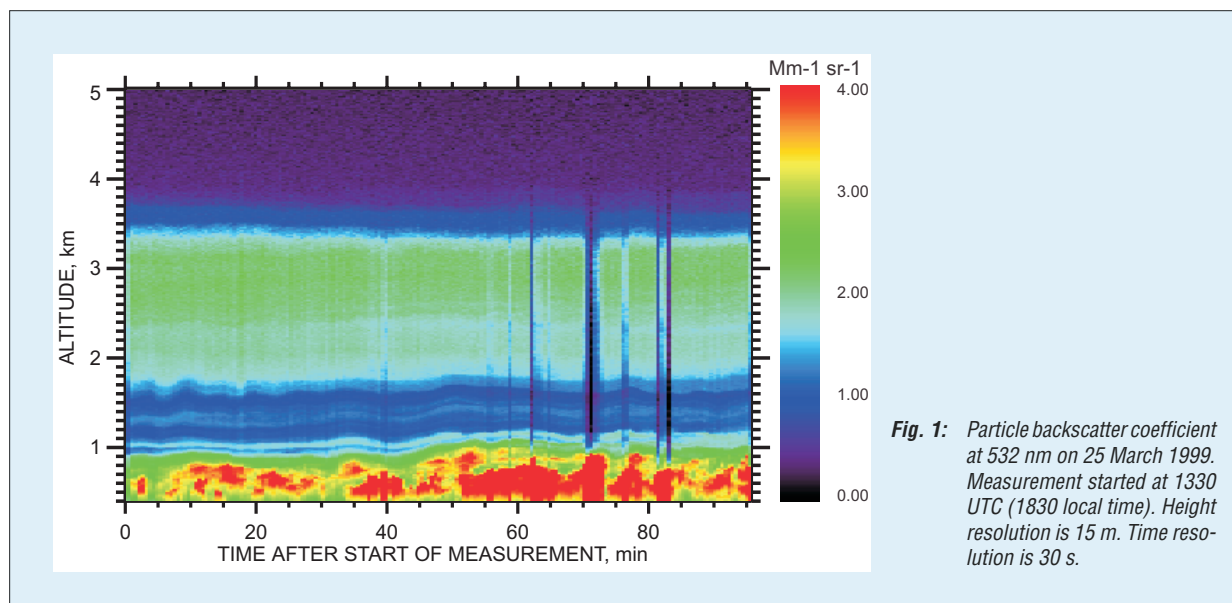
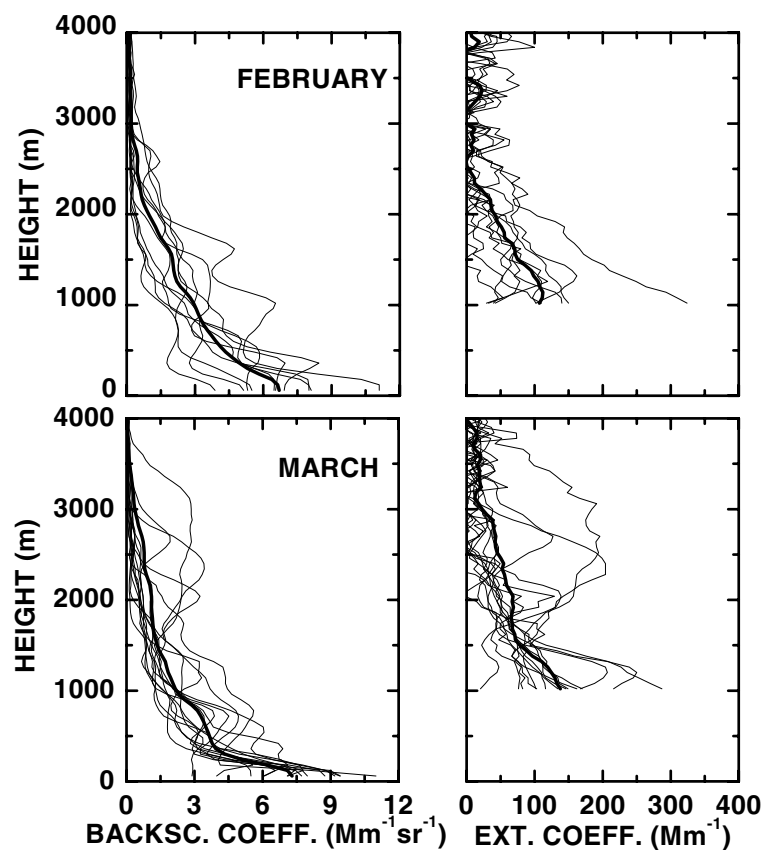


Fig. 2 shows all individual night-time measurements performed during the intensive field phase of INDOEX. The incomplete overlap between the laser beam and the receiver field of view restricts the minimum height for reliable extinction coefficients to 1000 m. In contrast, the backscatter coefficients at 532 nm can be derived down to the surface. Detailed analysis (Ansmann et al. 2000, Müller et al. 2000a, 2000b, 2000c) shows that during northeast monsoon in 1999 and 2000 multiple-layered particle plumes were frequently advected from India and southeast Asia. The maximum height of these layers reached 4 km.

the respective extinction profiles. The backscatter and the extinction coefficients were largest during the polluted northeast monsoon season. Very high lidar ratios of 75 sr at 532 nm, indicating strongly polluted air masses, were found in March 1999. Lower mean values between 45 and 65 sr were found during February 1999, which was characterized by advection of air from southeast Asia, and March 2000, which showed the advection of air masses from India and the arid and semi-arid regions to the northwest of India. In the case of advection from southeast Asia, these values indicate a mixture of aged aerosols



**Fig. 2:** Profiles of particle backscatter and extinction coefficients at 532 nm in February and March 1999, based on Raman measurements. Each of the individual profiles (thin solid lines) represents a 1-hour average of the respective measurement. The complement of the profiles represents all measurements performed after sunset during the intensive field phase of INDOEX. Also shown are the mean profiles of the particle backscatter and extinction coefficients (thick solid lines).

Fig. 3 shows the profiles of the monthly mean backscatter and extinction coefficients, and the lidar ratios at 532 nm based on all individual nighttime measurements. The mean lidar ratios below 1000 m height follow from the combined information of the integrated backscatter coefficient, columnar optical depth determined with the sunphotometer and optical depth above 1000 m height determined from

from anthropogenic pollution sources with marine particles. The lower values for March 2000 indicate a contribution by clean crustal particles. The pollution sources most-likely are biomass burning, and Diesel fuel and coal combustion (Müller et al. 2000a, 2000c). In general, the aerosol layering was more pronounced in March 2000 compared to the findings in the previous year.

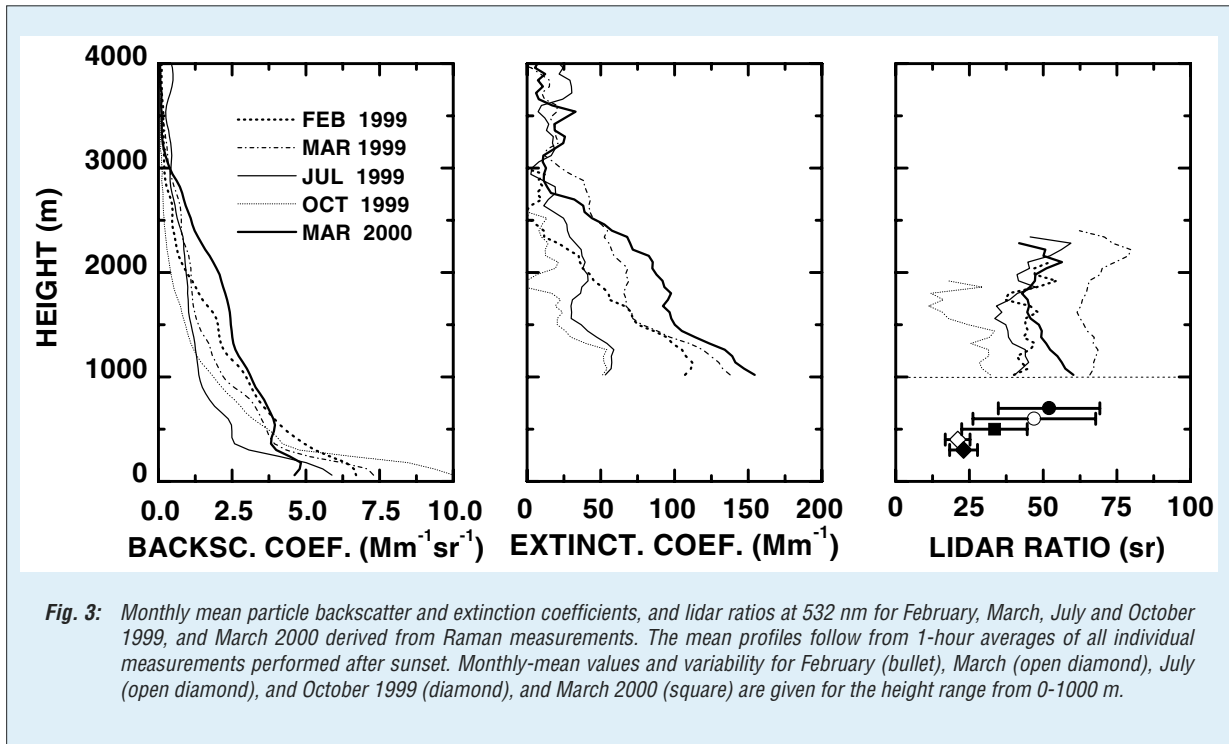
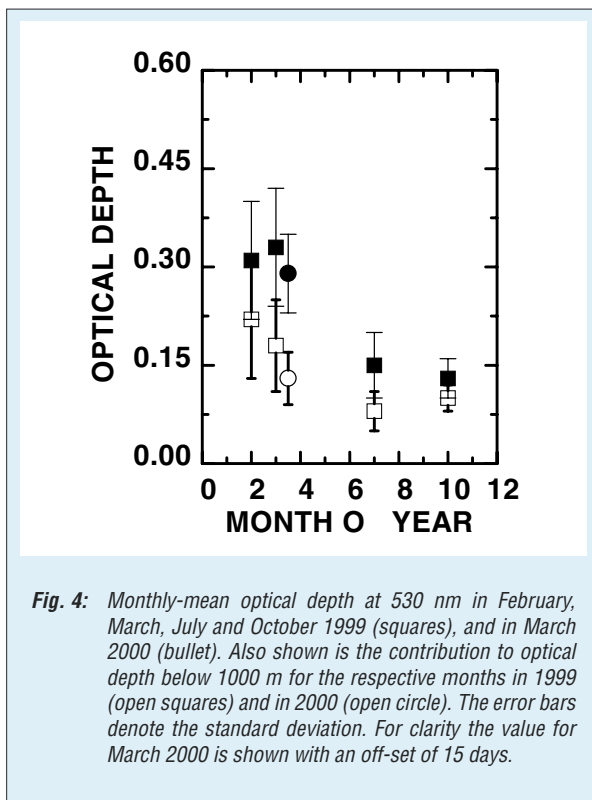


Fig. 4 shows the monthly mean columnar optical depth at 530 nm based on sunphotometer observations. The contribution to optical depth above 1000 m height follows from integration of the respective extinction profiles at 532 nm. During the northeast monsoon, elevated particle layers above a height of 1000 m contributed approximately 30-56% to the monthly mean optical depth of 0.29-0.32 at 530 nm.



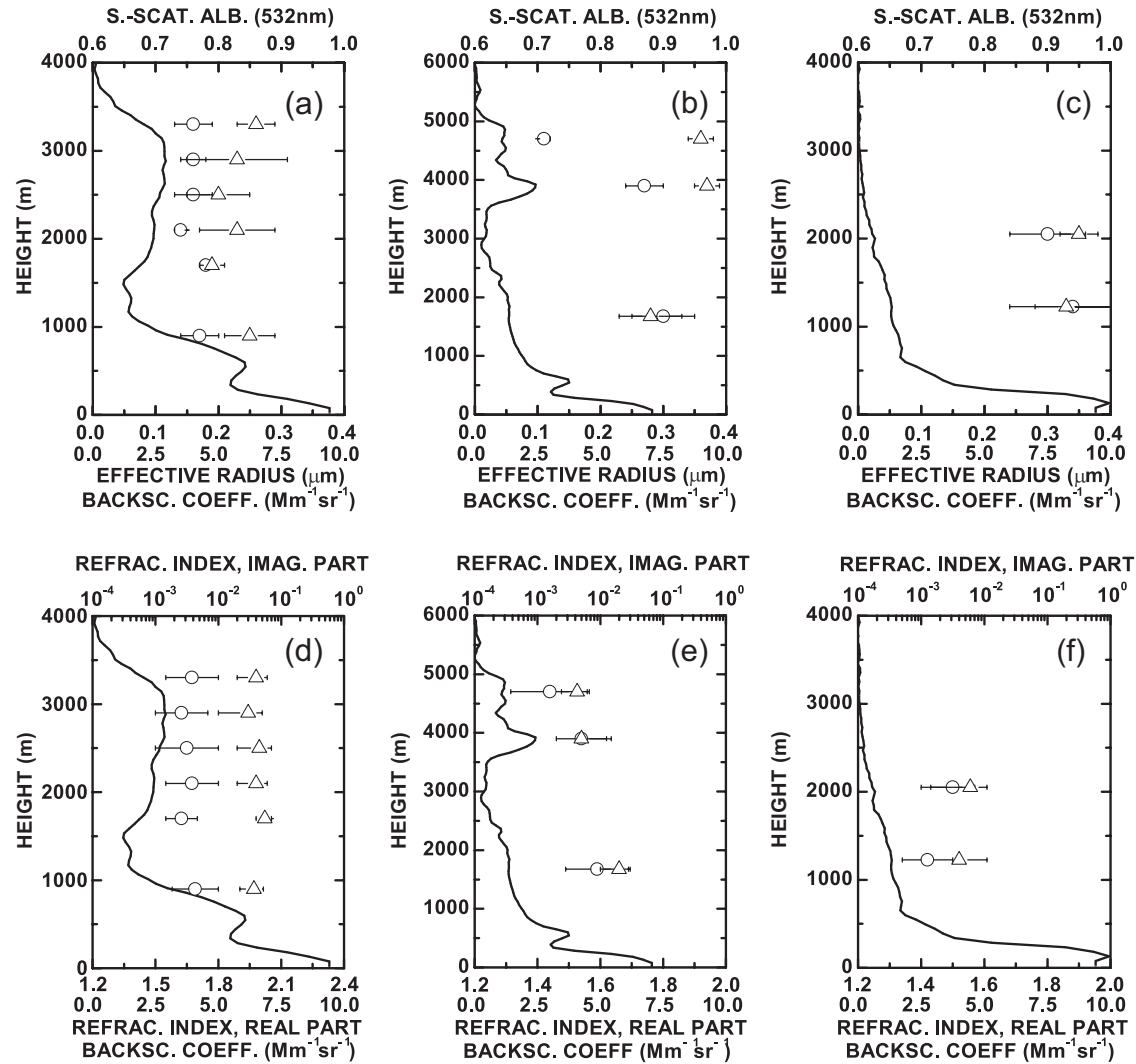
A combination of clean marine and clean continental conditions was found during the southwest monsoon in July 1999. Backtrajectory analysis showed the advection of air masses from the southwest of the Indian Ocean and eastern parts of Africa. In some cases, air was advected from the Arabian peninsula in maximum heights of 5 km. Accordingly, lidar ratios ranged between 35 sr near the surface, characteristic for a mixture of clean marine and clean continental aerosol, and 55 sr in elevated particle layers, characteristic for a mainly continental aerosol. Backscatter and extinction coefficients were considerably lower compared to the conditions found during the northeast monsoon. Mean optical depths were 0.15, with a contribution of almost 50% from layers above 1000 m. Clean marine conditions as the result of heavy wash-out processes caused by the passage of the Intertropical Convergence Zone prevailed during October 1999. Backtrajectory analysis showed the advection of air from the southwest of the Indian Ocean. Significant particle concentrations were found to maximum heights of 2.5 km. Lidar ratios ranged from 20-30 sr. Mean optical depths were 0.13.

Fig. 5 shows effective radius, single-scattering albedo, and complex refractive index for characteristic measurements during the northeast and southwest monsoon, and the passage of the ITCZ. The parameters follow from the inversion of the available optical data sets. A detailed description of the data evaluation is given in Müller et al. (2000a and 2000c). The measurement of March 25, 1999 of the northeast monsoon season was characterized by particles of low effective

radii  $<0.25 \mu\text{m}$  and mean complex refractive indices of  $\sim 1.6-0.05i$ . The single-scattering albedo ranged from 0.8-0.93 at 532 nm, reflecting the highly polluted conditions. Similar results were found for the measurements of February 18, 1999 characterized by the advection of air from southeast Asia, and March 22, 2000 characterized by advection of air from India (Müller et al. 2000c).

may have a great impact on e.g., the hydrological cycle in the Indian Ocean region.

In July and October 1999, particle sizes tended toward higher values below 1500 m. Effective radii of  $0.3-0.36 \mu\text{m}$  indicate marine particles. Considerably lower effective radii below  $0.2 \mu\text{m}$  were found in heights of 3-5 km on July 12, 1999. According to backtrajectory analysis, the origin



**Fig. 5:** Particle effective radius (circle) and single-scattering albedo at 532 nm (triangle), and real part (circle) and imaginary part (triangle) of complex refractive index for measurement from 25 March 1999 (a,d), 12 July 1999 (b,e), and 16 October 1999 (c, f). Also shown is the particle backscatter coefficient at 532 nm based on Raman measurements after sunset. Each measurement represents 1-hour average.

The extensive optical and physical parameter set allows for the first time radiative transfer calculations solely from lidar observations. Results for March 25, 1999 (Wagner et al. 2000) show a net radiative forcing at the top of the atmosphere of  $-6.5 \text{ W/m}^2$  for the entire day. This value amounts to a radiative cooling of  $-68 \text{ W/m}^2$  at the surface. The large difference between top-of-the-atmosphere and surface forcing indicates a considerable heating of the atmosphere, which

of the airmass in this height range was Arabia. In lower heights, the air was advected from the southwest of the Indian Ocean and eastern parts of Africa. Complex refractive indices were  $<1.6-0.02i$  for July 12, 1999, also reflecting the mixture of clean marine and clean continental particles. The single-scattering albedo was  $>0.88$  in lower heights and reached one in the elevated layer.

In October, the large effective radii and complex refractive indices in the range of  $1.4-0.005i$  show the



prevalence of clean marine particles. Accordingly, the single-scattering albedo was close to one. Backtrajectory analysis showed the advection of air from the Indian Ocean.

### Carbonaceous aerosol over the Indian Ocean

Carbonaceous material is a major fraction of atmospheric aerosol particles. Elemental carbon (EC) is of special interest due to its light-absorbing properties. Organic carbon (OC) contributes to the scattering of atmospheric particles (Penner 1995). A large variety of organic species contribute to OC. Their chemical nature strongly influences the physico-chemical properties of the aerosol.

Whereas EC is generally accepted to result almost entirely from anthropogenic combustion processes, OC can have several sources. These include direct emission due to incomplete combustion of fossil fuel or biomass and the atmospheric conversion of volatile organic compounds (VOCs) into less volatile species which subsequently condense onto the particulate phase. Both direct particle emission and the emission of particle OC precursors occur as a result of anthropogenic and natural processes. The knowledge about processes and budgets involving particulate organic material is rather incomplete. This has to do with the incomplete specification of organic compounds (only about 10-20% of the OC is specified to date (Rogge et al., 1993; Neusüß et al., 2000)).

Dicarboxylic acids are a main fraction of the known organic material in atmospheric particles (Saxena and Hildemann, 1996). Several measurements indicate their ubiquitous occurrence (e.g. Kawamura et al., 1996). Photochemical processes are the main sources of small dicarboxylic acids. Direct sources such as combustion of fossil fuels are of negligible importance (Schauer et al., 1996 and references therein).

In this contribution, detailed information is presented on the concentration of (i) EC, (ii) OC, and (iii) selected organic species in the marine boundary layer aerosol over the Indian Ocean sampled during the intensive field phase of the Indian Ocean Experiment. Organic species include small dicarboxylic acids, polycyclic aromatic hydrocarbons (PAH), and alkanes.

### Methods

Air was isokinetically sampled about 10 m above sea level in front of the ship's stack. Only air masses without contamination, indicated by number of particles, relative wind speed and direction, were sampled. Three-stage multi-jet cascade impactors (Berner et al., 1979) were used to determine carbon and organic species. The 50% aerodynamic cutoff diameters,  $D_p$ , were 10, 1.1, and 0.18  $\mu\text{m}$ ,

respectively.

In total, 41 samples for the determination of carbon have been taken continuously in time intervals of 12-48 h, depending on the available aerosol concentration. Mean concentrations are reported as time-averaged values. Seven samples have been analyzed for organic species.

Furthermore, a 7-stage multi-jet cascade impactor (50% cutoffs: 0.18/0.3/0.54/1.1/2.0/4.1/10.3  $\mu\text{m}$ ) was used to obtain three examples of the size distribution of carbon. The same impactor was used to obtain continuous size-segregated concentrations of major ions as measured by ion chromatography (Quinn, 1998).

Carbon was determined with a thermographic method by a commercial system (5500 c-mat, Ströhlein). The sample is placed in a quartz tube and heated rapidly. To separate between organic and elemental carbon (OC, EC), in a first step the sample is heated under nitrogen to 590 °C. Those carbon compounds which evaporate under these conditions are referred to as organic carbon. In a second step, the sample is heated under oxygen to 650 °C where all carbon except carbonate is oxidized. The respectively evaporated carbon is completely oxidized to  $\text{CO}_2$  ( $T = 850$  °C, CuO - catalysator) which is analyzed with an IR-detector. Quantification is performed by analyzing external standards.

The accuracy and precision is limited by blank values and the possibility for charring of volatile compounds leading to smaller OC and larger EC fractions. Blank values are subtracted. Errors are calculated from one standard deviation of field blanks. To convert organic carbon (OC) to organic matter (OM), a conversion factor of 1.6 was used. The absorption for submicrometer and supermicrometer particles was determined at 550 nm and 55% RH by measuring the change in transmission through a filter with a Particle Soot Absorption Photometer (PSAP, Radiance Research). Measured values were corrected for scattering, spot size, flow rate and the manufacturer's calibration according to Anderson et al. (1999) and Bond et al. (1999).

Aliphatic and hydroxylated organic acids and semivolatile compounds were determined using a combined method of capillary electrophoresis (CE) and Curie point pyrolysis gas chromatography/mass spectrometry (CPP-GC/MS). Both methods require only small sample amounts and avoid extensive purification or derivatization procedures. The methods are described in detail in Neusüß et al. (2000).

Particle mass was obtained by weighing the substrates before and after sampling. A Cahn Model 29 microbalance was used at a relative humidity of  $33 \pm 3\%$ . Thus, the mass includes water associated with the sampled particles at 33% RH.

## Results

Fig. 6 shows the total carbon concentration during the cruise.

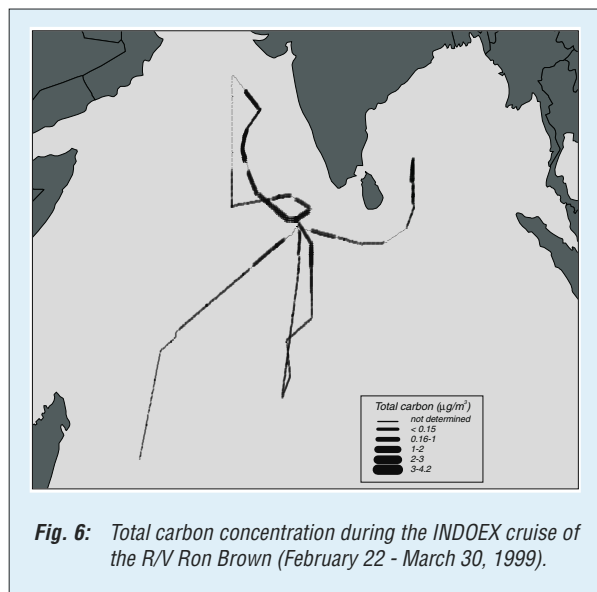


**Fig. 6:** Total carbon concentration during the INDOEX cruise of the R/V Ron Brown (February 22 - March 30, 1999).

The total carbon concentration ranged from only partly detected (supermicrometer OC) on the order of magnitude of  $0.1 \mu\text{g}/\text{m}^3$  in the southern Indian Ocean to more than  $4 \mu\text{g}/\text{m}^3$  southwest of India in the area of the Maldives. These differences are due to distinctly different air masses encountered during the cruise. The atmospheric concentration of carbon for air masses from the southern hemisphere is much lower than for air masses from the northern hemisphere. This behavior is most pronounced for EC for which the concentration can be more than two orders of magnitude higher in the Indian Ocean during air flow from the north ( $1.9 \mu\text{g}/\text{m}^3$  versus  $< 0.02 \mu\text{g}/\text{m}^3$ ). In these air masses, the concentration of OC in coarse particles which are dominated by sea salt particles (Quinn et al., 2001) is a factor of 5-10 higher than in the pristine southern air ( $0.6 \mu\text{g}/\text{m}^3$  versus  $0.07 \mu\text{g}/\text{m}^3$ ). EC is found mainly in submicrometer particles whereas OC is found both in sub- and supermicrometer particles.

The EC concentrations measured in the northern hemisphere are similar to remote continental concentrations in the United States (Penner, 1995) and to measurements in Falkenberg, Germany during the Lindenberg Aerosol Characterization Experiment 98 (LACE 98) (Neusüß et al., 2001).

The carbonaceous fraction of particulate mass is in the range 10 - 20%. Generally, the differences in OC and EC for different trajectory groups are less pronounced for the mass fraction of carbon compared to the concentration. This indicates that the change in the carbon concentration is dominated by meteorological phenomena that affect all chemical components. However, slightly

higher mass fractions of carbon are found for air masses with higher carbon concentrations. This points to a relative decrease in carbon amount, or an increase of secondary sulfate and nitrate with aging of the air mass.

An example of the size distribution of OC and EC for the "Arabian Sea / Coastal India" air mass is presented in Fig. 7.

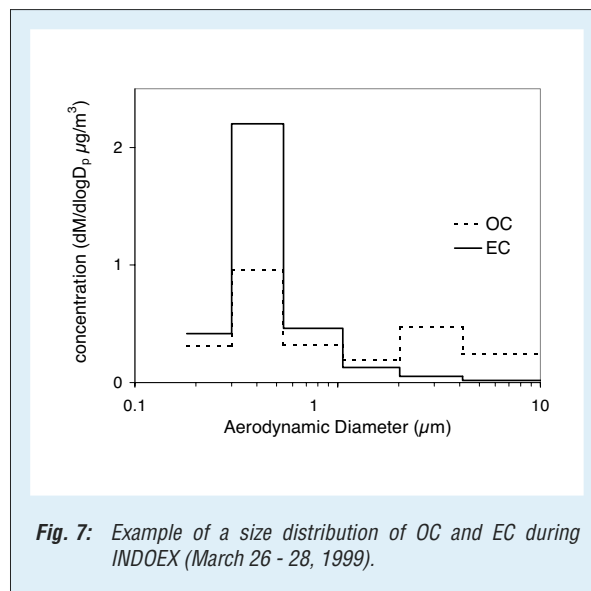


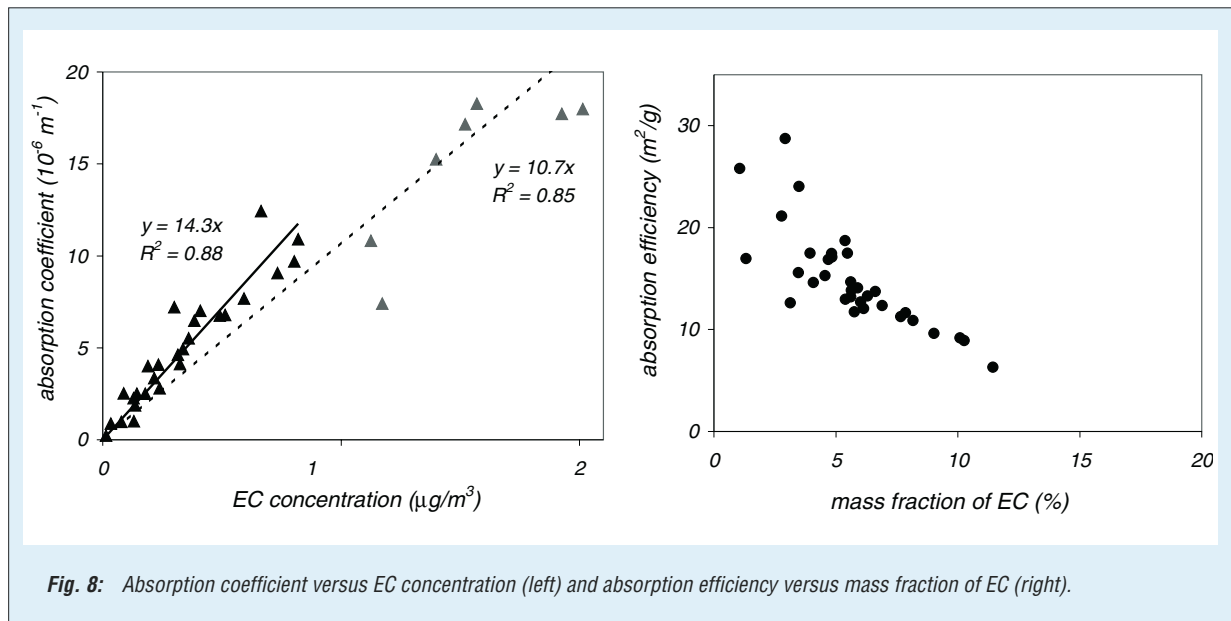
**Fig. 7:** Example of a size distribution of OC and EC during INDOEX (March 26 - 28, 1999).

EC shows a maximum in the size range  $0.3 \mu\text{m} < D_p < 0.54 \mu\text{m}$ . OC has its maximum in the same size fraction but in addition a secondary maximum in the range  $2 \mu\text{m} < D_p < 4.1 \mu\text{m}$  corresponding to the sea salt mode.

The absorption of submicrometer particles measured with a PSAP is correlated to the EC concentration (submicrometer) for all INDOEX samples in Fig. 8. For small carbon concentrations ( $\text{EC} < 1 \mu\text{g}/\text{m}^3$ ), a good regression ( $R^2 = 0.88$ ) is found. An absorption efficiency around  $14 \text{ m}^2/\text{g}$  is found for all air masses except the most polluted cases ( $10 \text{ m}^2/\text{g}$ ).

The good correlation of absorption and EC concentration shows that both measurements are in principle internally consistent and EC is responsible for most of the absorption of the aerosol. The absorption efficiencies obtained here ( $\pm 14 \text{ m}^2/\text{g}$ ) are comparable to the mean level of previous studies (Liousse et al., 1993). The dependence of the absorption efficiency on the mass fraction of EC is shown in Fig. 4. The decrease of the absorption efficiency with the increase of mass is likely to be due to an internal mixture of absorbing material.

Small amounts of primary organics were found. Alkanes, fatty acids and partly polycyclic aromatic hydrocarbons (PAHs) could be detected. PAHs have been detected in levels close to the detection limit in some of the most heavily loaded samples. The sum of phenanthrene, fluoranthene, and



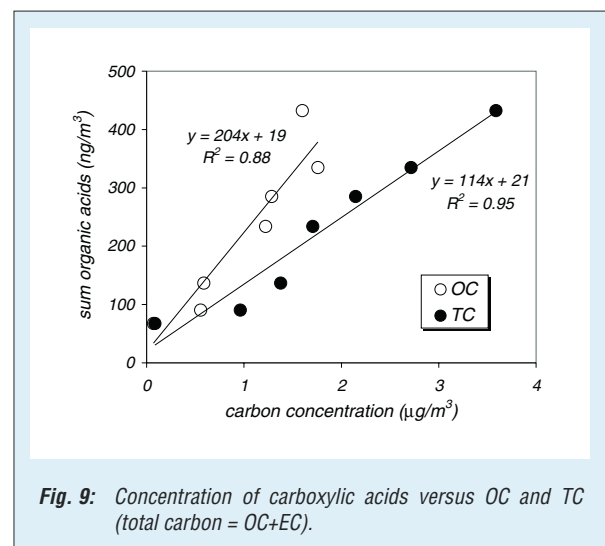
pyrene for sub- and supermicrometer particles was in the range of 0.2 - 0.5 ng/m<sup>3</sup>.

For alkanes, only small differences between the various air masses were observed both for the relative amount of single alkanes and their overall concentration.

Depending on air masses, large amounts of organic acids were observed. The anions of oxalic, malonic, succinic (including methylmalonic acid), tartronic, malic acid, tartaric and methanesulfonic acid were found regularly. In some samples, glutaric, adipinic and azelaic acid including their respective isomers were tentatively identified. Oxalic acid is the most abundant organic acid in aerosol particles followed by malonic and succinic acid for coarse mode particles. Nevertheless, malic and tartaric acid are almost as concentrated and sometimes exceed the oxalic acid concentration in submicrometer particles.

In pristine air masses of the southern Indian Ocean, the total concentration of the carboxylic acids was 30 ng/m<sup>3</sup> showing mostly up in supermicrometer particles. During the influence of air masses from south Asia, the concentration ranged up to 380 ng/m<sup>3</sup>.

In Fig. 9, the concentration of carboxylic acids versus organic and total carbon is shown for the sum of sub- and supermicrometer particles. The sum of dicarboxylic acids (as well as oxalic acid alone) shows a linear dependence with both OC and TC. Furthermore the regressions through the data points confirms a linear dependence for nitrate ( $R^2 = 0.85$ ) and sulfate ( $R^2 = 0.67$ ). This indicates similar sources for dicarboxylic acids (and precursors) and particulate carbon, nitrate, and to a lesser extent, sulfate.



### Hygroscopic properties of aerosol particles over the Indian Ocean

One of the important physical aerosol properties is the hygroscopicity. Hygroscopic properties of atmospheric particles may influence the number of cloud condensation nuclei and thus the resulting droplet size distribution which affects the albedo of the cloud. Besides the importance for cloud formation processes, hygroscopic data are also required to calculate microphysical aerosol properties such as size distribution or scattering for ambient conditions.

In general, aerosol particles can be classified in up to three groups according to their hygroscopicity: hydrophobic particles, less hygroscopic particles and more hygroscopic particles. Using a hygroscopic growth model, which needs the chemical composition and the hygroscopic growth as input parameters, the soluble volume fractions of the particles can be calculated. The ratio of

soluble and insoluble material in a particle has a high influence on the value of supersaturation at which the particle can be activated to form a cloud droplet (Swietlicki, 1999, Kulmala, 1996). It has been found that the increase of soluble mass decreases the supersaturation which is needed for the activation process.

### Air masses

During the cruise, aerosols of different age and origin resulting from differently polluted air masses were observed. Overall the backtrajectory analysis showed the air parcels coming either from the Northern or Southern Indian Ocean with no influence from land, or from the Bay of Bengal or the Arabian Sea under the influence of Pakistan, India or Sri Lanka. The air masses have been classified using backtrajectory analysis. The trajectories were calculated four times daily for three altitudes.

### Experimental setup

A Hygroscopic Tandem-Differential-Mobility-Analyzer (HTDMA) has been used for the hygroscopic growth measurements. The HTDMA measured continuously except for short time periods during which the system was calibrated. Hygroscopic growth factors have been determined for particles with initial dry sizes of 50, 150 and 250 nm. The spectra have been obtained at 30, 55, 75 and 90% RH. The acquisition of one data set lasted about 20 minutes because particle concentrations were generally low.

All data presented have been corrected for size shifts between the first and the second DMA. The relative humidity inside the second DMA has been checked several times each day by a salt calibration to obtain the real relative humidity of the measurement. The presented growth factors measured at 90% RH have been corrected for humidity uncertainties.

### Chemical inorganic composition

All data presented will be divided into three parts showing the first, the second and the third leg (Indian Ocean) of the experiment. The x-axis will be labeled as day of year. January 1 (12.00 at noon) will be denoted as 1.5.

In Fig. 10, the molar components of the major ions are presented. Fig. 11 a shows the molar composition of the first impactor stage ( $D_p = 80 - 184$  nm) whereas Fig. 11 b shows this composition for the second stage ( $D_p = 184 - 308$  nm).

During the first leg, high concentrations of sodium and chloride ions can be noticed sometimes for the first as well as for the second stage. These findings correspond to increasing wind speeds which lead

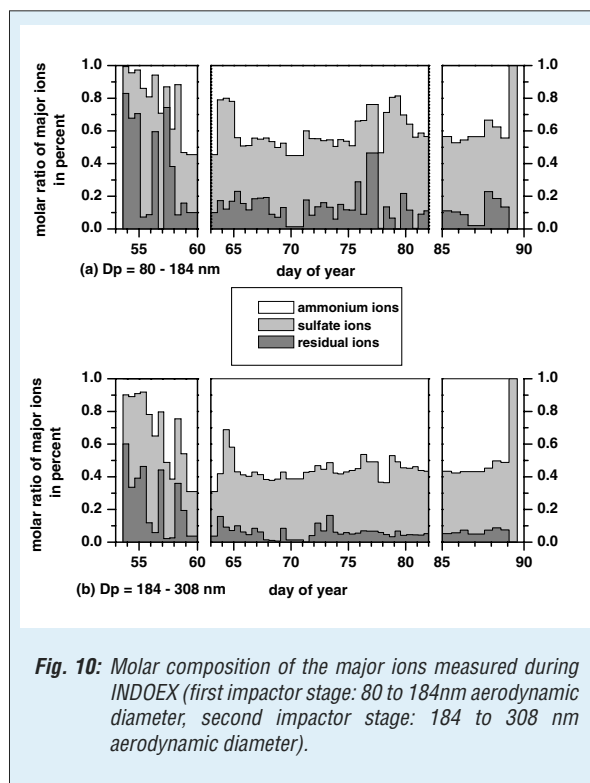


Fig. 10: Molar composition of the major ions measured during INDOEX (first impactor stage: 80 to 184nm aerodynamic diameter, second impactor stage: 184 to 308 nm aerodynamic diameter).

to sea salt production. For both cases ammonium and sulfate ions dominate the molar composition assuming that the major inorganic components of the investigated aerosol were a mixture of ammonium sulfate and ammonium bisulfate. For the second and third leg residual ions reach values of nearly 15% for the first and 10% for the second impactor stage.

In Fig. 11, the ratio of ammonium to sulfate ions is presented for both impactor stages ( $D_p = 80 - 184$  nm and  $D_p = 184 - 308$  nm).

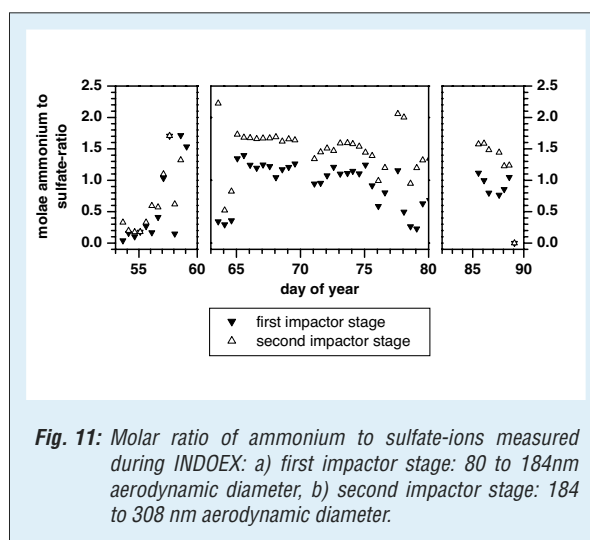


Fig. 11: Molar ratio of ammonium to sulfate-ions measured during INDOEX: a) first impactor stage: 80 to 184nm aerodynamic diameter, b) second impactor stage: 184 to 308 nm aerodynamic diameter.

For the first leg, this ratio shows high variations because of the high amounts of residual ions. For the second and third leg, the ammonium/sulfate ratio is relatively stable with values of nearly 1 for the first and 1.5 for the second impactor



stage. A reason for the increase of this ratio to higher particle diameters might be found in aging processes. These particles may have stayed for longer time in the atmosphere and water soluble material may have condensed on them or they have been cloud processed which leads to higher levels of neutralization. In the following analysis of TDMA data and hygroscopic growth, the inorganic chemical composition has been simplified to the major ions sulfate and ammonium which dominate for most of the time periods the molar distribution in the range between 80 to 300 nm (aerodynamic diameter).

### Hygroscopicity measurements

In Fig. 12, the measured growth factors at 90% RH are presented for particles with initial dry sizes of 50, 150 and 250 nm. More hygroscopic particles obviously have been observed during the whole cruise. The growth factors of these more hygroscopic particle fraction reach average values in the range between 1.68 and 1.73 for 50 nm particles, 1.82 and 1.89 for 150 nm particles and 1.88 and 1.98 for particles with dry diameters of 250 nm.

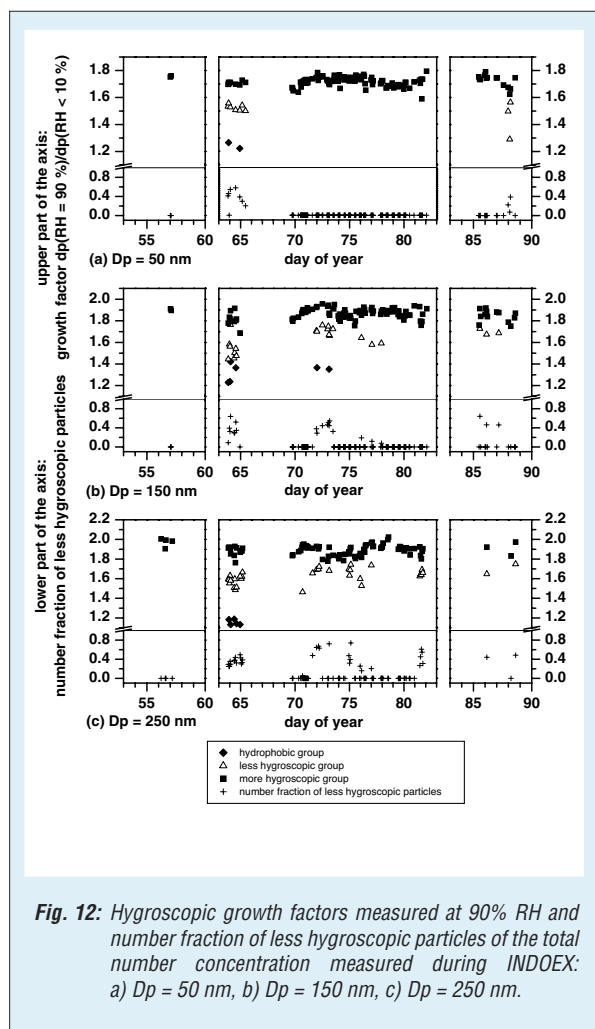


**Fig. 12:** Hygroscopic growth factors measured at 90% RH and number fraction of less hygroscopic particles of the total number concentration measured during INDOEX: a) Dp = 50 nm, b) Dp = 150 nm, c) Dp = 250 nm.

The change in air mass from period one (Indian Ocean) to period two (Indian Subcontinent) corresponds to changes of averaged hygroscopic growth factors from 1.89 to 1.82 for 150 nm particles and from 1.98 to 1.89 for 250 nm particles. Growth factors for 50 nm particles do not show significant variations with air mass.

During period two, air masses from the Indian Subcontinent were directly advected toward the ship's location. In this case, a less hygroscopic particle fraction occurred for nearly all observations besides the more hygroscopic particle mode. For this time period, the highest concentrations of elemental carbon were measured. Average growth factors for these particle groups are in the range between 1.5 and 1.6 depending on the examined size. In some cases hydrophobic particle groups appeared with values between 1.15 and 1.3.

Whereas the number fractions of less hygroscopic particles for this time period show values of 35 to 40%, the number fractions of hydrophobic particles are in the range of 5 to 7% and smaller. Hydrophobic particles are usually observed in urban areas, because their main sources are anthropogenic emissions by fossil fuel and biomass combustion. Here, these particles were found in air masses advected from the Indian Subcontinent. The trajectory analysis shows a travel time of 12 to 24 hours for these air masses between the ship and the continent.

Less hygroscopic particles in the 50 nm class also occurred for period five when air masses from the Arabian Sea contacting the Indian coast were investigated. These particles were sometimes observed during period three and four for particles with initial dry sizes of 150 and 250 nm. However, the smallest growth factors of less hygroscopic particles for 150 and 250 nm were measured during period two.

In general, the strong continental influence on air masses, which had crossed the Indian Subcontinent only one day before investigation, expressed itself in significant differences of the particles' hygroscopic properties. These differences were not seen for marine air masses of the Southern and Northern Hemisphere, which had no contact with land for at least six days.

For measurements performed at 75% RH, more hygroscopic and less hygroscopic particles were found whereas these groups could not be distinguished at 55 and 30% RH. Average growth factors of more hygroscopic particles reach values between 1.35 and 1.37 for 50 nm particles, 1.35 and 1.45 for 150 nm particles and 1.39 and 1.48 for particles with initial dry sizes of 250 nm. In contrast to this, less hygroscopic particles grow up to values of 1.15 and 1.29 depending on the examined size and air mass and they only

occur for time periods when less hygroscopic fractions of aerosol particles were also found in the 90% RH-measurements.

Looking at the data taken at 55% RH, a decrease in hygroscopic growth can be noted from period one (Indian Ocean) to period two (Indian Subcontinent). Especially for the accumulation mode particles, this decrease (from 1.26 to 1.19 for 150 nm particles and from 1.30 to 1.22 for 250 nm particles) is significant. Average values for 30% RH were 1.15 to 1.16 (period one) and 1.11 to 1.13 (period two). The variations in hygroscopic growth at 55 and 30% RH between different air masses were very small and only significant for the change in air mass from period one to period two and for particles with initial dry sizes of 150 and 250 nm.

For the calculation of soluble particle volume fractions, a hygroscopic growth model was used following Swietlicki (1999). The model assumes that the particles consist of a core, which is completely insoluble and coated by water soluble material such as ammonium sulfate or ammonium bisulfate.

The growth of the major soluble compounds serves here as input parameter. Therefore, the hygroscopic growth was experimentally derived as a function of the relative humidity (40 – 92% in steps of 1% and 0.5%, respectively) using the HTDMA. These measurements were done for different ammonium-to-sulfate ratios and particles with an initial dry diameter of 150 nm.

All calculations of soluble volume fractions have been made on the basis of the 90% RH hygroscopicity data with regard to the ammonium-to-sulfate ratio shown in Fig. 11. The calculations have only been done for those time periods when the molar fraction of ammonium and sulfate ions was higher than 80 percent of all ions (Fig. 10). In Fig. 13, the calculated soluble volume fractions for each hygroscopicity mode and size are presented. The smallest values of solubility for 150 and 250 nm particles were found for time period two when Indian Subcontinental air masses were investigated. This statement holds for the more hygroscopic particles as well as for the less hygroscopic particles. The more hygroscopic particles are on average 72% and 95% soluble for 150 nm and 250 nm particles, respectively. Less hygroscopic particles show soluble volume fractions of 37% (150 nm particles) and 50% (250 nm particles). It has to be taken into account that calculated solubilities for 250 nm particles are generally overestimated. The uncertainty for these values are however +/- 20%. Relatively small soluble volume fractions were found for 50 nm particles. Here, the average value for the more hygroscopic particles is 72%. Even smaller values of 66% were found for air masses from the Southern Hemisphere. Soluble volume

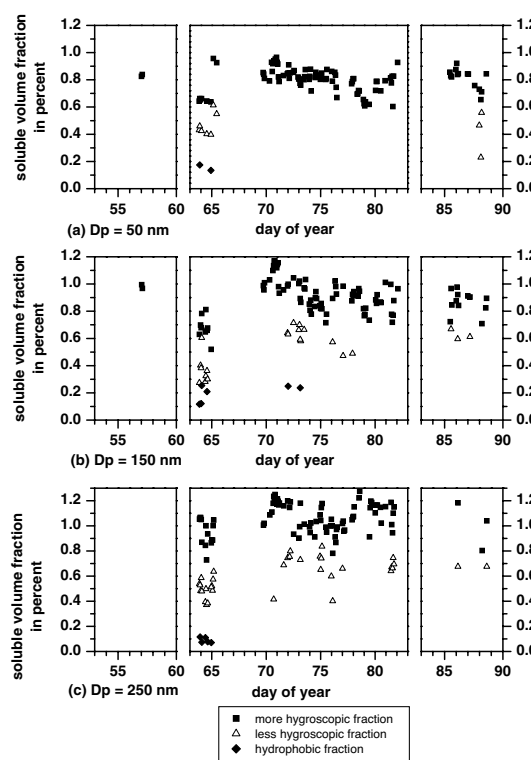


**Fig. 13:** Soluble volume fractions calculated on the basis of 90% RH-data during INDOEX: a)  $D_p = 50$  nm, b)  $D_p = 150$  nm, c)  $D_p = 250$  nm.

fractions found for less hygroscopic particles are generally smaller than 50%.

Nearly hydrophobic particle fractions for all particle sizes only were found for time period two (Indian subcontinental air masses) with one exception. Two observations were also found during period three (Mixed/Indian subcontinent and Middle East) for particles with initial dry sizes of 150 nm. Soluble volume fractions of this particle group is less than 25%.

In general, the smallest soluble volume fractions of accumulation mode particles were found for time period two, when highly continentally influenced air masses were observed. This has been found for more hygroscopic particles as well as for less hygroscopic particles. Soluble volume fractions of marine air masses of the Southern or Northern Hemisphere show significantly higher values.

## Conclusion

Routine lidar observations in February, March, July, and October 1999, and in March 2000 provide the seasonal cycle of optical and physical particle properties on a vertical scale over the Indian Ocean. During northeast monsoon, highly polluted aerosol layers in maximum heights of 4 km were advected from India and southeast Asia. From case studies follows a value of 0.8-0.93 for the single



scattering albedo at 532 nm. A mixture of clean continental and clean marine aerosol conditions prevailed during southwest monsoon. Particles were advected from Arabia in maximum heights of 5 km. The single scattering albedo was above 0.88. Mainly clean marine conditions as the result of heavy wash-out processes caused by the passage of the Intertropical Convergence Zone were found in October 1999. Particles were found in maximum heights of 2.5 km. The single scattering albedo was close to one.

A strong influence of southern Asia on the concentration of particulate carbonaceous material over the Indian Ocean has been observed. OC concentration was typically more than one order of magnitude higher in the northern compared to the southern Indian Ocean, both for submicrometer and supermicrometer particles. The mass fraction of carbonaceous material was in the range of 10-20%, showing less pronounced variation with air masses. A high degree of mixing with scattering material results in high absorption efficiencies. The absorption efficiency is lower for higher mass fractions. A large amount of organic material is of secondary origin since alkanes and polycyclic aromatic hydrocarbons have been found only in small amounts. This is confirmed by the good correlation of the sum of carboxylic acids with OC, EC, nitrate, and, to a lesser extent, sulfate.

Hygroscopic properties show differences depending on the air mass. Especially, strongly continentally influenced air masses, which have passed the Indian subcontinent only one day before investigation, show significant differences in their properties in contrast to marine air masses of the Southern and Northern Hemisphere, which had no land contact for at least six days.

A more hygroscopic fraction of aerosol particles was found for all particle sizes and for all air masses during the whole campaign at 90% RH. Less hygroscopic fractions only occur for continentally influenced air masses, whereas nearly hydrophobic particle groups were only observed for Indian subcontinental air masses. For this time period, a decrease in hygroscopic growth was observed in contrast to the marine aerosol of the Southern Hemisphere investigated before. The smallest soluble volume fractions of accumulation mode particles were found for time period two, when highly continentally influenced air masses were observed. This holds for more hygroscopic particles as well as for less hygroscopic particles. Soluble volume fractions of marine air masses of the Southern or Northern Hemisphere show significant higher values.

## References

- Althausen, D., Müller, D., Ansmann, A., Wandinger, U., Hube, H., Clauer, E. and Zörner, S. 2000.** Scanning six-wavelength eleven-channel aerosol lidar. *J. Atmos. Oceanic Technol.*, **17**, 1469-1482.
- Anderson, T.L., Covert D.S., Wheeler J.D., Harris J.M., Perry K.D., Trost B.E., Jaffe D.J., and Ogren J.A. 1999.** Aerosol backscatter fraction and single scattering albedo: measured values and uncertainties at a coastal station in the Pacific Northwest. *J. Geophys. Res.*, **104**, 26793 – 26807.
- Berner, A., Lurzer C., Pohl F., Preining O., and Wagner P. 1979.** The size distribution of the urban aerosol in Vienna, *Sci. Total Environ.*, **13**, 245 - 261.
- Bond T. C., Anderson T. L., and Campbell D. 1999.** Calibration and intercomparison of filter-based measurements of visible light absorption by aerosols, *Aer. Sci. Technol.*, **30**, 582-600.
- Kawamura K., Kasukabe H., and Barrie L. 1996.** Source and reaction pathways of dicarboxylic acids, ketoacids and dicarbonyls in arctic aerosols: one year of observations, *Atmos. Environ.*, **30**, 1709-1722.
- Kulmala, M., P. Korhonen, T. Vesala, H.-C. Hansson, K. Noone, B. Svenningsson, 1996.** The effect of hygroscopicity on cloud droplet formation, *Tellus*, **48B**, 347-360.
- Liousse C., Cachier H., and Jennings S. G. 1993.** Optical and thermal measurements of black carbon aerosol content in different environments: variation of the specific attenuation cross-section,  $\sigma$  ( $\sigma$ ), *Atmos. Environ.*, **27A**, 1203-1211.
- Müller, D., Wandinger, U. and Ansmann, A. 1999a.** Microphysical particle parameters from extinction and backscatter lidar data by inversion with regularization: Theory. *Appl. Opt.*, **38**, 2346-2357.
- Müller, D., Wandinger, U. and Ansmann, A. 1999b.** Microphysical particle parameters from extinction and backscatter lidar data by inversion with regularization: Simulation. *Appl. Opt.*, **38**, 2358-2368.
- Ansmann, A., Althausen, D., Wandinger, U., Franke, K., Müller, D., Wagner, F. and Heintzenberg, J. 2000.** Vertical profiling of the Indian aerosol plume with six-wavelength lidar during INDOEX: A first case study. *Geophys. Res. Lett.*, **27**, 963-966.
- Müller, D., Wagner, F., Althausen, D., Wandinger, U. and Ansmann, A. 2000a.** Physical particle properties of the Indian aerosol plume derived from six-wavelength lidar observations on 25 March 1999 of the Indian Ocean Experiment. *Geophys. Res. Lett.*, **27**, 1403-1406.



- Müller, D., Franke, K., Wagner, F., Althausen, D., Ansmann, A. and Heintzenberg, J. 2000b.** Vertical profiling of optical and physical particle properties over the tropical Indian Ocean with six-wavelength lidar, part I: Seasonal cycle. *J. Geophys. Res.*, in press.
- Müller, D., Franke, K., Wagner, F., Althausen, D., Ansmann, A. and Heintzenberg, J. 2000c.** Vertical profiling of optical and physical particle properties over the tropical Indian Ocean with six-wavelength lidar, part II: Case studies. *J. Geophys. Res.*, in press.
- Neusüß C., Wex H., Birmili W., Wiedensohler A., Koziar C., Busch B., Brüggemann E., Gnauk T., Ebert M., and Covert D. S. 2001.** Characterization and parameterization of atmospheric aerosol number, mass, and chemical size distributions in central Europe, *J. Geophys. Res.*, submitted.
- Neusüß C., Pelzing M., Plewka A., and Herrmann H. 2000.** A new analytical approach for size-resolved speciation of organic compounds in atmospheric aerosol particles: Methods and first results, *J. Geophys. Res.*, **105**, 4513-4527.
- Neusüß C., Gnauk T., Plewka A., Herrmann H., and Quinn P. K. 2000.** Carbonaceous aerosol over the Indian Ocean: OC/EC fractions and selected specifications from size-segregated samples taken onboard the R/V Ron Brown, *J. Geophys. Res.*, submitted.
- Penner J. E. 1995.** Carbonaceous aerosols influencing atmospheric radiation: Black and organic carbon, in *Aerosol forcing of climate: report of the Dahlem workshop on aerosol forcing of climate*, ed. R. J. Charlson and J. Heintzenberg, 91-108.
- Quinn, P. K., D. J. Coffman, V. N. Kapustin, T. S. Bates, D. S. Covert, 1998.** Aerosol optical properties in the marine boundary layer during ACE 1 and the underlying chemical and physical aerosol properties, *J. Geophys. Res.*, **103**, 16,547-16,563
- Quinn P. K., Coffmann D. J., Bates T. S., Miller T. L., Johnson J. E., Welton E. J., Neusüß C., Miller M., and Sheridan P. J. 2001.** Aerosol optical properties during INDOEX 1999: Means, variability, and controlling factors, *J. Geophys. Res.*, submitted.
- Rogge W. F., Mazurek M., Hildemann L. M., and Cass G. R. 1993.** Quantification of urban organic aerosols at a molecular level: Identification, abundance and seasonal variation, *Atmos. Environ.*, **27A**, 1309-1330.
- Saxena P. and Hildemann L. M. 1996.** Water-Soluble Organics in Atmospheric Particles: A Critical review of the Literature and Application of Thermodynamics to Identify Candidate Compounds, *J. Atmos Chem*, **24**, 57-109.
- Schauer J. J., Rogge W. F., Hildemann L. M., Mazurek M. A., and Cass G. R. 1996.** Source Apportionment of airborne particulate matter using organic compounds as tracers, *Atmos. Environ.*, **30**, 3837-3855.
- Svenningsson, B., H.-C. Hansson, A. Wiedensohler, J. A. Ogren, K. J. Noone, A. Hallberg, 1992.** Hygroscopic growth of aerosol particles in the Po Valley, *Tellus*, **44b**, 556-569.
- Voutilainen, A., F. Stratmann, J. P. Kaipio, 1999.** A new data inversion algorithm for DMPS and TDMA measurements (abstract), *J. Aerosol Sci.*, **30**, Suppl. 1, 775-776.
- Wagner, F., Müller, D. and Ansmann, A. 2000.** Comparison of the radiative impact of aerosols derived from vertically resolved (lidar) and vertically integrated (sun photometer) measurements: example of an Indian aerosol plume, *J. Geophys. Res.*, submitted.

### Funding

- Bundesministerium für Bildung, Wissenschaft, Forschung und Technologie (BMBF)

### Cooperation

- Center for Clouds, Chemistry and Climate, Scripps Institution of Oceanography, La Jolla, USA
- Florida State University, Tallahassee, USA
- Koninklijk Nederlands Meteorologisch Instituut, De Bilt, Netherlands
- Max Planck Institut für Chemie, Mainz
- Meteorological Service of the Maldives
- National Center for Atmospheric Research (NCAR), Boulder, USA
- National Oceanographic and Atmospheric Administration (NOAA), Boulder, USA
- University of Washington, Seattle, USA
- NOAA-PMEL, Seattle, USA



## Size segregated characterization of fine particulate matter in Leipzig and Melpitz

Erika Brüggemann, Thomas Gnauk, Hartmut Herrmann, Konrad Müller, Christian Neusüb, Antje Plewka, Gerald Spindler

### Introduction

The European standard for suspended particulate matter in air (PM<sub>10</sub>) will lead to strict regulations with regard to the mass concentration of PM<sub>10</sub> particulate matter (Tab. 1). For Saxonian cities the observance of these new regulations will

campaigns in winter 1999/2000 and in summer 2000.

Besides the chemical characterization of the main components of PM a set of ten trace metals was analysed as well as electron microscopic characterization of particles was performed by the UFZ Leipzig-Halle GmbH.

phase	integration time	limit value [ $\mu\text{g m}^{-3}$ ]	date of introduction
1	24 hours	50 (no more than 35 days exceeded per year)	01-01-2005
1	Year	40	01-01-2005
2 <sup>a)</sup>	24 hours	50 (no more than 7 days exceeded per year)	01-01-2010
2 <sup>a)</sup>	Year	20	01-01-2010
a) preliminary value			

Tab. 1: European limits for PM<sub>10</sub> in relation to human health.

be problematic. The Sächsisches Landesamt für Umwelt und Geologie (SLUG) charged the IfT to measure the size segregated particulate matter at three sites in NW Saxony to identify sources of the small particles during two measurement

The three sites (Fig. 1) selected for particle collection were a central cross road near the main railway station, the measuring platform of the IfT building and the IfT research station Melpitz.

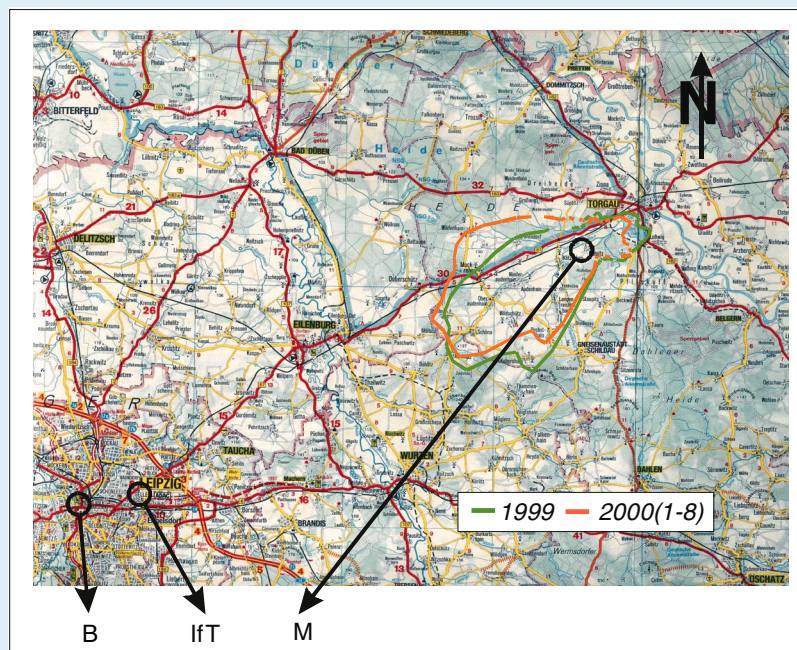


Fig. 1: Collection sites in Leipzig (B = City and IfT) and Melpitz (M) and wind rose for 1999 (green) and for the first eight months of 2000 (orange).

Nine typical dry winter days and eight typical dry summer days have been selected for the 24 hour collection of particles by five stage BERNER impactors (only four stages have been investigated: 0.05 – 0.14  $\mu\text{m}$ , 0.14 – 0.42  $\mu\text{m}$ , 0.42  $\mu\text{m}$  – 1.2  $\mu\text{m}$  and 1.2 – 3.5  $\mu\text{m}$ ), PM<sub>2.5</sub> high volume filter sampler and isokinetic collection on Nuclepore filters for electron microscopy, and X-ray microanalyses (EDX).

The chemical characterization of the impactor and filter samples was performed with regards to their ionic content (ammonium, sodium, potassium, magnesium, calcium, sulfate, nitrate, chloride and oxalate), OC-EC (Organic Carbon – Elemental Carbon), trace metals (V, Cr, MN, Co, Ni, Cu, Zn, Cd, Tl and Pb) and selected organic species (12 polyaromatic hydrocarbons (PAH), 13 alkanes and 2 oxy-PAH).

The REM (Raster Electron Microscopy) has been used to characterize the shape, including soot identification and number concentration. On selected particles the elemental composition was identified to characterize re-suspended crustal material.

### Selected results

Between the two measurement campaigns not only important differences but also commonalities have been identified. The traffic emissions were roughly constant at both campaigns. During the winter campaign the particulate matter composition was heavily influenced by individual household heating with brown coal briquettes, output from electrical power plants and heating power plants and by the lower boundary layer mixing height. During the summer campaign the influence of biogenic emissions must be taken into account.

The comparison of filter and impactor sampling was an important tool to explain some typical errors of the filter samplers using quartz fibre filters. Therefore, the main investigations have been carried out with the impactor samples. In Tab. 2 a summary of all collected samples give the mass distribution for the four size fractions.

The highest amount of particulate matter, nearly

80%, is found in particles below 1.2  $\mu\text{m}$ , which are most important because of their atmospheric stability, lung penetration and toxic effects.

### Stage 1 particles (50 – 140 nm)

The smallest particles mainly consist of elemental and organic carbon directly from traffic emissions or from gas to particle conversion or condensation of organics on particle surfaces. At the sampling site in the city of Leipzig, which is predominantly influenced by traffic (Fig. 2 and Fig. 3) the mean winter mass fraction of Total Carbon (TC = OC+EC) is 77%. From Leipzig city to the IFT and, further on to Melpitz a strong decrease in mass was observed for both summer and winter.

During winter nitrate was observed at all sites as the most important ionic component (13-17% of stage mass) whereas in the summer campaign sulfate was dominating (5-20% of stage mass).

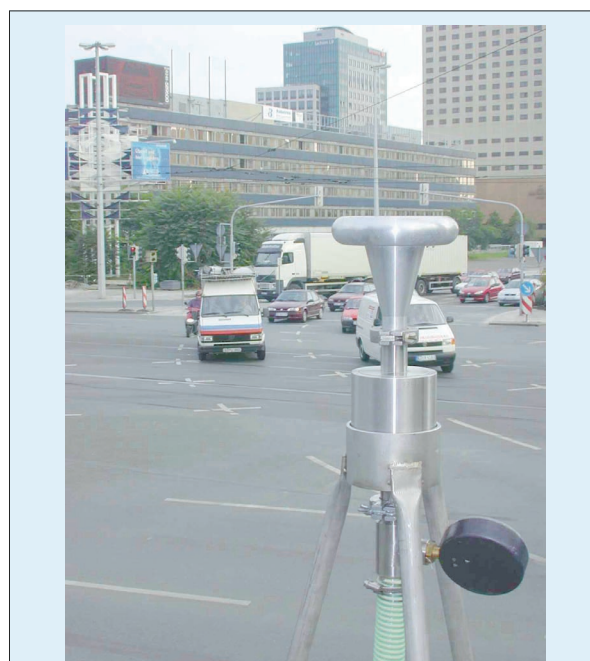
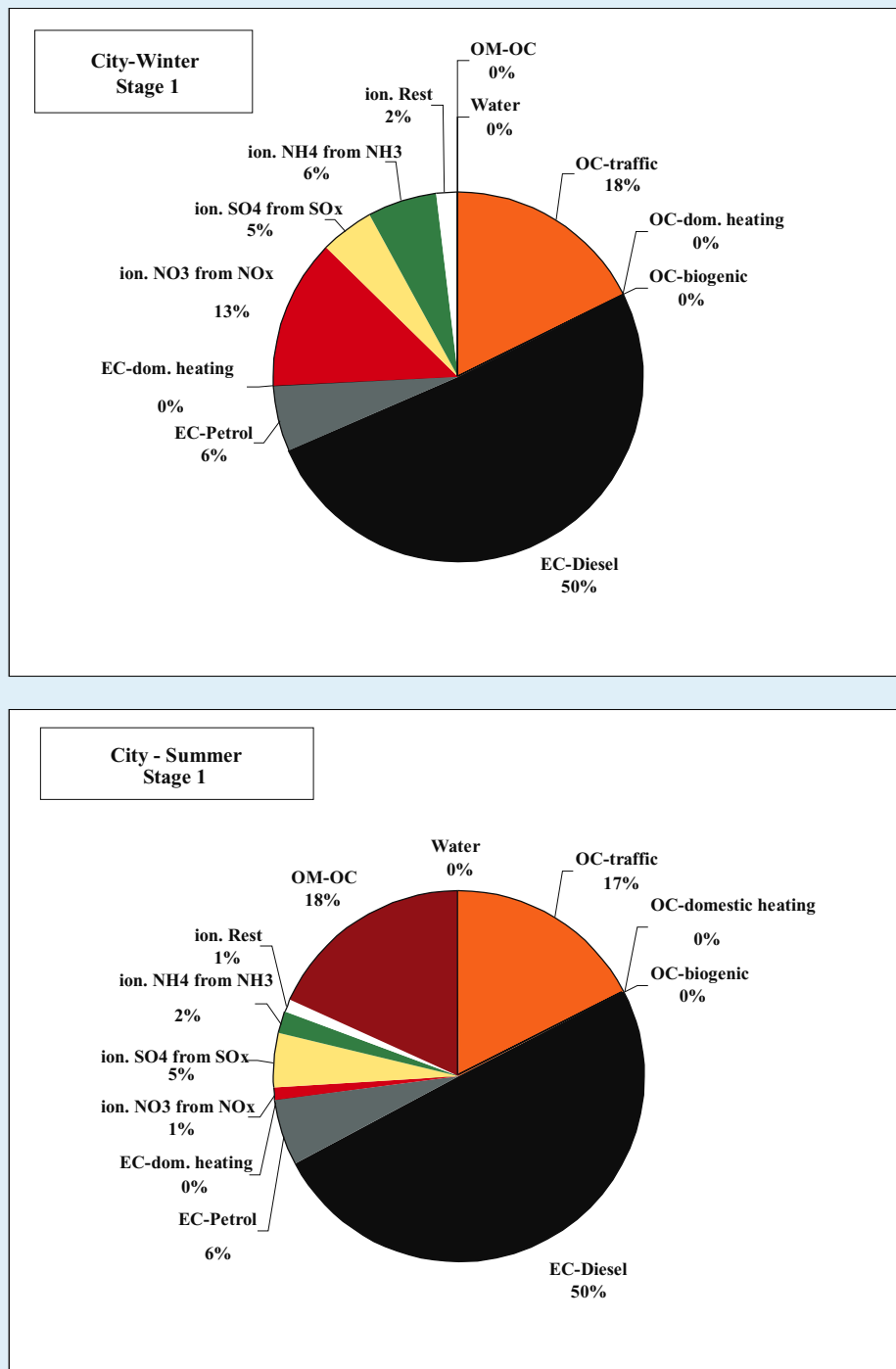


Fig. 2: View of the BERNER impactor at the measuring point in the Leipzig city at the cross road "Am Hallischen Tor" near the main station.

stage	mass concentration		minimum [%]	maximum [%]	standard deviation [%]	variation coefficient [%]
	$\mu\text{g m}^{-3}$	[%]				
1	1.31	(6)	3	15	4.6	77
2	4.27	(21)	16	24	3.3	16
3	10.38	(51)	43	57	5.1	10
4	4.85	(22)	17	27	4.1	10

Tab. 2: Mean values of the particle mass distribution on the four impactor stages.



**Fig. 3:** Estimated origin of particulate matter at the mainly traffic influenced measuring point in the city of Leipzig in the two periods of the project on stage 1 of the impactor.

### Stage 2 particles (140 – 420 nm)

These particles are older than the smaller ones and therefore aerosol import into the measurement region begins to play a role. During winter at IfT and in Melpitz the emissions from individual heating systems and from power plants are responsible for the main part of the EC/OC content, not traffic emissions. In the summer at all

sites, submicrometer crustal material and oxidized organic carbon represent 7 to 23% of mass.

The nitrate fraction during winter was between 18 and 21% of the stage mass whereas for sulfate only 8 to 10% was measured. In the summer campaign for nitrate 5-6% and for sulfate 16 to 25% were observed. The water content was estimated to 10% of the mass.

**Stage 3 particles (0.42 – 1.2 μm)**

About 51% of the mass was found on this stage, on which the ionic components dominate (33 – 55%). The winter carbon fraction was found between 31 and 14% dominated by traffic only at the city measuring point. The total carbon amount measured at these particle sizes decreased to 31 – 14% in comparison to smaller particles

(stage 1: 88-49%, stage 2: 58-29%). At the other sites the household emissions and the long range transport from power plants dominate (Fig. 4). During summer 5 to 6% of the mass on this stage are of biogenic origin. Following the results of McInnes et al. (1996) the water content was estimated to 20% of mass. Crustal material reaches 22 – 25% of the mass during the summer.

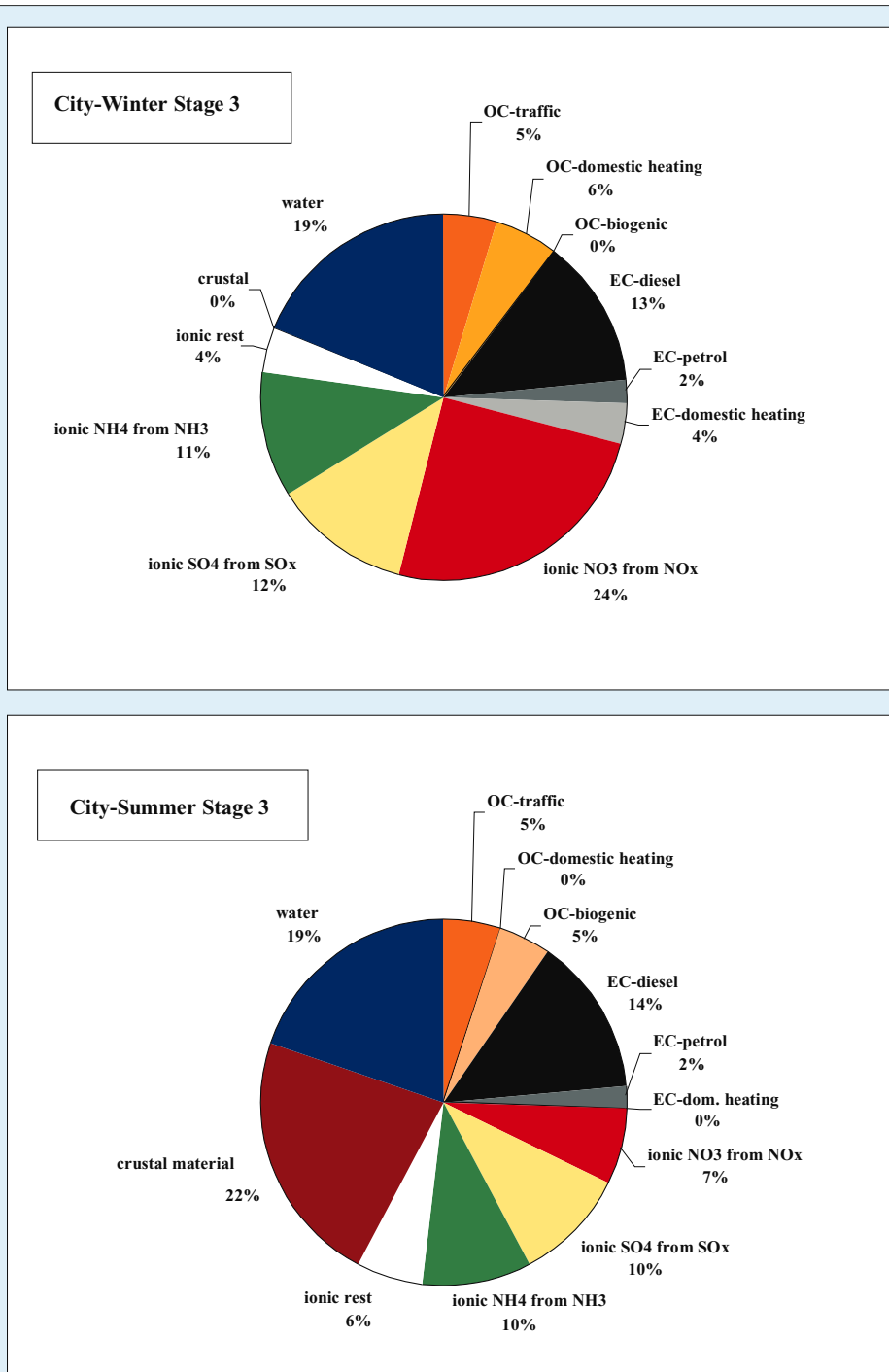


**Fig. 4:** Estimated origin of particulate matter at the mainly traffic influenced measuring point in the city of Leipzig in the both periods of the project at the mass rich stage 3 of the impactor.



### Stage 4 particles (1.2 – 3.5 $\mu\text{m}$ )

Aged particles and larger primary particles (sea salt, crustal material) dominate here. About 22% of the total mass was found on this stage. The mass concentration decreases in winter and summer from the city via the institute to Melpitz but the differences are small. The carbon fraction decreased to a minimum (23 – 13% of mass). Considering metal concentrations the origin of most particles was estimated as re-suspension of crustal material which is modified anthropogenically (e.g. tire abrasion). Their summer content reaches 29 – 35% of stage mass. The ionic concentration was quantified to 26 – 35% of mass in summer and during the winter campaign to 40 – 51% of mass. According to the content of ionic and crustal material the water content was estimated to 20% of the mass. In the summer the content of biogenic material was found to be between 6 and 8% of the mass.

#### Comparison of impactor and filter sampler

For filter sampling quartz fibre filters (Munktell, MK 360) have been used. During the winter measurements both methods have shown good conformity with some exceptions for the cations

ammonium, potassium and calcium. These ions were overestimated by the filter sampling method. The results are currently analyzed further. For ammonium the uptake of gaseous ammonia is enhanced because the winter aerosol is more acidic.

During the summer campaign the main differences were found for nitrate and chloride. The filter samples showed less nitrate and more chloride than the impactor samples. Depending on the temperature nitrate loss from quartz fibre filters was observed.

#### Group-specific results

##### Ionic components

Significant changes have been observed between winter and summer periods. Whereas the nitrate is the dominant ion during the winter in summer sulfate is the main ion in all samples. The ionic content decreases significantly from winter to summer, in mass concentration and mass percentage.

The history of the air mass is important for the ionic content of the PM because main parts of the ionic components result from particles transported over long distances. In Fig. 5 the differences are demonstrated.

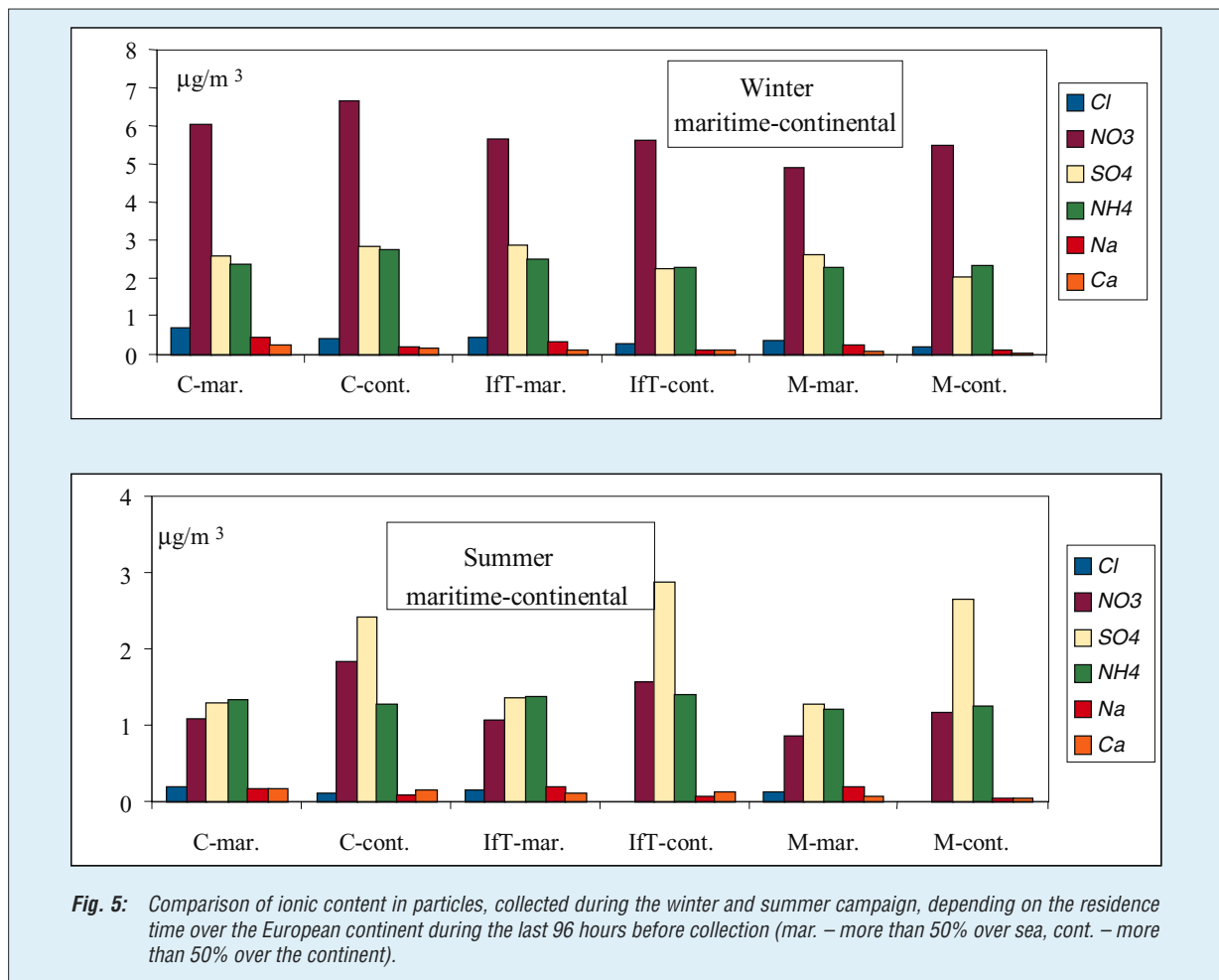


**Fig. 5:** Comparison of ionic content in particles, collected during the winter and summer campaign, depending on the residence time over the European continent during the last 96 hours before collection (mar. – more than 50% over sea, cont. – more than 50% over the continent).

OC-EC analyses

Source assignments of carbonaceous aerosol particles

Based on the following assumptions the calculations of source assignment were performed.

- 1) Traffic emissions were supposed to be nearly constant throughout the year (no seasonal variation)
- 2) TC of the fine particles on stage 1 at the city station B was supposed to originate entirely from traffic emissions. In this case the OC/EC ratio (mean value = 0.34) is set to be typically for pure traffic exhaust particles.

The carbon content of particles as a fraction of the stage mass decreases with increasing particle size. On the smallest stage of the impactor the differences between winter and summer are very small. With increasing particle diameter differences between summer and winter were observed depending on output from households - mainly stages 2 and 3 - and biogenic emissions -mainly stage 4 (Fig. 6).

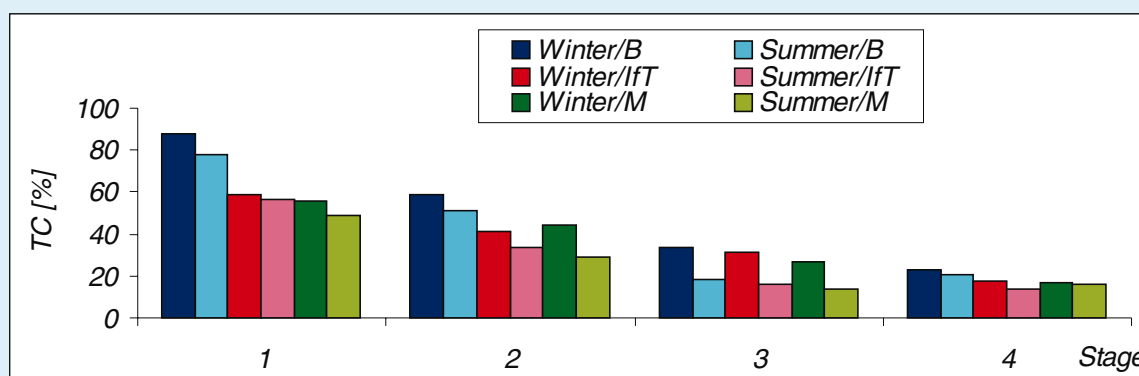


Fig. 6: Total carbon concentration related to the stage mass of the impactor (mean values).

- 3) TC parts on the higher impactor stages were assumed to be composed of

Winter: EC = part of aged traffic emissions, part of domestic heating (lignite fires)

OC = part of aged traffic emissions, part of domestic heating (lignite fires)

Summer: EC = aged traffic emission particles, i.e. EC(summer) = EC(traffic)

OC = part of aged traffic emissions, part of biogenic emissions.

- 4) Diesel vehicles were found to produce about 90% of mass of the traffic particle emission in Saxony (Gerike et al., 2000).
- 5) In the summertime the mixing layer height (MLH) is believed to be roughly twice as high during wintertime. Performing winter/summer comparisons a normalization to the same MLH is required, therefore MLH was reduced to 50% by doubling summer concentration values.

Calculations of the traffic contributions of OC and EC (segregated in diesel and gasoline part), domestic heating and biogenic emissions were performed for each stage.

Individual organic species

The analysis of samples was performed for polyaromatic hydrocarbons (PAH), selected oxy-PAH and the n-alkanes (C<sub>20</sub>-C<sub>32</sub>).

Some important results are:

1. PAH have their origin mainly in the individual heating by coal burning processes (about 80%) during the winter. The winter concentrations are typically much higher than in summer at all sampling stations. The differences between the three locations were small during wintertime whereas in the summer campaign a strong decrease of PAH concentrations was observed from the city via the IfT to Melpitz (Tab. 3).
2. During the winter period the PAH had their highest concentrations on stages 2 and 3 (household heating) – during the summer on stage 1 (traffic emission).
3. The alkanes had their origin during the winter mainly from burning processes. During summer they are of biological origin indicated by the  $CPI_{odd}$  on impactor stages 3 and 4 in the range of three to six ( $CPI$  - carbon preference index =  $c_{odd}/c_{even}$ ).



sampling station	Winter PAH [ng m <sup>-3</sup> ]	Summer PAH [ng m <sup>-3</sup> ]
Leipzig City	16.41	2.82
IfT	15.56	0.49
Melpitz	15.51	0.13

**Tab. 3:** Comparison of measured PAH mass concentration at all sampling points for both seasons (PM<sub>2.5</sub>-filters).

## Summary

Reflecting the specific regional source structure, the most important sources of particulate matter have been identified for four particle size classes in a winter and a summer period. The meteorological situation during both periods was not typical for the region with a very mild winter with good exchange conditions. The summer measurement period in July was untypically cold. During none of the

periods days with continental air masses from the East could be observed, showing higher particle mass concentrations in the past (K. Müller, 1999). An extrapolation of the data to the PM<sub>10</sub> standard of the European Union shows that the compliance to this standard will be problematical in Saxonian cities. The most important anthropogenic sources of small particles are traffic and household emissions.

## References

- McInnes, L. M., Quinn, P. K., Covert, D. S. and Anderson, T. L. 1996:** Gravimetric analysis, ionic composition, and associated water mass of the marine aerosol. *Atmos. Environ.*, 30, 869-884.
- Müller, K. 1999:** A 3 year study of the aerosol in northwest Saxony (Germany). *Atmos. Environ.*, 33, 1679-1685.
- Gerike, R., F. Zimmermann, V. Eichmann und U. Becker 2000:** Dynamisiertes Emissionskataster für Sachsen, Phase II. Untersuchungen im Auftrag des Institutes für Troposphärenforschung Leipzig an der Technischen Universität Dresden, Institut für Verkehrsplanung und Straßenverkehr, Lehrstuhl für Verkehrsökologie) Auftr.Nr.: IfT, 160104/80 (Endbericht) 115 Seiten

### Funding

- Sächsisches Landesamt für Umwelt und Geologie Dresden

### Cooperation

- Umweltforschungszentrum Leipzig – Halle GmbH



## Multiphase modeling and laboratory studies

Barbara Ervens, Diana Weise, Arno Walter, Johannes Hesper, Andreas Donati, Paolo Barzaghi, Hartmut Herrmann, Ralf Wolke, Oswald Knoth, Sabine Reutgen.

### Introduction

Multiphase processes, such as the uptake of gases and radicals by clouds or the production of gas phase halogenes from particulate halides, are of increasing importance for the understanding of tropospheric multiphase system. Phase transfer and chemical reactions modify the concentrations of trace gases and oxidants in either phase.

Whereas gas phase chemistry is currently described in very detailed models, many uncertainties exist with regards to the importance of the chemistry within the tropospheric particle phase. Therefore, further mechanism development is needed to complete mechanisms describing aqueous phase chemistry. At the current state of multiphase model development the mechanism CAPRAM (**C**hemical **a**queous **p**hase **r**adical **m**echanism) includes one of the most detailed descriptions of organic chemistry and radical processes within clouds. The correct formulation of chemical processes should be based on laboratory studies. To have a good basis for the estimation of unknown parameters systematic investigations in the laboratory are necessary leading to correlations between kinetic and extrakinetic data. The selection of investigated reactions should be directed to findings from field measurements where chemical compounds are identified. Therefore, further versions and extensions of the existing multiphase mechanism CAPRAM2.3/RACM (Herrmann *et al.*, 2000) were developed. Because it became evident that there is a lack of kinetic input parameters with regards to higher organic compounds, laboratory studies were performed to provide reliable input parameters for a proper formulation of processes in the mechanism.

The objective of the present work is the development of a cloud module which combines a complex multiphase chemistry with detailed microphysics. The description of both components should be given for a high resolution drop spectrum. Several numerical approaches for treating such processes have been investigated (Wolke and Knoth, 2000a, Wolke *et al.*, 2000). The droplets are subdivided into several classes. This decomposition of the droplet spectrum into classes is based on their droplet size and the amount of scavenged material inside the drops, respectively. The model equations resulting from such multiphase chemical systems

are nonlinear, highly coupled and extremely stiff. The very fast dissociations in the aqueous phase chemistry are treated as forward and backward reactions. The aqueous phase and gas phase chemistry, the mass transfer between the different droplet classes, among drops of the same class and with the gas phase are integrated in an implicit and coupled manner by the second order Backward Differential Formula (BDF) method. For this part a modification of the code LSODE (Hindmarsh, 1983) with special linear system solvers was used. These direct sparse techniques exploit the special block structure of the corresponding Jacobian. Furthermore, we utilize an approximate matrix factorization which decouples multiphase chemistry and microphysical exchange processes of liquid water (e.g., by aggregation, break up, condensation) at the linear algebra level. The sparse Jacobians are generated explicitly and stored in a sparse form. The efficiency and accuracy of our time integration schemes is discussed for three versions of the CAPRAM mechanism and for a different number of droplet classes.

### Mechanism development and model results

#### CAPRAM2.4 (MODAC mechanism)

Based on the former version of CAPRAM, version 2.3, the aqueous phase mechanism was evaluated and extended checking all kinetic parameters and – if more sufficient data were available – replacing them after evaluation of experimental studies. The updated version, called CAPRAM2.4 (MODAC mechanism) represents a model containing most recent findings on reaction patterns and kinetic data in the liquid phase. In comparison to the former version essential changes occur in the chemistry of transition metal ions (TMI), considering reactions of iron, manganese and copper ions. In both versions of CAPRAM the most detailed part is the chemistry of organic compounds considering not only C<sub>1</sub> organics as in other aqueous phase mechanisms known from literature but also reactions of the C<sub>2</sub> alcohols, aldehydes, carboxylic acids and peroxy radicals. Within the update the oxidation of organics by the radicals and radical anions X (OH, NO<sub>3</sub>, SO<sub>4</sub><sup>-</sup>, SO<sub>5</sub><sup>-</sup>, Cl<sub>2</sub><sup>-</sup>, Br<sub>2</sub><sup>-</sup> and CO<sub>3</sub><sup>-</sup>) is implemented explicitly including all alkyl and peroxy radicals. Furthermore the detailed oxidation of glyoxal, glyoxylic acid and oxalate by radicals and radical anions (OH, NO<sub>3</sub>, SO<sub>4</sub><sup>-</sup>, Cl<sub>2</sub><sup>-</sup>, Br<sub>2</sub><sup>-</sup>, CO<sub>3</sub><sup>-</sup>) was added. So the number



of reactions in this part was increased from 50 to 110 processes. The uptake of glyoxal linking its chemistry to the gas phase and its further hydration was included. The sulfur chemistry considering the reactions of  $\text{SO}_x^-$  radical anions ( $x = 3, 4, 5$ ) consists of 43 reactions. Here the essential extension was a split of  $\text{HMS}^-$  oxidation into elementary steps. 34 reactions of the  $\text{HO}_x^-$ -radicals ( $\text{OH}$  and  $\text{HO}_2$ ) and transition metal ions ( $\text{Cu}^{+/2+}$ ,  $\text{Fe}^{2+/3+}$ ,  $\text{Mn}^{2+/3+}$ ) are considered. Because many reactions of the ferryl ion ( $\text{FeO}^{2+}$ ) and the dynamic behavior of several manganese species was implemented here the number was extended to 59 reactions. 25 reactions of the nitrogen chemistry are implemented including reactions of the  $\text{NO}_3$  radical. This part was further completed with six additional or split reaction pathways. The halogen chemistry ( $\text{Cl}_2^-/\text{Br}_2^-$ ) and the carbonate chemistry ( $\text{CO}_3^-$ ) was changed only in some few points (2, 3 and 4 processes added, respectively). In the updated version the photolysis processes of  $[\text{Fe}(\text{C}_2\text{O}_4)_2]^-$ ,  $[\text{Fe}(\text{C}_2\text{O}_4)_3]^{3-}$ ,  $\text{NO}_3$  (assumed to be the same as in the gas phase) and  $\text{CH}_3\text{OOH}$  were added.

Because of the changes within the revision of CAPRAM2.3 to CAPRAM2.4 (MODAC mechanism) in the description of the transition metal chemistry the concentration levels of the  $\text{HO}_x^-$ -radicals ( $\text{OH}$  and  $\text{HO}_2$ ) are influenced. With CAPRAM2.4 (MODAC mechanism) a time dependent redox cycling of

the concentration levels of iron can be modeled, so that during night more iron(III) is present and during day the iron(III) complexes are photolysed forming iron(II).

In CAPRAM2.4 (MODAC mechanism) the total S(IV) is oxidized within a few hours of simulation by hydrogen peroxide in agreement with findings from other model studies (e.g., Warneck, 1999). This is due to three different effects: (1) The direct oxidation of copper by oxygen leads to a high  $\text{O}_2^-/\text{HO}_2$  concentration. These species form  $\text{H}_2\text{O}_2$  by reactions with  $\text{Fe}^{2+}/\text{Cu}^+$ . (2) The change of the Henry's Law constant for formaldehyde causes an increase of the  $\text{OH}$  concentration because  $\text{HCHO}$  can act as a very effective sink for  $\text{OH}$  leading also to an enhanced  $\text{HO}_2$  concentration. (3) Due to the consideration of the iron-oxalato-complexes a significant fraction of the iron exists in a complexed form: under urban conditions the concentration of the mono-oxalato-complex is about  $10^{-6}$  M (20% of the total iron). So, less  $\text{Fe}(\text{II})$  being an important sink for hydrogen peroxide is available. In total, all these effects lead to a higher  $\text{H}_2\text{O}_2$  concentration (a factor of 2 during day, and even a factor of 100 during night) compared to CAPRAM2.3 so that radical pathways of the sulfur oxidation formerly having more importance in CAPRAM2.3 are compensated.

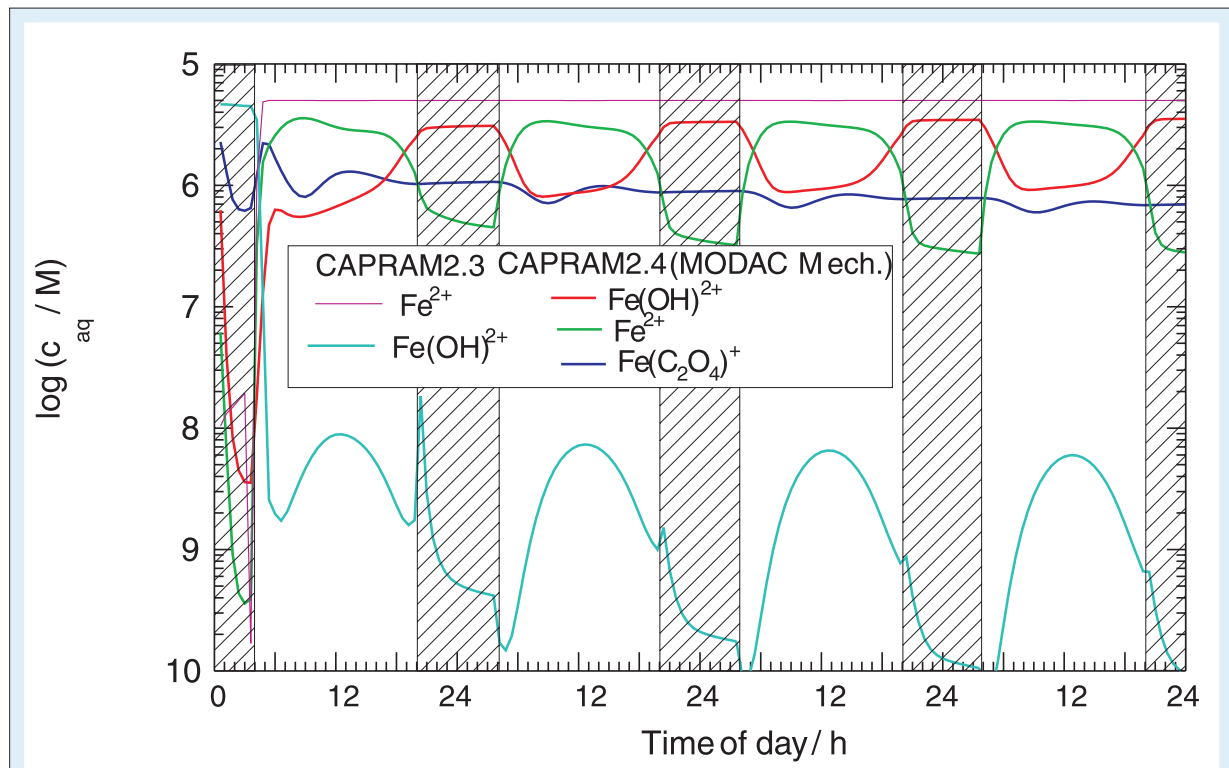


Fig. 1: Comparison of the concentration levels of Fe(II) and Fe(III) in CAPRAM2.3 and CAPRAM2.4 (MODAC-mechanism).

The C<sub>2</sub> organic chemistry was further completed considering the difunctional C<sub>2</sub> compounds glyoxal, oxalate/ oxalic acid and glyoxylic acid. The chemistry of glyoxal in the gas phase is restricted to the formation mainly by peroxy radicals from aromatics and the photolysis and the reaction with OH and NO<sub>3</sub> as loss processes. The latter two processes are very slow so that glyoxal accumulates during night if uptake and further aqueous processes are not considered. It could be shown that these species are oxidized very effectively in the aqueous phase forming glyoxylic acid and oxalate. In the urban case after three days of simulation maximum concentrations for CH(OH)<sub>2</sub>CH(OH)<sub>2(aq)</sub>, CH(OH)<sub>2</sub>COOH<sub>(aq)</sub> and HC<sub>2</sub>O<sub>4</sub><sup>-</sup> of 4·10<sup>-8</sup> M, 4·10<sup>-8</sup> M and 3·10<sup>-8</sup> M, respectively, can be found. It is interesting to note that the oxalate concentration is independent of the fact whether an initial concentration for oxalate (estimated equal to iron) is used or not. So, it can be concluded that oxalate may be formed indirectly from the aromatics oxidation in the gas phase. This could be a hint to explain high oxalate concentrations found in particles in field measurements (Neusüß *et al.*, 2000).

To give a more realistic picture of cloud chemistry, emissions and depositions were implemented to the box model. The total oxidation of initialized species (e. g. SO<sub>2</sub>, NO<sub>x</sub>, ozone, organics) in the box is avoided permitting the renewal of the trace gases in the box and keeping the concentration levels of these species more or less constant during the whole simulation time. If emissions are considered as additional sources several reaction patterns discussed before are changed: e.g., the concentration of the OH<sub>(aq)</sub> radical is decreased from 1.2·10<sup>-12</sup> M to 2·10<sup>-14</sup> M in the urban case after 36 h hours of simulation. On the one hand many organics are emitted consuming OH in the gas phase; formaldehyde gains in importance as sink species in the aqueous phase (with emissions 47% of 4.9·10<sup>-6</sup> M s<sup>-1</sup>; without emissions 19% of 1.9·10<sup>-8</sup> M s<sup>-1</sup>). On the other hand the relatively high emission of SO<sub>2</sub> and the additional source of formaldehyde lead to significant concentrations of the HMS<sup>-</sup> complex being also an efficient sink species for OH.

#### **CAPRAM2.4 (MODAC mechanism)-reduced**

A reduced version of the mechanism was developed to facilitate the use in higher scale models. The basis of the reduction was the output of CAPRAM2.4 (MODAC-mechanism) considering emissions/depositions. Species were selected for which the concentrations should be equal (± 5%) in the reduced scheme compared to the complete scheme: OH, S(IV), NO<sub>x</sub> (= NO + NO<sub>2</sub>), NO<sub>3</sub>, H<sub>2</sub>O<sub>2</sub>, O<sub>3</sub> and H<sup>+</sup>. The criteria for removing processes

were contributions of < 1% to the total production / loss of the target species at t = 36 h and t = 48 h. The removed processes were investigated and such processes were resumed which were either links between acids and their anion or the only sink for a species or essentially for CAPRAM2.4 (e.g. oxidation of C<sub>2</sub> species). Finally the number of aqueous phase reactions was reduced from 409 to 183, one phase transfer process was also removed. The number of species in CAPRAM2.4 (MODAC mechanism)-reduced is 195 instead of 225. In the reduced version of the mechanism no chemical processes of manganese containing species and none of the carbonate radical anion are included anymore, because the fluxes of their reactions are so small that they do not influence the concentration levels of the target species. An important evidence is the fact that the oxidation of organics can largely be described by the reactions of OH only; the contributions of the oxidation by other radicals/radical anions (NO<sub>3</sub>, SO<sub>4</sub><sup>-</sup>, Cl<sub>2</sub><sup>-</sup>, Br<sub>2</sub><sup>-</sup>, SO<sub>5</sub><sup>-</sup> and CO<sub>3</sub><sup>-</sup>) are negligible.

#### **Extension of the organic chemistry**

It is known from analytical studies of field measurements that within tropospheric clouds and aerosols many higher hydrocarbons beyond C<sub>2</sub> from biogenic and anthropogenic sources exist: Besides the class of dicarboxylic acids (oxalic, malonic and succinic acid) found in cloud water or aerosol samples gas phase measurements of water soluble C<sub>3</sub> species are available (e.g., ketones, aldehydes). Consequently the organic chemistry in CAPRAM surely represents one of the most incomplete part of the mechanism. The kinetic data of reactions of C<sub>3</sub> and C<sub>4</sub> organic compounds determined in the laboratory studies (see section there) were implemented directly in an extension to CAPRAM2.4 (MODAC mechanism)-reduced. In total this extension includes 70 additional processes describing the explicit oxidation of C<sub>3</sub>- and C<sub>4</sub> organic compounds.

The results with this extended mechanism clarify that, dependent on the scenario, the C<sub>3</sub>-organics (mainly propanol) can have essential contributions to the decay of the OH-radical in the aqueous phase. Consequently in common aqueous phase mechanisms the concentration level of OH is overestimated significantly, because its main sinks are reactions with organics. Furthermore, chemical sink processes for dicarboxylic acids (oxalic/ malonic/ succinic acid and their anions) are included describing possibly formation and sink processes of these species which are found in high concentrations in aerosol samples. Model calculations with this extended version of CAPRAM2.4 (MODAC mechanism)-reduced give hints that chemical processes in clouds can modify



the composition of the organic fraction in the particle phase in such a way that the composition of the organic carbon, e.g., the accumulation of dicarboxylic acids or pyruvic acid / pyruvat, found in aerosol samples can at least partly be explained by chemical processes in clouds.

### Aromatic module

Whereas in the gas phase mechanism RACM the oxidation of some aromatic compounds is considered, the corresponding reaction patterns in the aqueous phase are not known. Although the kinetic data for the loss processes of aromatics by radicals are available, they are not included in models for cloud chemistry so far. It is known that aromatics appertaining to the VOCs are important for ozone formation. It could be shown that in polluted scenarios (initial concentrations of aromatics: 10 ppb) the oxidation processes of aromatics within the aqueous phase can lead to an essential increase of the  $\text{HO}_{2(\text{aq})}$ -concentration (+ 23%) because of the high solubility of the OH- substituted aromatics phenol and cresols. Furthermore the nitration of aromatics in the aqueous phase was included in the extended aromatic module considering the effective formation of toxic nitrophenols in clouds.

### Halogen module

The extension of CAPRAM2.3 describing halogen activation under marine and urban conditions was further developed showing that in tropospheric clouds halides can be activated leading to the formation of  $\text{X}_2$ ,  $\text{XNO}_2$  or  $\text{HOX}$  ( $\text{X} = \text{Br}$  or  $\text{Cl}$ ) which evaporate to the gas phase where they are photolysed into halogen atoms influencing the ozone budget. Compared to other mechanisms (e.g., Sander and Crutzen, 1996) describing marine halogen activation from sea salt aerosols CAPRAM2.3+Marine was initialized for cloud conditions (low ionic strengths, low pH and high liquid water content was assumed). It could be shown that under these conditions radical reactions within tropospheric clouds can cause halogen production resulting in halogen atom concentrations of  $10^6 \text{ cm}^{-3}$  ( $\text{Cl}$ ) and  $10^3 \text{ cm}^{-3}$  ( $\text{Br}$ ). The halogen module was developed further and more radical processes are considered and more detailed sink reaction paths for the species considered are added. But also uncertainties became evident describing certain processes sufficiently which are possibly important (e.g.,  $\text{BrCl}$ ). Further development is underway.

### Laboratory studies

When reducing chemical mechanisms it became evident that organic oxidation processes can in general be described by reaction of OH. Higher organics ( $> \text{C}_2$ ) have not been treated in aqueous phase models up to now because of the lack of kinetic (temperature dependent) input parameters. To obtain these parameter for the extension of the reaction scheme, laboratory studies have been performed to gain better insight into chemical conversions in clouds and wet tropospheric particles.

species	$k_{25^\circ\text{C}} / \text{M}^{-1} \text{s}^{-1}$	$E_A / \text{kJ mol}^{-1}$
formate	$2,4 \cdot 10^9$	$9 \pm 5$
tert-Butanol	$4,3 \cdot 10^9$	$10 \pm 3$
oxalate <sup>1)</sup>	$1,9 \cdot 10^8$	$23 \pm 4$
oxalate <sup>2)</sup>	$1,6 \cdot 10^8$	$36 \pm 10$
acetaldehyd <sup>3)</sup>	$7 \cdot 10^9$	--
ethanol	$2,1 \cdot 10^9$	$10 \pm 5$
glyoxylic acid	$3,6 \cdot 10^8$	$8 \pm 3$
glyoxylate	$2,6 \cdot 10^9$	$36 \pm 8$
1-propanol	$3,2 \cdot 10^9$	$8 \pm 6$
propionic acid	$3,2 \cdot 10^8$	$19 \pm 8$
propionate	$7,2 \cdot 10^8$	$15 \pm 4$
acetone	$9,0 \cdot 10^7$	$15 \pm 10$
methylglyoxal	$1,1 \cdot 10^9$	$13 \pm 6$
pyruvic acid	$1,2 \cdot 10^7$	$23 \pm 4$
pyruvate	$7,0 \cdot 10^8$	$19 \pm 4$
malonate <sup>1)</sup>	$6,0 \cdot 10^7$	$11 \pm 5$
succinic acid	$1,1 \cdot 10^8$	$11 \pm 6$
succinate <sup>2)</sup>	$5,0 \cdot 10^8$	$11 \pm 5$
<sup>1)</sup> monoanion	<sup>2)</sup> dianion	<sup>3)</sup> $k_{10^\circ\text{C}}$

Tab. 1: Reaction rates and activation energies of reactions of the OH-radical in aqueous.

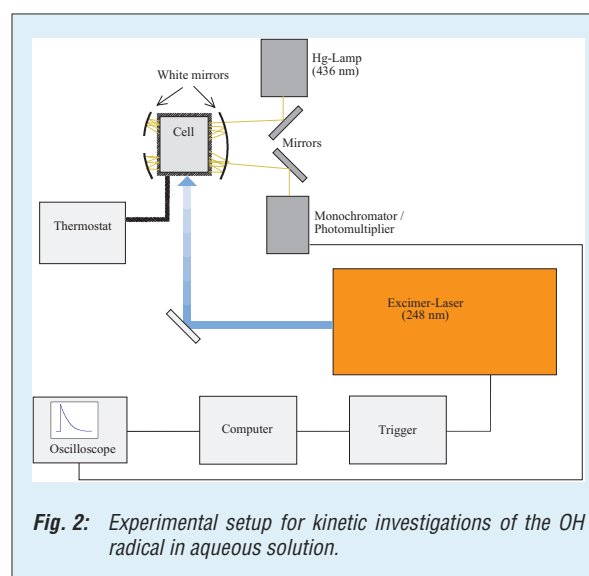


Fig. 2: Experimental setup for kinetic investigations of the OH radical in aqueous solution.

The kinetic experiments were performed with a laser-photolysis-long-path-absorption set-up. The investigations of reactions of the OH radical were performed by competition kinetics with (SCN)<sub>2</sub><sup>-</sup> as reference substance. The temperature dependence of the reference reaction was characterized to develop a reliable basis for further investigations with this method.

On the one hand processes of C<sub>2</sub> organic compounds were investigated for which no temperature dependence in CAPRAM2.4 (MODAC mechanism) is included, on the other hand reactants with three and four carbon atoms were selected being possibly important in the tropospheric multiphase system. The kinetic data investigated are summarized in Tab. 1. These data were implemented directly extending the organic chemistry in CAPRAM2.4 (MODAC-mechanism)-reduced.

It is assumed that reactions between organics and the OH radical take place via an abstraction of the weakest bonded hydrogen atom. After Evans and Polanyi (1938) correlation exists between the bond dissociation energy (BDE) and the activation energy (E<sub>A</sub>) for a given type of chemical reaction. Based on the data measured and additional literature data such correlation could be found.

With the equations obtained the activation parameters and reaction rates for reactions of the OH radical with similar reactants can be estimated and implemented into models to further complete the organic part of the mechanism.

## Size-resolved simulations

### Model formulation

In the real atmosphere, multiphase chemistry is in close interaction with microphysical cloud processes. These essential interchange effects have to be taken into consideration also for the development of numerical techniques for more complex models. As a first step, the present

work focuses on the treatment of the multiphase chemistry for a size-resolved droplet spectrum in a box model (one "grid cell" of an Eulerian grid model). The droplets are segregated into *M* classes. This decomposition of the droplet spectrum into classes is based on their droplet size and the amount of scavenged material inside the drops. We assume that the size distribution and all other microphysical parameters are given a priori by a microphysical cloud model. In each of the *M* droplet classes, *N<sub>A</sub>* aqueous phase species are considered. Some of these aqueous phase species interact with one of the *N<sub>G</sub>* gas phase species. Note that the number of species in the gas phase must not be necessarily the same as the number of aqueous species which occur in all droplet classes.

In a box model the multiphase chemical processes can be described by the system of mass balance equations (1) and (2), where *L<sub>k</sub>* denotes the volume fraction [*V<sub>k</sub>* / *V<sub>box</sub>*] of the *k*-th droplet class inside the box volume. The vectors *c<sup>k</sup>*, *k*=1,...,*M*, are the liquid-phase concentrations of the species in the *k*-th liquid water fraction and the vector *c<sup>G</sup>* stands for the concentrations of the gas phase species. The chemical reaction terms are denoted by *R<sup>G</sup>* and *R<sup>k</sup>*. The second term on the right hand side describes the interchange between the gas and aqueous phases. It will be referred to as Henry term in the following. The indicator *κ<sub>k</sub>* is equal to 1 if the species is soluble. In the other cases, the Henry term will be dropped in both equations. The term *T* in (2) stands for the mass transfer between different droplet classes by microphysical exchange processes of liquid water (e.g., by aggregation, break up, condensation). The *Q* terms are time-dependent natural and anthropogenic emissions. The velocities for dry and wet deposition are denoted by *v<sub>D</sub>*. The interchange between the gas and liquid phases is specified by the Schwartz approach (Schwartz, 1986). The value *H<sub>l</sub>* denotes Henry's law coefficient for the *l*-th species. The

$$\frac{dc_{l^*}^G}{dt} = R_{l^*}^G(t, c_1^G, \dots, c_{N_G}^G) - \kappa_l \sum_k L_k \cdot k_t^{kl} \cdot \left[ c_{l^*}^G - \frac{c_l^k}{H_l} \right] + Q_{l^*}^G - v_D^G c_{l^*}^G \quad (1)$$

$$\begin{aligned} \frac{d(L_k c_l^k)}{dt} &= L^k \cdot R_l^A(t, c_1^k, \dots, c_{N_A}^k) + \kappa_l \cdot L_k \cdot k_t^{kl} \cdot \left[ c_{l^*}^G - \frac{c_l^k}{H_l} \right] \\ &+ T(L_1 c_l^1, \dots, L_M c_l^M) + Q_l^k - v_D^k L_k c_l^k, \end{aligned} \quad (2)$$

$$l^* = 1, \dots, N_G; \quad l = 1, \dots, N_A; \quad k = 1, \dots, M,$$



mechanism	number of species			number of reactions				
	total	gas	aqua	total	gaseous	Henry	disso	aqueous
CAPRAM2.3	162	82	80	508	237	34	27	210
CAPRAM2.4	220	83	137	654	237	34	55	328
CAP2.4_Reduced	195	83	107	416	237	33	37	109

**Tab. 2:** Characteristics of the CAPRAM2.3, CAPRAM2.4 and the reduced CAPRAM2.4 mechanisms.

mass transfer coefficient depends on the droplet size, the gas diffusion coefficient, the molecular speed and the mass accommodation coefficient of the  $l$ -th species.

From the microphysical point of view the exchange of liquid water between droplet classes by aggregation and break up, for instance, takes place on a slower time scale than the aqueous phase chemistry and the phase interactions. The liquid water fluxes transport the corresponding fractions of all included aqueous phase species into other classes. In the ODE system (1), (2) the species within one class are coupled through the chemical reaction system. Furthermore, two types of coupling between different droplet classes can be identified. First, the aqueous phase species within different classes interact directly by the exchange term  $T$ . Additionally, they are indirectly coupled via the gas phase by the phase interchange described by the Henry term.

The chemistry in the aqueous phase differs from the gas phase chemistry by the occurrence of fast dissociations in equilibria. In our approach these fast dissociations are considered as forward and backward reactions. Most of the dissociations

include  $H^+$  or  $OH^-$  ions. Therefore the behavior of the system depends very strongly on the underlying pH value. In contrast to other authors (e.g., Chaumerliac et al., 2000), the pH value is not prescribed a priori. The  $H^+$  concentration as part of the chemical system is computed for each droplet class dynamically.

In our implementation, the modification or substitution of the chemical reaction system (gas and aqueous phases, phase transfer according to Schwartz) can be done very easily, because the mechanism is read from a file. The syntax to describe the system is very easy and allows large flexibility. For our tests three different versions of the CAPRAM mechanism are used, see above. Typical characteristics of these mechanisms are given in Tab. 2.

### Numerical Method

The main task in an implicit method is the approximate solution of linear systems of the form

$$(I - \beta \Delta t J) \Delta c = b, \quad (3)$$

which involve the Jacobian  $J$  of the right hand

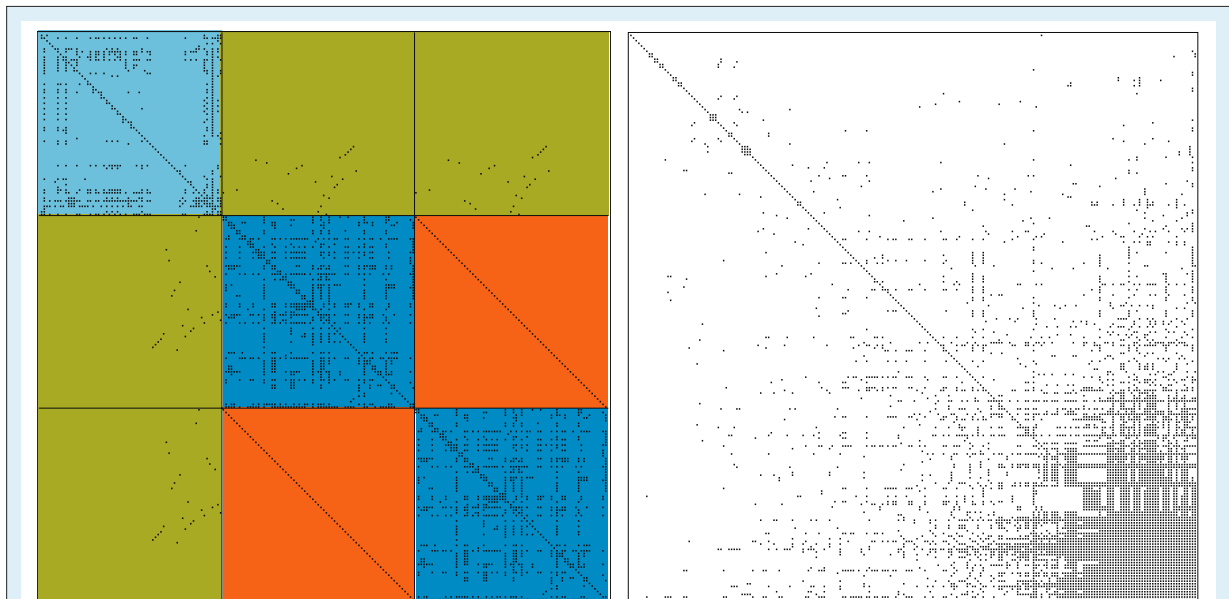


**Fig. 3:** Sparse structure of Jacobian and LU decomposition for CAPRAM2.3 and two droplet classes.

side of the ODE system. For an efficient solution of these systems the properties of the Jacobian (e.g., sparsity, block structure, different types of coupling) have to be utilized. The solution of linear systems during the integration of system (1), (2) is only practicable by applying sparse techniques. In atmospheric gas phase chemistry, the sparse linear system (3) can be solved by linear Gauss-Seidel iterations (Knoth and Wolke, 1995). Unfortunately, for aqueous chemistry mechanisms the Gauss-Seidel iteration converges only slowly or even fails (Wolke and Knoth, 2000b).

The Jacobian structure of the right hand side in system (1), (2) is given in Fig. 3. The blue blocks in the diagonal are the Jacobians of the gas phase and aqueous phase reaction terms, respectively. In our example, the upper left block stems from the gas phase. The other two diagonal blocks coming from the aqueous phase chemistry have the same sparse structure. The green left and upper boundary blocks represent the phase interchange according to Schwartz (1986). The orange diagonal matrices include the coupling terms resulting from the mass transfer between the droplet classes. In the implementation the sparse block matrices are generated explicitly and stored in a sparse form. By utilizing an approximate matrix factorization, the multiphase chemistry part and the part from microphysical exchange processes (e.g., by aggregation, break up) are decoupled at the linear algebra level. The sparse factorization is stored and performed only when the Jacobian  $J$  has to be recalculated. The sparse Jacobians are generated explicitly and stored in a sparse form.

The sparse linear system (3) is solved by a sparse LU decomposition (i.e., a factorization into a lower

and upper triangular matrix) with diagonal pivoting. An optimal order of the pivot elements to avoid fill-in is determined by a diagonal Meis-Markowitz strategy (e.g., Sandu et al., 1996). This strategy is coupled with a approximate matrix factorization approach and adapted to the special structure of the Jacobian (Wolke and Knoth, 2000a). In Fig. 4 the number of operations for the LU decomposition and the CPU times for a 48 hours simulation are presented.

By using this sparse strategy, a linear behavior in the required number of operations is inevitably reached for the three chemical mechanisms. This measure depends only on the dimension of the linear system as well as on the non-zero entries in the Jacobian. On the contrary, the CPU time is markedly influenced by the computation of the reaction constants. Fig. 4 shows that the numerical costs for the reduced CAPRAM2.4 and the CAPRAM2.3 mechanism are comparable. The numerical behavior opens up real possibilities to handle complex multiphase reaction mechanisms within multidimensional models.

### Simulation example

In Fig. 5 an example of the influence of a size-resolved cloud droplet spectrum onto concentration levels is given. These concentration levels for the OH radical are calculated in droplets with radii of 1  $\mu\text{m}$ , 4  $\mu\text{m}$ , 16  $\mu\text{m}$  and 64  $\mu\text{m}$ , respectively. It is evident that the concentration of OH in the droplet decreases with increasing droplet radius due to dilution and changing size of the phase interface. If the uptake in the droplet would be controlled only by the physical solubility the aqueous phase concentration in every droplet class should be

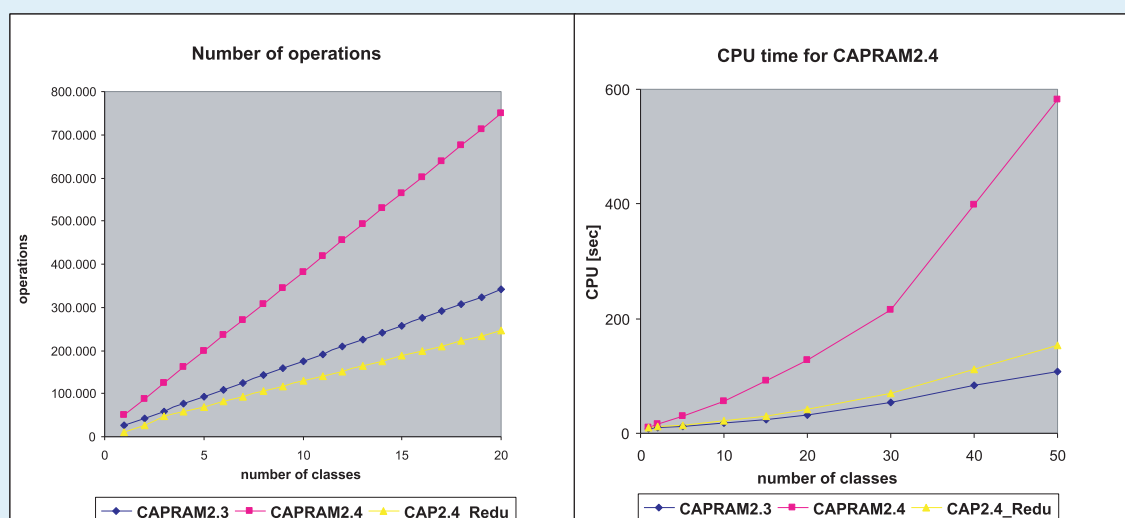
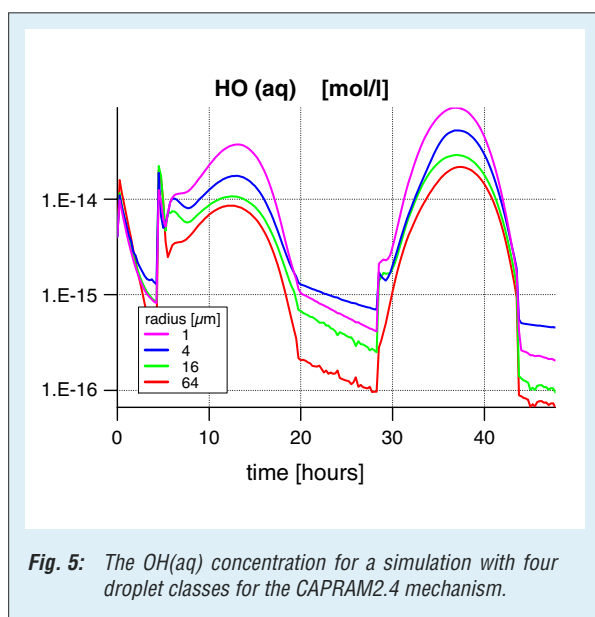


Fig. 4: The number of operations for one LU decomposition and the CPU times for an 48 hours simulation for three mechanisms of different complexity.



**Fig. 5:** The OH(aq) concentration for a simulation with four droplet classes for the CAPRAM2.4 mechanism.

same as predicted by the Henry's Law coefficient. It is interesting to note that there is no exact correlation between the droplet radius and the

concentration of OH in the aqueous phase showing that also the concentrations of precursors and/or sink reactants of OH in both phases are influenced by the variation of the droplet radius. Therefore, it can be concluded that a changing phase surface area between the gas and aqueous phase can lead to different reaction patterns in the multiphase system.

## Conclusion

The treatment of cloud processes requires complex multiphase chemistry mechanisms as well as detailed microphysics. The phase interchange depends strongly on the phase surface area. Therefore, a high resolution drop spectrum has to be considered for an appropriate description of the chemistry in both phases and its coupling. The developed numerical techniques allow the handling of complex multiphase systems also within multidimensional models. Investigations in this direction are underway.

## References

- Chaumerliac, N., Leriche, M. and Audiffren N., 2000.** Modeling of scavenging processes in clouds: Some remaining questions about the partitioning of gases among gas and liquid phases. *Atmos. Res.*, **53**, 29-43.
- Herrmann, H., Ervens, B., Jacobi, H.-W., Wolke, R., Nowacki P., and Zellner, R., 2000:** CAPRAM2.3: A Chemical Aqueous Phase Radical Mechanism for Tropospheric Chemistry. *J. Atm. Chem.*, **36**, 231-84.
- Hindmarsh, A.C., 1983.** *ODEPACK, A systematized collection of ODE solvers.* R.S. Steplman et. al. (Ed.), In *Scientific Computing*. North-Holland, Amsterdam, 55-74.
- Knoth, O. and Wolke, R., 1995.** Numerical methods for the solution of large kinetic systems. *Appl. Num. Math.*, **18**, 211-221.
- Schwartz S.E., 1986.** *Mass transport considerations pertinent to aqueous phase reactions of gases in liquid water clouds.* W. Jaeschke (Ed.), In *Chemistry of Multiphase Atmospheric Systems*. Springer Verlag, Berlin, 415-471.
- Sander, R. and Crutzen, P. J., 1996:** Model study indicating halogen activation and ozone destruction in polluted air masses transported to the sea. *J. Geophys. Res.*, **101**, 9121-9138.
- Sandu, A., Potra, F.A., Charnichael, G.R. and Damian, V., 1996.** Efficient implementation of fully implicit methods for atmospheric chemical kinetics. *J. Comput. Phys.*, **129**, 101-110.
- Warneck, P., 1999:** The relative importance of various pathways for the oxidation of sulfur dioxide and nitrogen dioxide in sunlit continental fair weather clouds. *Phys. Chem. Chem. Phys.*, **1**, 5471-5483.
- Wolke, R. and Knoth, O. 2000a.** Time-integration of multiphase chemistry in size-resolved cloud models. *Appl. Num. Math.*, submitted.
- Wolke, R. and Knoth, O. 2000b.** Implicit-explicit Runge-Kutta methods applied to atmospheric chemistry-transport modelling. *Environ. Model. Software*, **15**, 711-719.
- Wolke, R., Knoth, O. and Herrmann, H., 2000.** *Numerical treatment of aqueous phase chemistry in atmospheric chemistry transport modelling.* Gryning, S.E. and Schiermeier, F.A. (Ed.), In *Air Pollution Modeling and Its Application XIV*. Kluwer Academic / Plenum Publishers, New York, in press.

### Funding

- European Commission, Brussels.

### Cooperation

- University of Leeds,
- University of Strasbourg,
- University of Utrecht,
- University of Lyon.



## The micro-scale meteorological model MITRAS: An overview

Detlef Hinneburg, Oswald Knoth, Michael Lambrecht, Eberhard Renner, Ralf Wolke

### Introduction

The building-resolving micro-scale meteorological model MITRAS combines the advantages of both micro- and meso-scale atmospheric models. Essential features are the complete prognostic description of the boundary layer including the relevant energy and particle fluxes over heterogeneous terrain as well as the explicit high resolution of single obstacles, buildings or complex structures. The model was deduced from the original meso-scale model METRAS (Schlünzen, 1988) and receives the building-relevant information from a preprocessor.

In the preprocessor the geometry of the buildings is created and simultaneously converted to physically operating quantities for the basic meteorological equations. For a complete implementation of buildings in all physical processes, a systematic and detailed revision of all meteorological, physical and technical procedures and conceptions was required. Some brief explanations are quoted in the following sections (see also Schlünzen et al., 2001). Results of several model tests and applications demonstrate the state and capability of the model.

Similar to the mesoscale model, MITRAS is adapted to the chemical transport model MUSCAT (Knoth and Wolke, 1998). The micro-scale meteorological-chemical transport model set consisting of MITRAS and MUSCAT (including the building-preprocessor and the 1-dimensional meteorological pre-run model) has been employed to simulate particle transport through synthetic and real street canyons. As an example the application to a highly polluted city quarter in Leipzig is offered.

### Preprocessor for buildings

The preprocessor is necessary to establish the geometry of the building structure and to determine so-called mask functions, which precisely and simply adapt to the physical quantities of the meteorological model. Its characteristic feature is to remodel the real buildings as a complex of walls that are strictly directed along the faces of the model grid cells while preserving information about the coverage of the faces and the volumes. Two alternative forms of input patterns for the building geometry are provided. The positions of the buildings and quarters are allowed to be rotated and shifted subsequently by any amount

desired. All these calculations and experiments are managed by the preprocessor requiring a run-time of a few seconds in any case.

After the determination of grid intersections caused by the buildings, the relative coverage of each grid cell volume and face is calculated. A set of 3-dimensional fields for the ratios (amounting between 0 and 1) of free volume and free x-, y-, and z-face area of the model grid cells (i.e. the mask functions) can thus be placed at the disposal of the meteorological model. Possible deformations of the buildings or the city quarter, respectively, due to the derived mask functions are avoided by means of skilfully accumulating all building units in a cell before analysing the resultant grid intersections.

The criteria for a sensitive detection of buildings in a cell as well as the calculation rules for the area and volume coverage are very sophisticated. Proper relations between the mask function values of a grid cell and a blowing-up procedure for all objects by a small tolerance amount in each direction prevent discrepancies such as unjustified disappearance of a building because of inexact grid fitting. Special attention is given to cases of thin detached walls with open cells on both sides and to the occurrence of various (partially) closed faces in the same grid cell. Moreover, an exact adaptation of the coordinate system and consistent boundary conditions are established between the preprocessor and the meteorological model. Finally, the possibility of smoothing all buildings to fit the grid cells (without cut cells) is allowed.

The preprocessor also performs a mapping of the distance of each grid cell to the nearest building and of the wall roughness, both being used in the processes of turbulent diffusion. The quantity of wall roughness was introduced in the preprocessor and the meteorological model (similar to the surface roughness) in order to manage buildings with heterogeneous face properties.

### General aspects of the meteorological model

Maximum possible congruency between the 3-dimensional model MITRAS and its 1-dimensional pre-run version with regard to state and sequence of all routines is declared. Thus, the damping process in the uppermost layers is realized in both models with consistent time proportionality, which results in steady conditions for the time integration during the transition from the 1-dimensional pre-



run to the 3-dimensional simulation. In the case of fixed inflow conditions mostly applied in the studies, the damping procedure is constrained to the inner model region. Also the calculations for the turbulent kinetic energy and dissipation (and therefore the diffusion coefficients) are unified and stabilized in regard of the temporal changes of production terms. In order to control immediately the time step for the overall integration cycle of the models, the appropriate routines are arranged after the calculation of the corresponding coefficients (especially of diffusion).

The mask functions from the building-preprocessor are utilized in the MITRAS model (see Lambrecht and Knoth, 1999) by way of

- 1) additional factors joined to the corresponding quantities (fluxes and similar terms), and
- 2) criteria within logical switches (e.g., decisions on wall friction).

The filter routine for damping accidental oscillations of the wind velocity components throughout the model domain is constructed such as to exclude undesired influences due to formal and unrealistic values in empty (i.e. completely covered) grid cells. In order to approach to the real geometric structure, incompletely covered (i.e. cut) grid cells are allowed for in all processes and formulae of the model (see following sections). Buildings that touch or cross the boundaries of the model region are also taken into account by the corresponding routines (lateral boundary conditions, flux control).

### Initialization of obstacles/buildings

In perfect analogy to the gradual rise of orography (diastrophism), the buildings and mask functions, respectively, are initialized as well (optionally). The values of the mask functions describe a no-building situation at the very beginning of the temporal integration and arise during the diastrophism phase until the predetermined values are reached. Consequently, peculiar situations and exaggerative properties of the flow situation are prevented in the start phase anyway and at the boundaries in general. The realization of the flux conservation by the dynamic pressure-solver is facilitated significantly.

In the initialization phase two different cases of cut cells or faces are to be distinguished:

- a) Genuine cut cells or faces reside (at least partially) outside a building and are defined for the usual quantities such as wind velocity and scalar atmospheric characteristics (e.g., temperature).
- b) Provisional cut cells or faces are placed completely inside a building and are not equipped with real atmospheric properties.

They are handled like a porous material of stepwise diminishing permeability. The individual quantities of these cells during the diastrophism period are prescribed such, that wind velocity, turbulent kinetic energy and diffusion coefficients decrease with proceeding time, starting from the initial atmospheric values and vanishing at the end.

After the initialization period, all mask functions relating to cells or faces entirely inside the buildings receive zero values which cancel the improper terms in the equations.

### Advection

Advection is the primary, but at the same time rather simple process to be mastered by the model. The customary advection formulae retain their validity, when the following appositions are considered:

- 1) Effective fluxes are scheduled in multiplying the usual transporting fluxes with the locally defined face-mask functions.
- 2) The gradients of the advection fluxes are normalized to (divided by) the corresponding volume mask to account for the limited free space in the grid cell.

In the case of provisional cut cell faces the flux mask factors are redundant because of the prescribed descending fluxes (see point b above). This fact includes the advective effect of the ventilation inside the buildings on the wind outside (during diastrophism).

In contrast to the wind vector, the influence of the scalar quantities in covered cells (i.e. buildings) on the atmospheric properties is substituted by diagnostic specifications in the cells adjacent to the buildings. Apart from these cells, special provision is also required for indirectly adjacent cells in order to convert the modelled second order advection (Knoth and Wolke, 1998) into first order (upstream) techniques. The modifications of both the advection and the diffusion (see below) have impact on the routines for the lateral boundary conditions which are concentrated in a separate routine.

### Turbulent diffusion

Dependent on the vicinity of a surface (earth or building walls), the formulae for the turbulent diffusion split into different parts: The turbulent exchange that couples cells outside the buildings remains unaffected, whereas wall friction is calculated in generalized analogy to the friction on the earth surface. This part of the model was expanded in order to allow for partially closed faces of different number within a grid cell.



For this purpose all cells adjacent to at least one (partial) building wall are treated separately. According to the effective face coverage  $f$ , the turbulent diffusion through a cell face is treated both as wall friction weighted by the factor  $f$  and as open-air diffusion weighted by  $(1-f)$ . The proper part of the wall that is exposed to the free cell volume part and, therefore, causes wall friction (i.e. the effective face coverage) is re-created by the model as the ratio of the face coverage and the volume coverage of the cell in question.

As for wall friction, the following impact quantities are accounted for in the calculations: roughness, distance, and direction of the walls, relative face coverage by the buildings, and the wall(face)-parallel wind speed projection. Various walls exposed to the same grid cell give rise to an accumulation of the corresponding friction fluxes. Similar to the earth surface, the friction velocity relative to a wall is found from the parallel wind component, the wall roughness and the wall distance. This quantity also determines diagnostically the turbulent kinetic energy, its dissipation as well as the diffusion coefficient of this cell (Ehrhard, 1999).

### Dynamic pressure correction

The diagnostic non-hydrostatic determination of the dynamic pressure is in general based on the enforcement of conservation upon the pressure-corrected momentum fluxes in each grid cell and at each time step. Considering the grid cells adjacent to a building, the usual equations retain their validity provided that the fluxes are multiplied with the appropriate face-mask functions. These factors consequently appear in the corresponding terms of the Poisson matrix.

In the cases of provisional cut cell faces (i.e. inside the buildings during the diastrophism period), however, the pressure gradients are multiplied additionally with the actual mask functions in order to achieve a stepwise transition to vanishing pressure corrections on hard walls after the diastrophism phase. The described procedure also holds for the multigrid pressure solver where the mask functions are defined analogously on several differently resolved grids.

### Simulation example

The complete model MITRAS, connected with the chemical transport model MUSCAT (Knoth and Wolke, 1998), was applied to a complex of three crossing street canyons in the inner north-east part of Leipzig (Eisenbahnstrasse). These quarters belong to those city regions which are most affected by traffic emissions. The investigations were focussed on the transport of traffic-emitted

diesel soot through the quarters, and to the infiltration from the streets into the backyards. The six quarters are partially open and in the backyards some back premises are existent. The individual building geometry considers the real flat and saddle roofs.

The quarters are enclosed by a model region of 420 m length, 184 m width and 500 m height. The corresponding grid spacing is chosen as 4 m x 4 m in the horizontal and variable for the 34 vertical layers (in the figures only a smaller section is shown). For the wind speed of 2 m/s (from west) a simulation time of 10 minutes was found to be sufficient for achieving a rather stationary wind field.

Fig. 1 shows the west-east directed wind field at a height of 2 m above ground. Due to the unsymmetrical arrangement of the buildings and quarters, the flow through the central street canyon (Eisenbahnstrasse) is pushed away from the axis. The distribution of diesel soot emitted by traffic at about 08:00 LT on a weekday can be found on Fig. 2.

At two points, in a side-street and in a neighbouring back yard, vertical profiles of the soot concentration were drawn at several times (Figs. 3 and 4). They demonstrate that on a time scale of few minutes the emitted and transported particles are spread in the vertical direction and induce a progressive mixing even into the "clean" back yards.

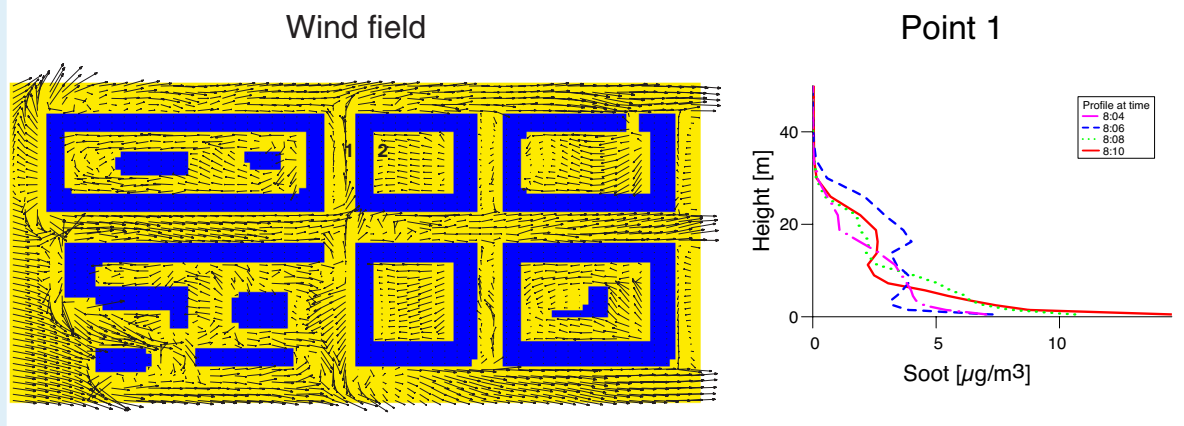


**Fig. 1:** Wind field at a height of 2 m above ground for the city quarter "Eisenbahnstrasse in Leipzig".

**Fig. 3:** Vertical profiles of diesel soot concentrations at different times after release of traffic emissions for a side-street position (cf. point 1 on Fig. 1).

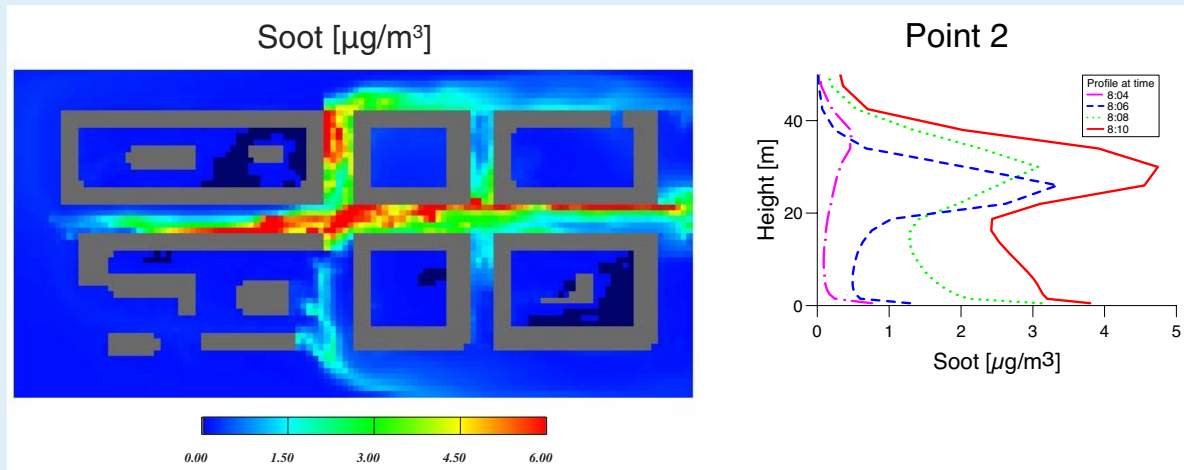


**Fig. 2:** Diesel soot concentration at a height of 2 m above ground 08:00 LT for the city quarter "Eisenbahnstrasse in Leipzig".

**Fig. 4:** Vertical profiles of diesel soot concentrations at different times after release of traffic emissions for a backyard position (cf. point 2 on Fig. 1).

## References

- Ehrhard, J. 1999.** Untersuchung linearer und nichtlinearer Wirbelviskositätsmodelle zur Berechnung turbulenter Strömungen um Gebäude. Fortschritt-Berichte VDI, Reihe 7, Nr. 367.
- Knoth, O. and Wolke, R. 1998.** An explicit-implicit numerical approach for atmospheric chemistry-transport modeling. Atmos. Environ., **32**, 1785-1797.
- Lambrecht, M., Knoth, O. and Renner, E. 1999.** Development of numerical schemes for high-resolution urban scale models. Proceedings from the EUROTRAC Symposium '98, P.M. Borrell and P. Borrell (Eds.), 542-546.
- Schlünzen, K. H. 1988.** Das mesoskalige Transport- und Strömungsmodell "METRAS" – Grundlagen, Validierung, Anwendung. Hamburger Geophysikalische Einzelschriften, **88**, Universität Hamburg und MPI für Meteorologie Hamburg.
- Schlünzen, K. H., Bischof, G., Hinneburg, D., Knoth, O., Lambrecht, M., Leitl, B., Lopez, S., Lüpkes, C., Pankus, H., Renner, E., Schatzmann, M., Schoenemeyer, T., Trepte, S. and Wolke, R. 2001.** Flow and transport in the obstacle layer – First results of the micro-scale model MITRAS. Submitted to J. Atmos. Chem.

### Funding

- Bundesministerium für Bildung, Wissenschaft, Forschung und Technologie (BMBF)

### Cooperation

- Alfred Wegener Institut Bremerhaven
- Meteorologisches Institut der Universität Hamburg





*Short contributions  
to current research projects*







## Submicrometer particles in the tropopause region (CARIBIC)

Markus Hermann, Hartmut Haudek, Alfred Wiedensohler, Jost Heintzenberg

### Introduction

**CARIBIC** (Civil Aircraft for Regular Investigation of the atmosphere Based on an Instrument Container) is an international project with the goal to measure trace gas and aerosol particle concentrations in the upper troposphere and lower stratosphere (UT/LS). For these measurements, a standard air freight container is equipped and flown regularly aboard a commercial aircraft (B-767) of LTU International Airways (cf. Brenninkmeijer et al., 1999). IFT is one of the three founding institutes of the project, which started in 1994, and is responsible for all aerosol measurements within this project. This includes the construction and characterization of a new aircraft-borne aerosol inlet (Hermann et al., 2001) and the development and operation of two aerosol units (Hermann, 2000). The two units contain three modified condensation particle counters (CPCs, cf. Hermann and Wiedensohler, 2001), yielding number concentrations for ultrafine particles (4 nm < diameter < 12 nm) and Aitken and accumulation mode particles (12 nm < diameter < 1.5 μm) and a particle sampler which collects all particles larger than 65 nm for subsequent chemical analysis.

### Development

With the Ph. D. thesis of Hermann (2000), the technical development of the present CARIBIC aerosol system has been completed. Since March 1999, the second aerosol unit, containing the aerosol sampler and the third CPC, is flown regularly together with unit one. To date, more than 50 successful long distance flights have been carried out, from Germany to the Indian ocean. These flights covered south-east Europe and a substantial part of west and southern Asia, including the Indian Ocean, a large, but scarcely investigated region of the atmosphere. Since May 2000, the flight routes were extended to the African continent (Windhuk/Namibia, cf. Fig. 2).

### Results

Up to now, CARIBIC collected more than 1.5 million single particle concentration measurements. This unique data set can be used, for instance, to create geographical and seasonal distributions of the concentrations of ultrafine particles and Aitken and accumulation mode particles in the UT/LS. As an example, Fig. 1 shows the probability distribution of

ultrafine, i.e. recently formed particles for summer.

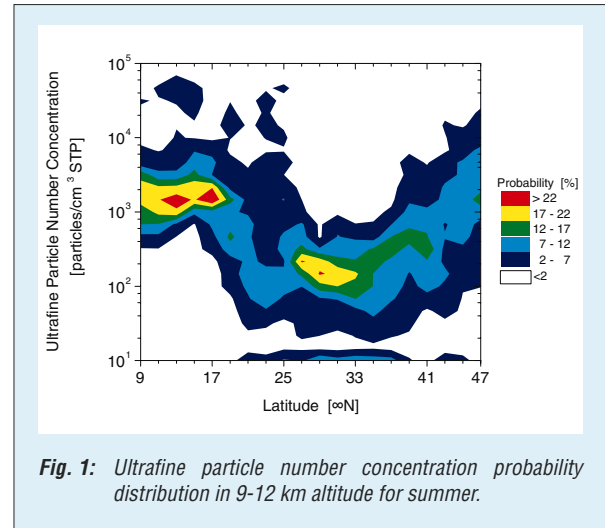


Fig. 1: Ultrafine particle number concentration probability distribution in 9-12 km altitude for summer.

Fig. 1 shows high ultrafine particle number concentrations in the tropics and at mid-latitudes, indicating regions of particle formation, whereas in the subtropics concentrations are generally low. This picture is in agreement with the global meridional vertical circulation pattern. In the tropics, deep convective transport carries particles as well as particle precursor gases (like  $C_2H_6S$ ,  $OCS$ , and  $SO_2$ ) from the surface to higher altitudes. During transport, the precursor gases are oxidized leading to homogeneous particle nucleation of the oxidation products (mainly sulfuric acid) at higher altitudes. In the subtropics, this kind of upward motion is mostly lacking and large-scale subsidence is prevailing, making particle formation less likely. In contrast to the tropics, no single reason for the higher concentrations at mid-latitudes can be given. Here, several sources, such as aircraft emissions, mixing of tropospheric and stratospheric air, and upward motion of anthropogenically polluted surface air contribute to the observed values.

To expand the observation area of CARIBIC, in 2000 a second flight route to the African continent was made available. Fig. 2 shows the Aitken and accumulation mode particle number concentration for the first flight on May 18<sup>th</sup>. Clearly visible are high particle concentrations caused by deep convective cells in the Intertropical Convergence Zone (ITCZ). The extension to this second flight route allows to investigate atmospheric regions and processes, which are important but relatively unknown, like the southern hemisphere, the tropics,



and African biomass burning plumes. The CARIBIC aerosol research activity of the

last two years is reflected in eight published or submitted manuscripts.

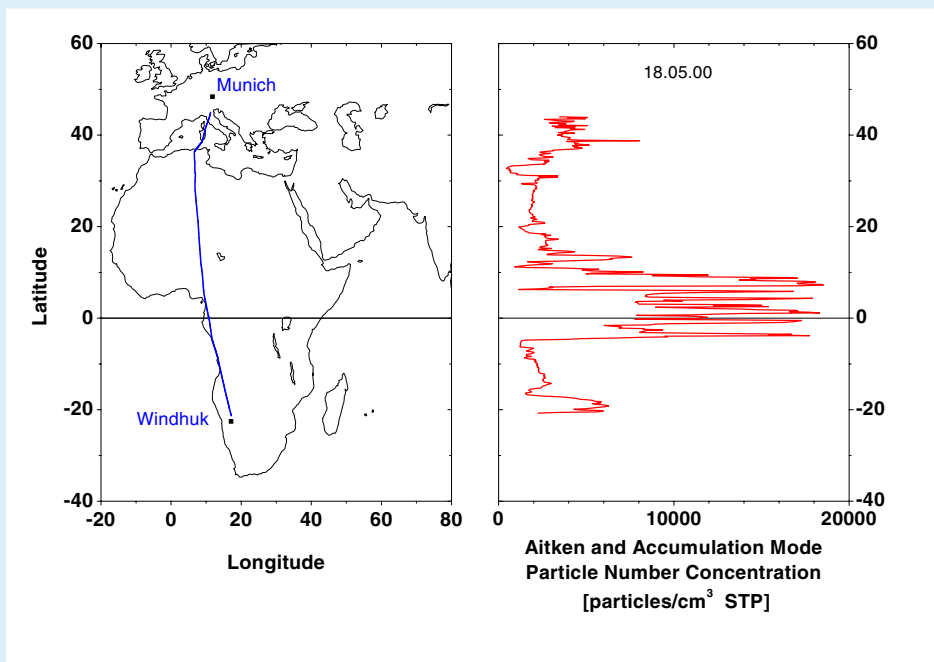


Fig. 2: Aitken and accumulation mode particle number concentration for the first Africa flight to Windhuk/Namibia, yielding a meridional section through the tropics.

## References

Brenninkmeijer, C. A. M., Crutzen, P. J., Fischer, H., Güsten, H., Hans, W., Heinrich, G., Heintzenberg, J., Hermann, M., Immelmann, T., Kersting, D., Maiss, M., Pitscheider, A., Pohlkamp, H., Scharffe, D., Specht, K., and Wiedensohler, A. 1999. CARIBIC civil aircraft for global measurement of trace gases and aerosols in the tropopause region. *J. Atmos. Oceanic Technol.*, 16, 1373-1383.

Hermann, M., 2000. Development and Application of an Aerosol Measurement System for Use on Commercial Aircraft. Ph. D. thesis, Universität Leipzig, Germany.

Hermann, M., Stratmann, F., Wilck, M., and Wiedensohler, A., 2001. Sampling characteristics of an aircraft-borne aerosol inlet system. *J. Atmos. Oceanic Technol.*, 18, 7-19.

Hermann, M. and Wiedensohler, A., 2001. Counting efficiency of condensation particle counters at low-pressures with illustrative data from the upper troposphere. *J. Aerosol Sci.*, in press.

### Funding

- European Commission, DG 12
- LTU International Airways

### Cooperation

- Max-Planck-Institut für Chemie, Abteilung Chemie der Atmosphäre, Mainz
- Forschungszentrum Karlsruhe, Institut für Meteorologie und Klimaforschung, Karlsruhe
- Royal Netherlands Meteorological Institute, De Bilt, Netherlands
- University of Lund, Dept. Nuclear Physics, Lund, Sweden
- Max Planck Institute for Aeronomy, Katlenburg-Lindau, Germany
- University of East Anglia, Norwich, Great Britain
- LTU International Airways, Düsseldorf, Germany



## Temperature profiling in the troposphere using a Raman lidar

Dietrich Althausen, Albert Ansmann, Ina Mattis, Ulla Wandinger

Optical and physical properties of atmospheric particles depend on relative humidity. Hence the knowledge of relative humidity is essential for investigations of atmospheric aerosols. The water vapor channel installed in the IFT Raman lidar permits the determination of the water vapor mixing ratio by measuring the Raman shifted signal of water vapor and nitrogen molecules. Measuring simultaneously temperature and water vapor mixing ratio within the same atmospheric volume would allow to determine the relative humidity.

For investigations of particle dispersion within the planetary boundary layer the height of the convective (daytime) boundary layer, its variability and the entrainment zone are required. Temperature profiles can be used for the determination of these parameters. At daytime this requires temperature profiles every 10 min. Radiosondes cannot be used for observations on this time-scale. The rotational Raman lidar technique offers an elegant way of measuring temperature profiles with high temporal resolution.

In cooperation with the Institute for Atmospheric Optics, Tomsk, Russia a temperature channel has been installed in the Raman lidar (Wandinger et al. (1998)). The temperature dependent intensities of the pure rotational Raman lines result from the Boltzmann statistics of the population of the rotational energy states. The temperature is determined from the ratio of two portions of the pure rotational Raman spectrum. The full width at half maximum of a pure rotational Raman line is about  $0.05 \text{ cm}^{-1}$ . The distance between the lines is about  $8 \text{ cm}^{-1}$ . A double grating monochromator within the temperature channel of the Raman lidar realizes the spectral separation. With the first grating the wavelength region is selected which comprises the nitrogen and oxygen pure rotational Raman lines. This grating works also as a first blocking filter for the elastically backscattered light. With the second grating the necessary suppression of the elastic backscattered light to  $10^{-6}$  is achieved.

A temperature profile measured with the lidar during the night of 15 November 1999 is shown in Fig. 1 in comparison with the profile acquired with a concurrent radiosonde launched at the lidar site. The statistical error of the rotational Raman temperature measurements is calculated according to Arshinov et al (1983) and Behrendt et al. (2000). For the average temperature profile taken between 21:54 and 23:27, UTC the statistical error amounts

to about 0.3 K at 8-km height, about 1 K at 10 km, and about 1.5 K in the tropopause region.

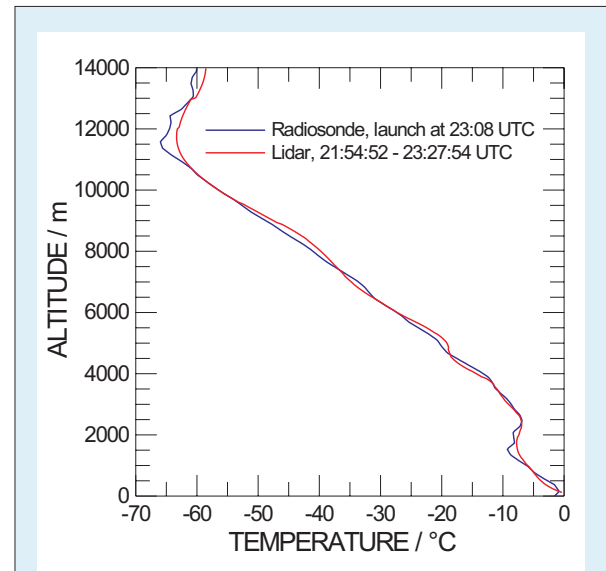


Fig. 1: Measurement on 15 November 1999 (Lidar site 51.35 N, 12.43 E): Average temperature profile measured with pure rotational Raman lidar and temperature profile measured with radiosonde.

The measurements with 5-min averaging time are depicted in Fig. 2. The range is limited to 4 km. The statistical error is below 1 K up to this height.

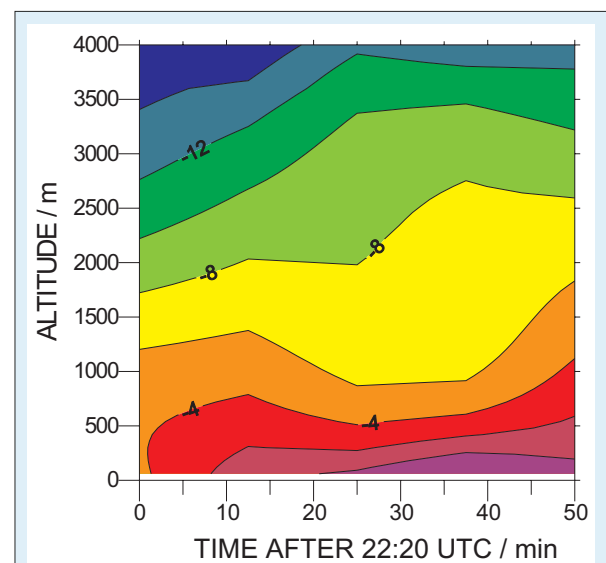


Fig. 2: Time-height contour of temperature measured with the Raman lidar. The temporal resolution is 5-min.



For daytime measurements it is important to suppress the wide spectral regions between the temperature-sensitive pure rotational Raman lines as these regions only contain background light. In the current set-up of the Raman lidar system, which uses a double grating monochromator the sky background between the pure rotational Raman lines is not filtered out. Thus the low signal-to-background ratio up to now only allows temperature determination below 2 km during daytime. If this spectral portion could be filtered out, the signal-to-background ratio could be theoretically increased by a factor up to  $160 = 8 \text{ cm}^{-1} / 0.05 \text{ cm}^{-1}$  (Arshinov et al. (1999)). Calculations have shown that the use of two state-of-the-art Fabry-Perot interferometer (FPI) would lead to a background reduction by a factor of 50.

Up to now only first pilot experiments have been carried out (Althausen et al., 2000). The Raman lidar was equipped with an FPI installed in front of the double grating monochromator. As a result, the ratio of the signal maximum to the sky background was enhanced by a factor of 6. This is less than the expected factor of 16 and in part caused by the degradation of the plate separation of the FPI with time. To improve the stability, an automated tuning of the plate separation has to be set up in the future.

### Acknowledgement

The authors acknowledge the Saxonian Government for financial support of the cooperative research.

### References

- Althausen, D., Arshinov, Yu. F., Bobrovnikov, S. M., Serikov, I., Ansmann, A., Mattis, I. und Wandinger, U. 2000.** Temperature profiling in the troposphere using a pure rotational Raman lidar. Fifth International Symposium on Tropospheric Profiling: Needs and Technology, Adelaide, Australia, 4 to 8 December, 2000. 31-33.
- Arshinov, Yu. F., Bobrovnikov, S. M., Zuev, V. E. und Mitev, V. M. 1983.** Atmospheric temperature measurements using pure rotational Raman lidar. *Appl.Opt.*, **22**, 2984-2990.
- Arshinov, Yu. F., und Bobrovnikov, S. M. 1999.** Use of a Fabry-Perot interferometer to isolate pure rotational Raman spectra of diatomic molecules, *Appl.Opt.*, **38**, 4635-4638.
- Behrendt, A., und Reichardt, J. 2000.** Atmospheric temperature profiling in the presence of clouds with a pure rotational Raman lidar by use of an interference-filter-based polychromator, *Appl.Opt.*, **39**, 1372-1378.
- Wandinger, U., Mattis, I., Ansmann, A., Arshinov, Yu. F., Bobrovnikov, S. M. und Serikov, I. 1998.** Tropospheric temperature profiling based on detection of Stokes and Anti-Stokes rotational Raman lines at 532 nm. 19<sup>th</sup> International Laser Radar Conference, NASA Langley Research Center, USA, NASA/CP-1998-207671/PT1. 6 to 10 July, 1998. 297-299.

#### Cooperation

- Institute for Atmospheric Optics, Siberian Branch of the Russian Academy of Sciences, Tomsk, Russia



## National and transboundary effects of emission changes on components of precipitation in Saxon border regions (OMKAS-Project)

Erika Brüggemann, Wolfgang Marquardt, Annelie Thomas

Natural and anthropogenic emissions (pollutants) can be transported many hundreds of kilometers downwind from their sources before they are deposited (either wet or dry) on the earth's surface. The deposition of atmospheric components can affect terrestrial and aquatic ecosystems (forest decline, lake and soil acidification and/or eutrophication) and cause deterioration of ancient monuments. The effects of acidic precipitation at example of Erzgebirge is shown in Fig. 1 for forest decline. Concentrations of pollutants in precipitation are dependent on the pattern and amount of emissions incorporated into cloudy air masses. Large changes of emissions can cause a significant change of concentrations of pollutants in precipitation.

The experimental method is based on the collection of precipitation samples of periods  $\leq 4$  hours and tracking the raining air masses over 24 hours by three-dimensional backward trajectories starting at 900 hPa level, calculated in one-hour steps.

Precipitation samples were collected at stations of the German Weather Service in Carlsfeld/Westerzgebirge (from March 1993 to December 1999, to 1995 within the project SANA - Scientific programme of recovery of the atmosphere) and Mittelndorf/Ostsächsische Schweiz (from October 1996 to December 1999). Furthermore, data from the sampling site Seehausen/Altmark (from October 1982 (to September 1991 within the investigation of the former GDR, to December 1995 within the project SANA) to December 1999) are included.

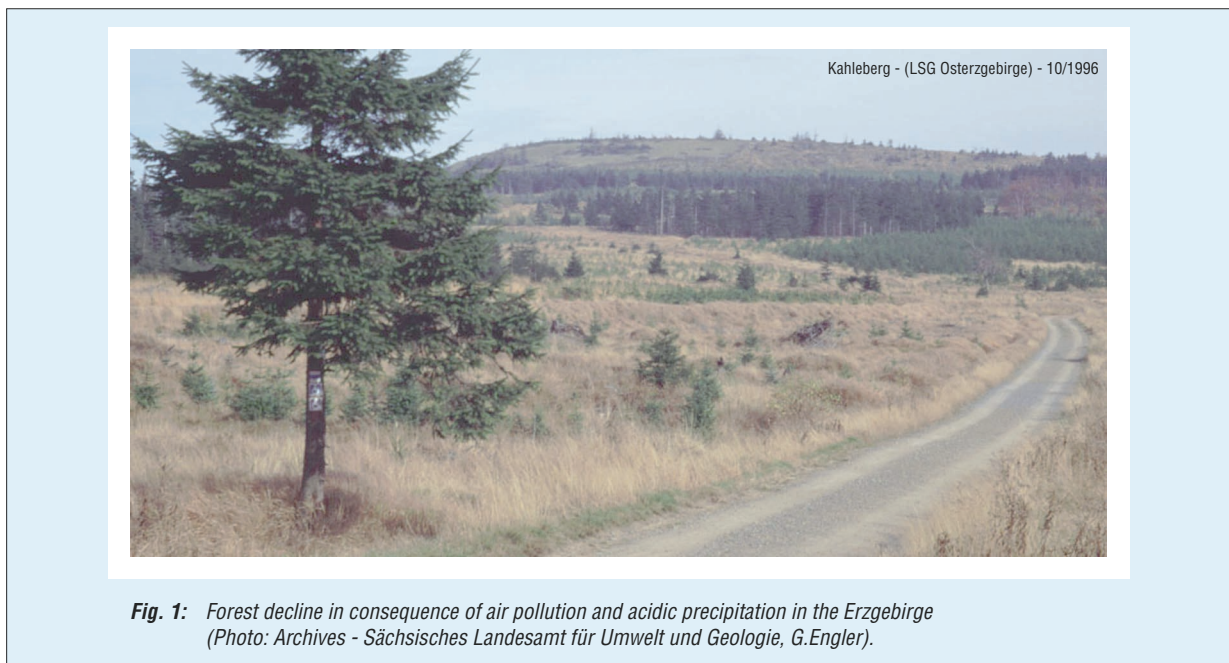


**Fig. 1:** Forest decline in consequence of air pollution and acidic precipitation in the Erzgebirge (Photo: Archives - Sächsisches Landesamt für Umwelt und Geologie, G.Engler).

The border region (also called Black Triangle) which is the industrial region between South Saxonia (Germany), Silesia (Poland), and North Bohemia (Czech Republic) was gravely marked by high  $\text{SO}_2$ ,  $\text{NO}_x$ ,  $\text{NH}_3$ , and dust emissions. In this region the change of pollution and acidification in precipitation was investigated in the course of the redevelopment, modernization, and closure of lignite burning power and heating plants within the project OMKAS (Optimization of the measures to reduce the emission and to control the development of pollution and acidity in precipitation in the border region of Saxony) in the time period from 1996 to 1999.

Thus, the data set of Seehausen covering over 17 years in Seehausen is the longest uninterrupted time series regarding short time collection and evaluation by backward trajectories and was used as reference data.

All sampling sites had automatic wet only collectors. In the precipitation eight main components - chloride ( $\text{Cl}^-$ ), nitrate ( $\text{NO}_3^-$ ), sulfate ( $\text{SO}_4^{2-}$ ), sodium ( $\text{Na}^+$ ), ammonium ( $\text{NH}_4^+$ ), potassium ( $\text{K}^+$ ), calcium ( $\text{Ca}^{2+}$ ), and magnesium ( $\text{Mg}^{2+}$ ) - were analysed by ion chromatography (Metrohm System, Switzerland). Acidity (pH-value), conductivity, and meteorological parameters were registered as well. The data capture for rain events was 85%.



Starting from the collection site so-called entry sectors (EzS) of precipitating clouds were defined, in which regions with similar emission or specific geographical characteristics are combined. These entry sectors were selected in a manner, such that industrial centres in East Germany, Poland, Czech Republic, and also relatively clean regions in West Germany can be distinguished:

- the main emission areas of East Germany (the former GDR, now: the new Federal States) – sectors H (at Seehausen) and 51 (at Carlsfeld),
- Czech Republic/North Bohemian industrial region – sectors 53 (at Carlsfeld) and 63 (at Mittelndorf),
- Poland/Silesia – the sector 62 (at Mittelndorf),
- West Germany (the old Federal States) – sectors I+J (at Seehausen) and 54 (at Carlsfeld),

The total investigation period can be subdivided into three time periods. The first period (1983 - 1989/90) is the time before the unification of Germany and was marked by large emissions of SO<sub>2</sub> (no desulfurization of flue gases), NO<sub>x</sub> (obsolete industrial techniques), and dust (insufficient dust removal in flue gases). At the site Seehausen the annual mean concentrations in this period were larger for sulfate (275 µeq/l) by a factor of two, for nitrate (70 µeq/l) about two, for ammonium (152 µeq/l) about three, for calcium (158 µeq/l) about three, and, finally, acidity (45 µeq/l) was equal for the entry sector East Germany compared to West Germany. The high emissions of acidifying components (SO<sub>2</sub> and NO<sub>x</sub>) were compensated by alkaline components (Ca and NH<sub>3</sub>), so that the acidity in rain water was about equal to that in the sectors under the influence of the West Germany. In the second period (1991 to 1995) the reformation and modernization of industry and agriculture brought different effects on the emissions and consequently on the components in precipitation. The alkaline components were reduced efficiently by dust removal: calcium decreased by two thirds and ammonium by one third. The acidic components sulfate decreased by one half and nitrate increased by 40%. As a consequence, the acidity of rain water strongly rose, partly by a factor of five compared to that in rain from West Germany.

The third period (1996 to 1999) shows by the effects of reformation of industry in the other eastern

regions also and was studied in the Black Triangle (South Saxonia, North Bohemia, and Silesia). In this phase desulfurization in the power plants of East Germany was established. The same took place in North Bohemia nearly two years later. Therefore, the rain water concentration of components decreased once more, at the site Carlsfeld more than in Seehausen, and the acidity had about the same value in 1999 as in the first period. The ionic components in precipitation from East Germany, Czech Republic, and Poland (EzS H, 51, 53, 63, and 62) are still more abundant than in rain from West Germany (EzS I+J and 54). But now the contents are at an much lower level compared to before (cf. Fig. 2).

It remains to be seen in the coming years if the pollution of rain water from the eastern regions will decrease further.

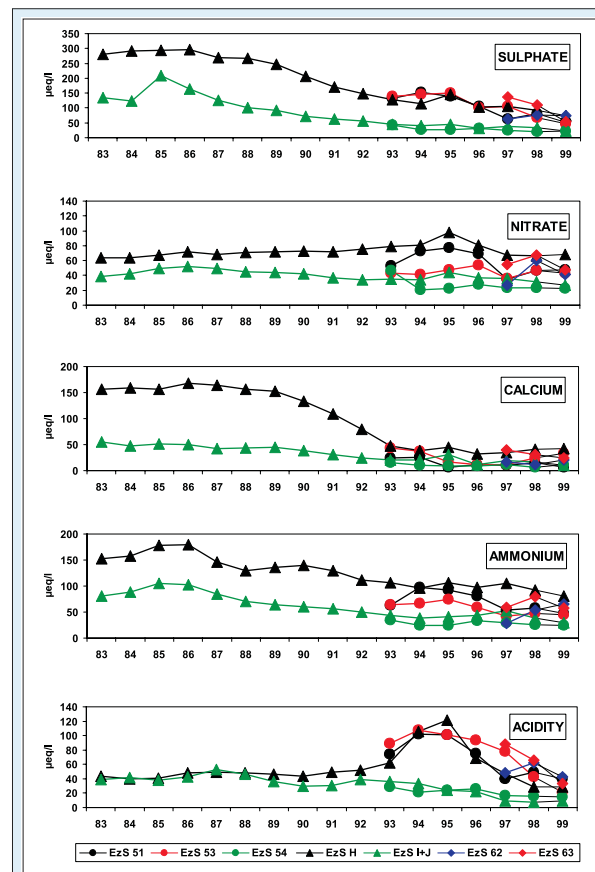


Fig. 2: Annual average volume-weighted concentration of sulfate, nitrate, calcium, ammonium, and the acidity in precipitation for the entry sectors from East Germany: H (at Seehausen) and 51 (at Carlsfeld), Silesia: 62 (at Mittelndorf), North Bohemia: 53 (at Carlsfeld) and 63 (at Mittelndorf), and West Germany: I+J (at Seehausen) and 54 (at Carlsfeld).

**Funding**

- Sächsisches Landesamt für Umwelt und Geologie Dresden

**Cooperation**

- Deutscher Wetterdienst
- Brandenburgische Technische Universität Cottbus



## Cloud water analysis with high pressure liquid chromatography in combination with mass spectrometry

Diana Hofmann

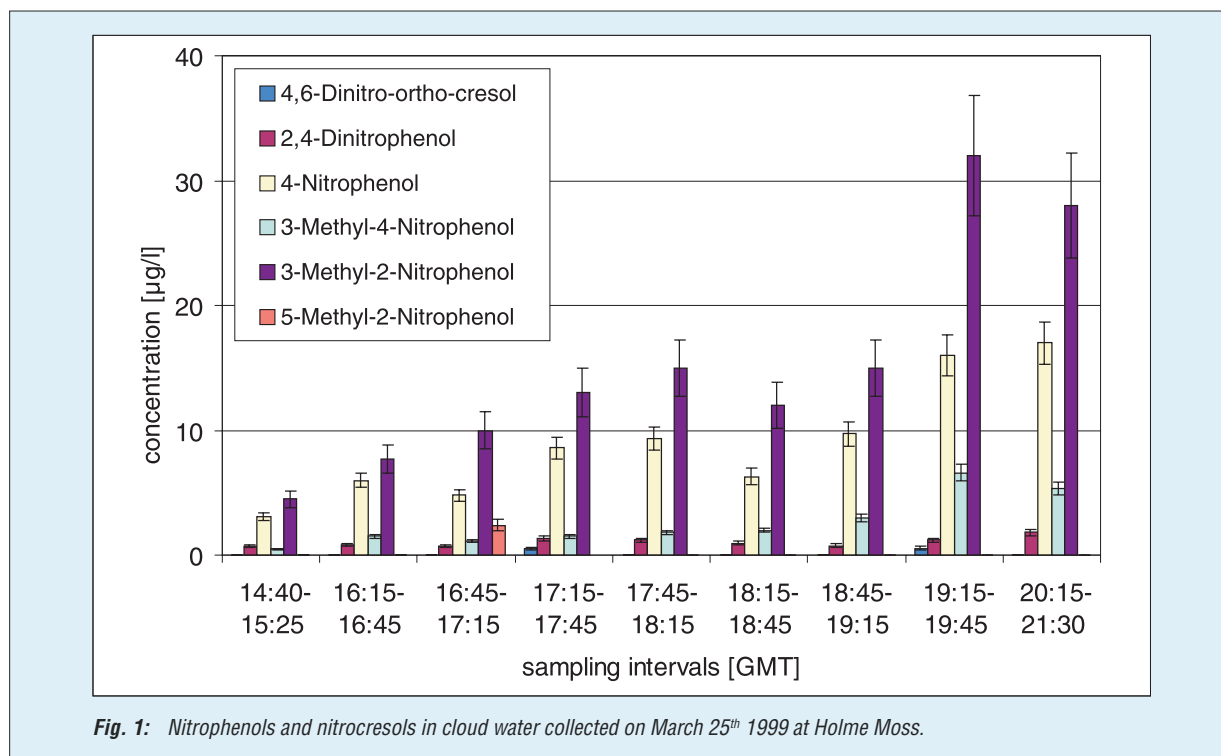
Reactions of organic pollutants in the atmospheric multiphase system are not well known. The products of these reactions contribute to particle modification and cloud formation. Some of them are more hazardous to the biosphere than primary pollutants. In the past new particle formation and particle modification by cloud passage was investigated with the main focus on inorganic precursor gases and aerosol and cloud constituents. Smog chamber experiments with organic substances, e.g., aromatics, show high aerosol yields. In the atmosphere, such processes will lead to an increase of particulate secondary organic carbon (SOC).

For a better understanding of tropospheric oxidation processes of organic compounds a field experiment was performed in March 1999 (negligible biogenic influence), mainly directed towards the physical and chemical aerosol characterization. The chemical

components by a factor of 100 was achieved with methyl-*tert*-butylether as solvent in an modified and miniaturized light phase rotary perforator. The recovery of the analytes was between 70 and 100%. The extracts were examined with high pressure liquid chromatography in combination with mass spectrometry (HPCL-MS) after atmospheric pressure chemical ionisation in the negative mode.

In some samples besides 4-nitrophenol (NP) and 2,4-dinitrophenol (2,4-DNP) additional compounds were identified. By the combination of source-collision induced dissociation and MS/MS it was found that these substances are nitrocresols and 4,6-dinitro-*o*-cresole (4,6-DNOC), respectively.

The analytes were quantified with deuterated standards (4-NP and 2,4-DNP) and with previously determined response factors, respectively.



modification of an urban aerosol by a cloud passage was characterized downwind of Manchester (Great Britain) at Holme Moss mountain site.

Following methodical investigations for the characterization of nitro- and dinitrophenols in the water phase, cloud water samples from the Holme Moss experiment were analyzed.

The preconcentration of the polar organic

The samples of the individual days show uniformity predominantly with regard to the detected main component. Most samples show 4-NP as the main component, where the highest values of 4-NP (up to 260 µg/l) are found in the samples of March 12<sup>th</sup>, the only day which was influenced by continental air. The comparison with values from literature is shown in Tab. 1.



location	time	investigator	content
Cloud - Great Dun Fell	04-05/1993	Lüttke	0,05-5 µg/l (GC-MS)
Cloud - Brocken	06/1994	Lüttke	6-49 µg/l (GC-MS)
Cloud - Fichtelgebirge	07/1998-03/1999	Hottenroth et al.	5-170 µg/l (GC-MS) 0,1-73 µg/l (HPLC-MS)
Cloud - Fichtelgebirge	07/1989	Herterich & Herrmann	57 µg/l (GC-MS)
Rain - Fichtelgebirge / Alpes	05-08/1989	Herterich & Herrmann	4-17 µg/l (GC-MS)
Fog - Fichtelgebirge	07-08/1997	lft	2-20 µg/l (HPLC-MS)
Cloud - Holme Moss	03/1999	lft	1-260 µg/l (HPLC-MS)

**Tab. 1:** Comparison of 4-nitrophenol-contents from Holme Moss samples with literature data.

Only March 17<sup>th</sup> shows 2,4-dinitrophenol as main component (20-54 µg/l) because the pH-value of the cloud water was about five. Under these circumstances the 2,4-dinitrophenol is more dissociated and the gas-liquid-equilibrium is shifted to the liquid phase. In these samples we also identified and quantified larger amounts of 4-nitrophenol (7-28 µg/l) and 4,6-dinitro-o-cresol (0,5-11 µg/l).

An interpretation of the results is underway with regards to (i) meteorological conditions (wind direction and wind velocity, trajectories, radiation) as well as (ii) chemical precursor concentrations (nitrogen oxides NO<sub>x</sub> and aromatics like benzene, toluene, ethylbenzene and xylene - BTEX) and (iii) acidity of the cloud droplets.

## References

**Herterich, R. and Herrmann, R., 1990.** Comparing the distribution of nitrated phenols in the atmosphere of two German hill sites. *Environ. Technol.*, 11, 961-972

**Hottenroth, S., Völkel, W., Fechner, T., Bopp, S., Römpf, A., Klemm, O., and Frank, H., 2000.** HPLC-MS-MS: A powerful tool for sensitive detection of nitrophenols in cloud water samples. Poster, 1<sup>th</sup> International Symposium on Advances in Chromatographic and Electrophoretic Separations (ACES), Bayreuth, 17.-19. April

**Lüttke, J., 1996.** Untersuchungen zu Vorkommen, Entstehung und Abbau von Phenolen und Nitrophenolen in der Troposphäre. Dissertation, Universität Hannover

### Cooperation

- University of Manchester, Institute for Science and Technology
- Universität Lund
- Technische Universität Wien



## Cloud processing of mineral dust particles and the effects on cloud microphysics

Sabine Wurzler, Yan Yin, Tamir Reisin, Zev Levin

### Introduction

In the Mediterranean region sulfate is found in most aerosol particles. Among these, mineral dust particles coated with soluble substances are found. The amount of soluble material on the mineral dust particles was found to be related to their surface area. The soluble coating of the mineral dust particles could significantly change their ability to serve as cloud condensation nuclei (CCN). Evidence for the activation of these large CCN was observed during in-cloud measurements, where a few large drops containing both dust and sulfate were found (Levin et al., 1996). The processes responsible for the sulfate coating of dust particles are still not identified. Possible coating mechanisms are heterogeneous surface reactions or sedimentation of dust particles onto sea water and subsequent resuspension. Another more likely coating mechanism is the cloud processing of mineral dust particles. In it, mineral dust particles are collected by cloud drops that have been nucleated on soluble aerosol particles. Additional sulfate is added by gas scavenging and subsequent liquid phase oxidation. In mixed phase clouds, mineral dust particles and drops can be collected by ice particles. Melting of these ice particles contributes to the number of drops which contain mineral dust and soluble materials. After cloud evaporation, mineral dust particles coated with soluble material are released with other cloud processed aerosols. In order to investigate the effects of cloud processing of mineral dust particles, model simulations with a parcel model and a two dimensional dynamic cloud model with detailed description of cloud microphysics have been carried out.

### Model results

The numerical simulations (Wurzler et al., 2000) show that one possible path for the formation of the sulfate coating is through the interaction of clouds with dust particles. Three cycles through a cloud formed on a marine aerosol size distribution including a tail of large mineral dust particles were studied. The mineral dust concentrations were based on typical background concentrations. With increasing number of cycles through the cloud more large particles are formed, among which there are coated mineral dust particles. In a subsequent study, the effects of the cloud

processed mineral dust particles on cloud micro- and macrostructure as well as on precipitation development were investigated (Yin et al., 2000a) using a two dimensional cloud model (Yin et al., 2000b) with detailed description of warm and cold cloud microphysics (Reisin et al., 1996, Tzivion et al., 1987). Figs. 1 and 2 show the model results after 40 minutes of simulation.

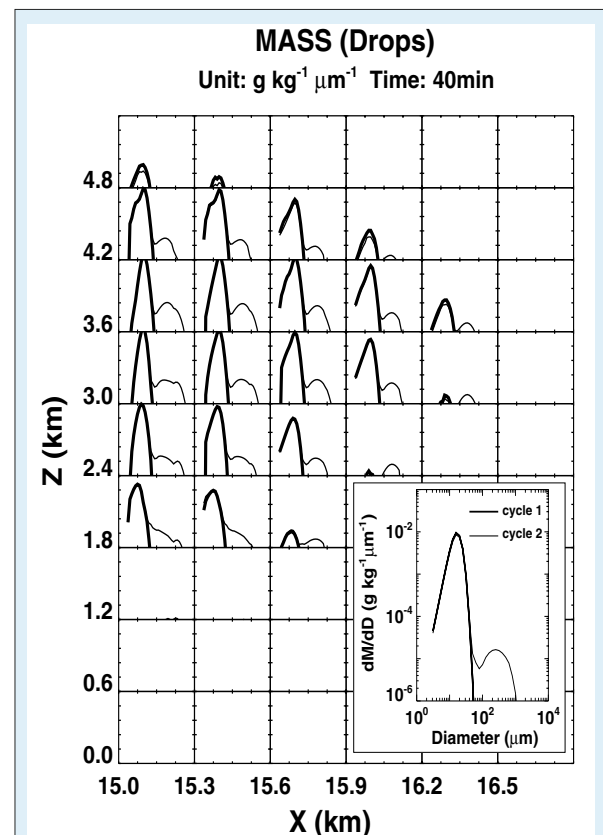
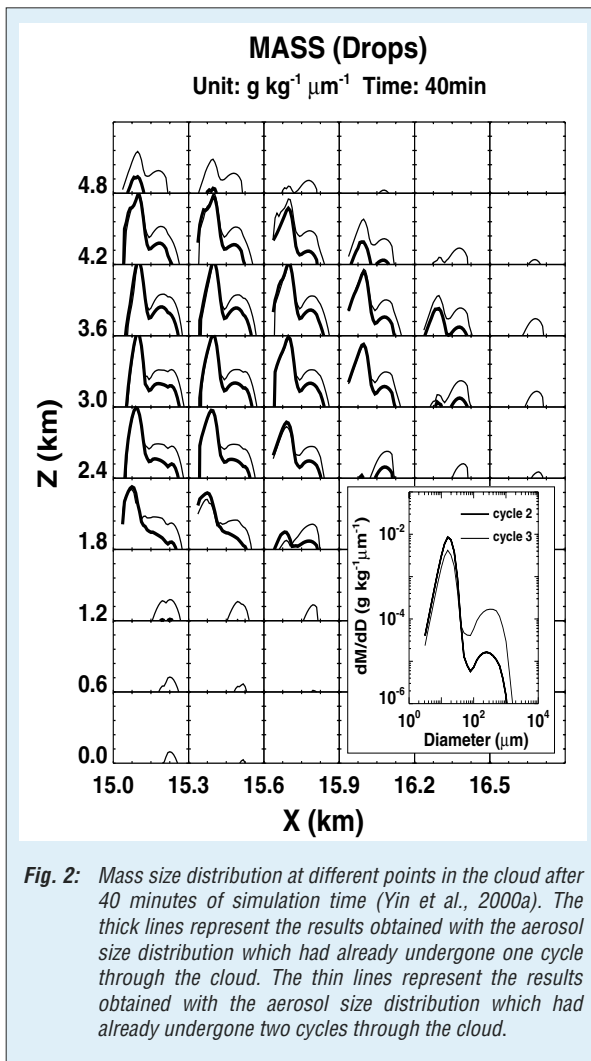


**Fig. 1:** Mass size distribution at different points in the cloud after 40 minutes of simulation time (Yin et al., 2000a). The thick lines represent the results obtained with the initial unprocessed aerosol size distribution. The thin lines represent the results obtained with the aerosol size distribution which had already undergone one cycle through the cloud.

Fig. 1 shows the distribution of the liquid water content obtained during the first (thick line) and the second (thin line) cycle of the aerosol particles through the cloud. After 40 minutes of simulation time only a narrow drop size population without precipitation sized drops has formed during the first cycle. In contrast, in the second cycle after 40 minutes, the cloud formed on the cloud processed aerosol particles has already developed precipitation sized drops. Fig. 2 shows the water



mass distribution of the model cloud during the second (thick line) and the third (thin line) cycle of the aerosol particles through the cloud. In the third cycle the development of precipitation was even more efficient than in the second cycle. Note that the situation might look otherwise for a sandstorm situation, where the production of further CCN can lead to the suppression of precipitation.

### Conclusions

The simulations with the parcel model show that one possible path for the formation of sulfate coating of mineral dust particles is through the interactions of clouds with dust particles. The simulations with the two dimensional cloud model show that when ingested in subsequent growing clouds, these cloud-processed aerosol particles, among which there are also coated mineral dust particles, can trigger the development of precipitation and increase the precipitation efficiency (Yin et al., 2000a). This can be seen from the drop size distributions formed on the cloud processed aerosol particles, which have developed a second maximum in the range of precipitation sized drops (cf. Figs. 1 and 2).

### References

- Levin, Z., Ganor, E. and Gladstein, V. 1996.** The effects of desert particles coated with sulfate on rain formation in the eastern Mediterranean. *J. Appl. Meteor.*, **35**, 1511-1523.
- Reisin, T.G., Levin, Z. and Tzivion, S. 1996.** Rain production in convective clouds as simulated in an axis-symmetric model with detailed microphysics. Part II. Effects of varying drop and ice initialization. *J. Atmos. Sci.*, **53**, 1815-1837.
- Tzivion, S., Feingold, G. and Levin, Z. 1987.** An efficient numerical solution to the stochastic collection equation. *J. Atmos. Sci.*, **44**, 3139-3149.
- Wurzler, S., Levin, Z. and Reisin, T. 2000.** Modification of mineral dust particles by cloud processing and subsequent effects on drop size distributions. *J. Geophys. Res.*, **105**, 4501-4512.
- Yin, Y., Wurzler, S., Reisin, T. G. and Levin, Z. 2000a.** Modification of the size and composition of CCN by cloud processing of mineral dust particles and the effects on cloud microphysics. *Proc. 13<sup>th</sup> Internat. Conf. on Clouds and Prec.*, Aug. 14-18 2000, Reno, Nevada, USA, **2**, 936-939.
- Yin, Y., Levin, Z., Reisin, T.G. and Tzivion, S. 2000b.** The effects of giant nuclei on the development of precipitation in convective clouds. *Atmos. Res.*, **53**, 91-116.

#### Funding

- Bundesministerium für Bildung, Wissenschaft, Forschung und Technologie (BMBF)
- German Israeli Foundation (GIF)

#### Cooperation

- School of the Environment, University of Leeds, Leeds, UK
- Soreq Nuclear Research Center, Yavne, IL
- Department of Geophysics and Planetary Sciences, Tel Aviv University, Tel Aviv, IL



## On the influence of large-eddy simulation (LES)-based turbulence parameters on mesoscale cloud forecast

Jürgen Helmert, Olaf Hellmuth

### Motivation

It is a common view, that with today's computational capabilities modelling of the atmosphere will not be carried out at vertical and horizontal resolutions sufficient to resolve eddies, which are responsible for turbulent transport of heat, mass and momentum in the planetary boundary-layer (PBL). Therefore it seems reasonable to assume that large-scale and mesoscale models will continue to require some form of parameterization of turbulent processes. The description of these subscale effects is a major limitation of present-day weather and climate models.

A general methodology for the improvement of parameterization schemes of mesoscale and large-scale models is provided by the employment of high resolution models in conjunction with data sets for validation.

Owing to the well-known difficulties in performing spatial and temporal high-resolution measurements over areas comparable to the size of a single grid cell of a mesoscale model, we decided to use LES for the generation of datasets suitable for the development of parameterizations for mesoscale and large-scale models. At present, these new parameterizations be implemented in the PBL scheme of the DWD Lokal-Modell. The aim is to elucidate the sensitivity of the mesoscale prediction of clouds and precipitation against the turbulence parameterization, i.e. turbulent PBL fluxes of momentum, heat and humidity.

Here, we use a large-eddy simulation model in cooperation with the Max-Planck-Institut für Meteorologie Hamburg as a high resolution model, that provides time dependent, three dimensional fields of velocity, pressure, temperature and passive scalars.

LES separates the turbulent flow into two parts: a large-eddy (or resolvable-scale) field and a residual (or subgrid-scale) field. The reason for this division is that large scales in a turbulent flow contain most of the energy and flux and therefore are of prime importance. The small-scale motions contain appreciably less energy and are more isotropic and universal in their behaviour.

LES allows to simulate realistic flow conditions in a controlled fashion and gives an insight into PBL properties that have been measured only poorly, if at all.

### Results

First large-eddy simulations of a moist convective boundary layer with developing shallow cumulus clouds using a LES model setup from the 6<sup>th</sup> GCSS (GEWEX Cloud System Study, GEWEX (Global Energy and Water Cycle Experiment)) model intercomparison have been performed.

This setup is based on an idealization of observations made at the Southern Great Plains ARM (Atmospheric Radiation Measurement program of the U.S. Department of Energy) site on 21<sup>st</sup> June 1997. On this day, cumulus clouds developed at the top of a convective boundary layer. The large scale forcing was weak compared to the surface forcing.

This LES run provides a reference data set for the derivation of turbulence parameters, such as variances of wind velocity and temperature, the autocorrelation-length scale and the peak wavelength of the variance spectrum which are the base of new parameterizations for the moist convective boundary layer. Fig. 1 shows the horizontal and time averaged profiles of the wind velocity components and the potential temperature at different output times of the model run. These profiles indicate a convective boundary layer with well developed mixed layer.

The autocorrelation-length scale plays an important role in determining the eddy diffusivity in simple down-gradient flux parameterizations of mesoscale and large-scale models. A review of previous length scale parameterizations reveals large differences, especially in the upper part of the PBL.

We determine this length scale for the vertical velocity and the potential temperature from the high resolution large-eddy simulation run of a convective boundary layer and compared with previous parameterizations. Fig. 2 shows these length scale profiles for the vertical velocity and the potential temperature together with estimated fit functions and commonly used profiles from the literature.

The difference between the LES results and results from the literature are clearly visible.

Obtained turbulence length scale profiles are also implemented in a conceptual model of the turbulence-induced nucleation process of a binary system.

Besides the determination of the autocorrelation length, we use the large-eddy simulation data to determine the peak wavelength profiles of the



variance spectra of the vertical velocity and the potential temperature. The peak wavelength is defined as that wavelength, where the normalized spectral-density function attain its maximum. It is closely related to the autocorrelation-length scale. Both, the peak wavelength and the autocorrelation-length scale serve as important parameters in turbulence parameterization schemes of mesoscale and large-

scale models. The profiles of the peak wavelength for the vertical velocity and the potential temperature are shown in Fig. 3 together with estimated fit functions and commonly used profiles from the literature. The estimated fit functions form the base for the creation of improved turbulence parameterizations of mesoscale and large-scale models.

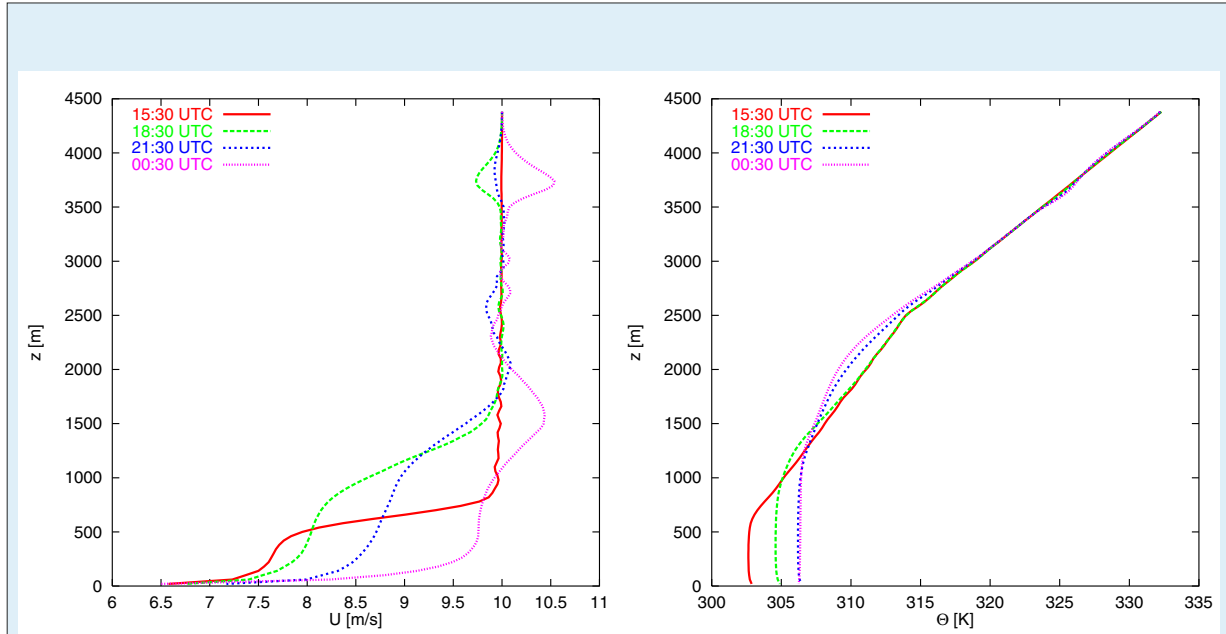


Fig. 1: Vertical profiles of the mean horizontal wind (left) and the mean potential temperature (right) at different output times.

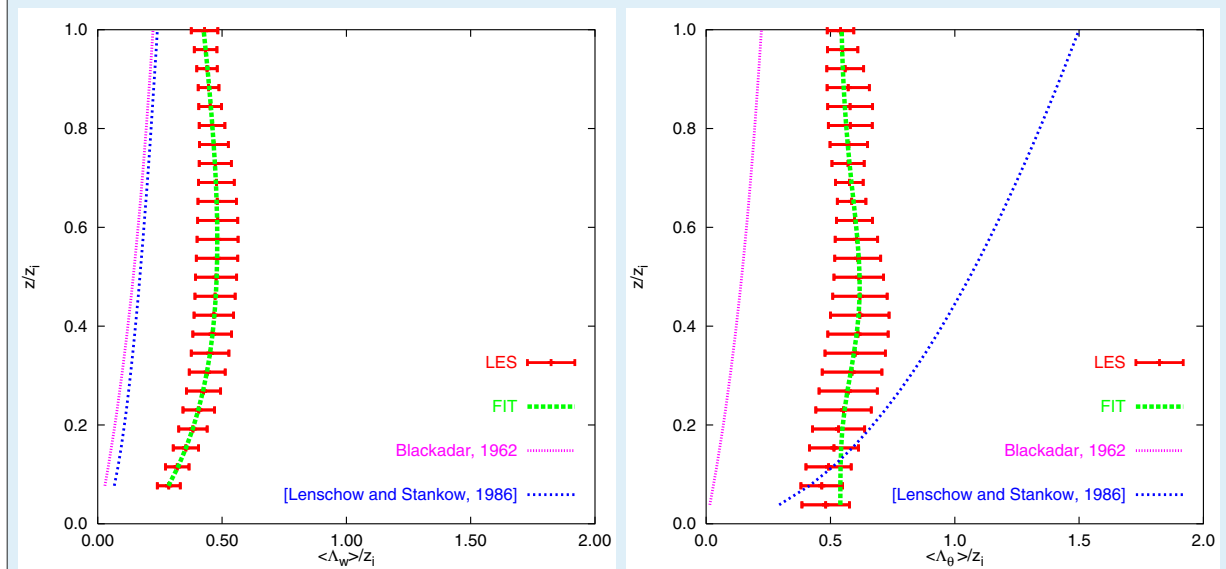
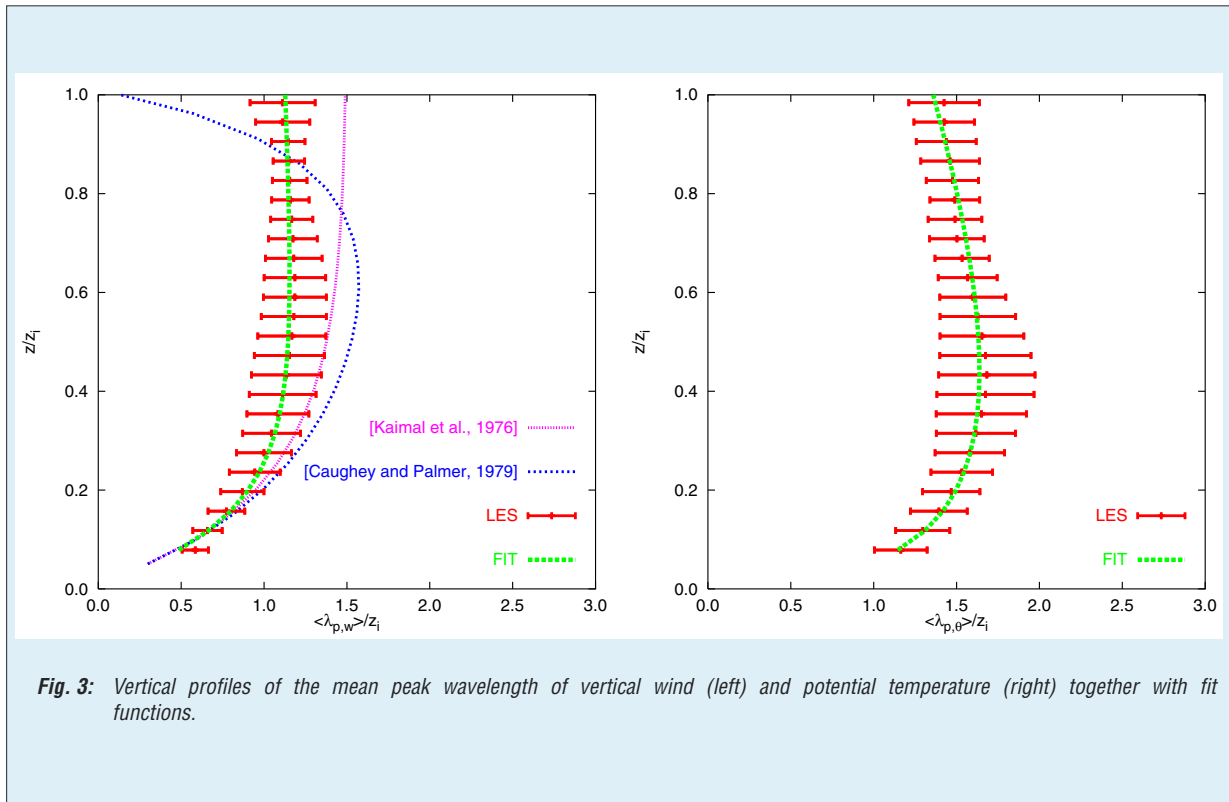


Fig. 2: Vertical profiles of the mean integral length scale of vertical wind (left) and potential temperature (right) together with fit functions.



## References

- Ayotte, K. W., Sullivan, P. P., Andr n, A., Doney, S. C., Holtslag, A. A. M., Large, W. G., McWilliams, J. C., Moeng, C.-H., Otte, M. J., Tribbia, J. J. und Wyngaard, J.C. 1996. An evaluation of neutral and convective planetary boundary-layer parameterizations relative to large-eddy simulations. *Bound.-Layer Meteor.*, **79**, 131-175.
- Blackadar, A. 1962. The vertical distribution of wind and turbulent exchange in a neutral atmosphere. *J. Geophys. Res.*, **67**, 3095-3102.
- Caughey, S. J. and Palmer, S. G. 1976. Some aspects of turbulence structure through the depth of the convective boundary layer. *Q. J. Roy. Meteor. Soc.*, **105**, 811-827
- Hellmuth, O., Helmert, J., Muschinski, A., Sullivan, P. 2000. Determination of convective length scales from a large-eddy simulation of the convective boundary layer. Submitted to the *J. Atmos. Sci.* .
- Kaimal, J.C., Wyngaard, J.C., Haugen, D.A., Cot , O.R., Izumi, Y., Caughey, S.J. and Readings, C.J. 1976. Turbulence structure in the convective boundary layer. *J. Atmos. Sci.*, **33**, 2152-2169.
- Lenschow, D. H. and Stankov, B. B. 1986. Length scales in the convective boundary layer. *J. Atmos. Sci.*, **43**, 1198-1209.

### Cooperation

- Max-Planck-Institut f r Meteorologie Hamburg
- Deutscher Wetterdienst (DWD), Abteilung Forschung und Entwicklung, Offenbach
- Meteorologisches Observatorium Lindenberg



## Tethered balloon measurements with MAPS-Y

Thomas Conrath, Jost Heintzenberg, Dörthe Müller, Sebastian Schmidt, Holger Siebert, Ulrich Teichmann, Manfred Wendisch

Clouds are important for the Earth's climate and the atmospheric radiation budget because they modify significantly the transfer of solar and terrestrial radiation within the atmosphere. One of the major characteristics of clouds is their high spatial and temporal inhomogeneity, especially of their microphysical properties. It is argued that these inhomogeneities are partly responsible for the serious controversy concerning cloud enhanced absorption (i.e. measured absorption is larger than that predicted by models). Turbulent processes may cause part of these cloud inhomogeneities. Thus, in order to resolve reasons for the enhanced cloud absorption, fine-scale turbulent processes have to be investigated. Because of their fast velocity, aircraft cannot deliver all the required measurements with sufficient resolution. Therefore we have started to use a tethered balloon system as platform for meteorological, microphysical and radiative cloud measurements.

The tethered balloon, MAPS-Y (**M**obiles **A**utonomes **P**ositionierungs**S**ystem), is operated by the German army in Elpersbüttel by the North Sea. It is unique in Germany due to its capability to carry a payload of up to 150 kg to a ceiling of 1.1 km with a maximum climb rate of  $3 \text{ m s}^{-1}$ . It is filled with  $400 \text{ m}^3$  of hydrogen and can be maintained for the measurements or in a parking position for several days without re-filling. The balloon has a length of 26 m and a diameter of 6.5 m (cf. Fig. 1).

MAPS-Y carries our new measurement platform, which consists of meteorological (sonic anemometer, a new, very fast wire-resistance thermometer, Lyman- $\alpha$ -hygrometer, navigation system) as well as aerosol (condensation particle counter) and drop (particle volume monitor) microphysical sensors, which allow a sampling frequency between 100 and 500 Hz. The instruments are mounted in a rigid metal frame hanging below the balloon (cf. Fig. 2). Two



**Fig. 1:** MAPS-Y is filling up with hydrogen before start.



campaigns with MAPS-Y, partly combined with concurrent aircraft measurements, have been conducted in April and September/October 2000. An example of vertical profile data sampled through an elevated fog layer is shown in Fig. 3.

The vertical temperature structure is clearly correlated with the cloud layer. At the cloud top a temperature inversion is observed. In the vertical

profile of the liquid water content there are obvious inhomogeneities. The detailed analysis of the measurements is done within the PhD thesis of Holger Siebert. For future measurements we plan to complement the equipment with further drop microphysical (Fast FSSP, forward scattering spectrometer probe) and radiation (albedometer) sensors.



**Fig. 2:** MAPS-Y with the measurement payload.

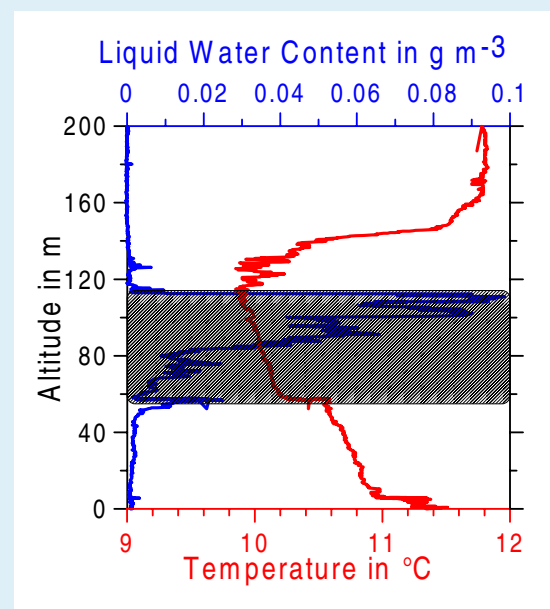


**Fig. 3:** Vertical profiles of liquid water content (blue line, upper axis) and temperature (red line, lower axis) through an elevated fog layer. The cloud region is indicated by the hatched area.

#### Cooperation

- Wehrtechnische Dienststelle für Schiffe und Marinewaffen (WTD71), Bundeswehrrprobungsstelle Elpersbüttel
- Institute of Geophysics, University of Warsaw
- National Center of Atmospheric Research (CNRN), Meteo France, Toulouse



## Particle formation and growth in the lFT laminar flow tube (lFT-LFT)

Torsten Berndt, Olaf Böge, Sylvia Bräsel, Frank Stratmann, Martin Wilck, Markus Witter

A laminar flow tube, the lFT-LFT, was constructed to investigate new particle formation and growth for substances that are relevant in the atmosphere. Two different scenarios, i.e. particle formation in the  $H_2SO_4$ - $H_2O$ -system and in the  $O_3$ - $\alpha$ -pinene-system have been investigated.

### $H_2SO_4$ - $H_2O$ -system

To describe the fluid flow and the particle dynamical processes occurring in the lFT-LFT and to interpret measured size distributions a numerical model was developed. Fluid flow and mass transfer are solved for using the CFD-Code (computational fluid dynamics - Code) Compact-2D (Patankar, 1980). Particle dynamical processes (nucleation, condensation, coagulation) are described utilizing the multicomponent aerosol dynamics modal approach system (MADMAcS) I model (Wilck, 1999). Main emphasis was given to the

quantification of the local binary nucleation rate, i.e. its dependence on the local  $H_2SO_4$  and  $H_2O$  concentrations. The total particle number concentration at the outlet of the lFT-LFT was considered. In Fig. 1 measured number concentrations are plotted as function of  $H_2SO_4$  concentration for three relative humidities (r.h.). Measured (symbols) and modeled (lines) values are depicted.

In Fig. 1 it can be seen that the observed increase of total particle number concentration with increasing  $H_2SO_4$  concentration and r.h. is consistently predicted by the model.

In Fig. 2, the measured r.h. dependence of the total particle number concentration is plotted for different relative acidities (r.a.). For low r.h. values, particle number concentration and consequently the nucleation rate, are strongly dependent on r.h. For higher r.h. a saturation behavior can be observed.

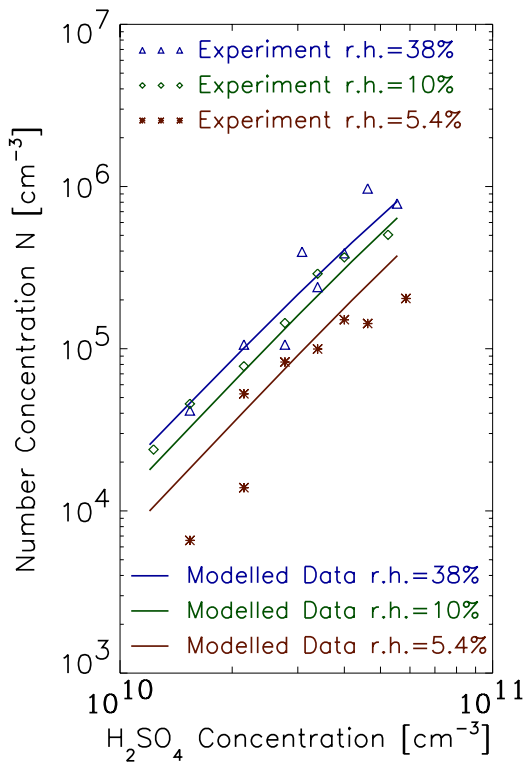


Fig. 1: Total particle number concentration as function of  $H_2SO_4$  concentration.

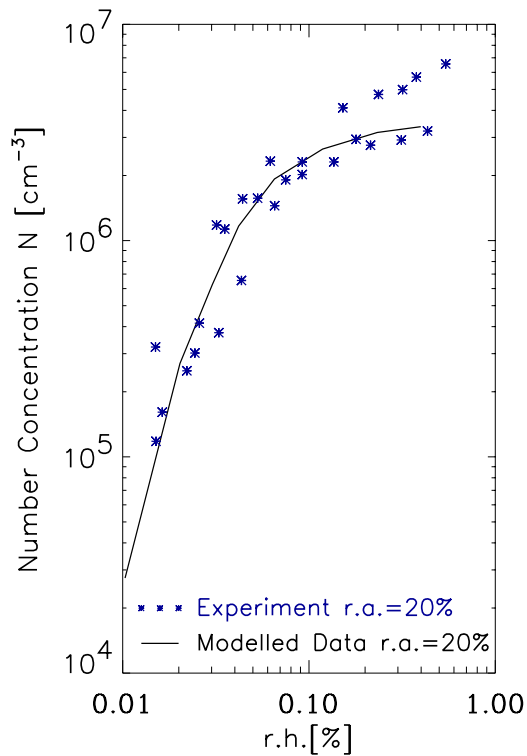


Fig. 2: Total particle number concentration as function of relative humidity.



To describe the measured  $\text{H}_2\text{SO}_4$  and r.h. dependencies in the numerical model, a nucleation rate  $J$  based on a kinetic approach had to be implemented. In this nucleation rate, a stable cluster of a  $(\text{H}_2\text{SO}_4)_2$  and  $n$   $\text{H}_2\text{O}$  molecules was assumed. With the adjustable coefficients  $A$  and  $B$

$$J = \frac{A \cdot [\text{H}_2\text{SO}_4]^2 \cdot [\text{H}_2\text{O}]^n}{B + [\text{H}_2\text{O}]^n}$$

With this approach the measured  $\text{H}_2\text{SO}_4$  and r.h. dependencies could be modeled consistently, i.e. with only one set of coefficients  $A$  and  $B$ . The saturation behavior at high r.h. values is due to i) the increasing influences of coagulation and ii) a reduced exponent  $n$  for the water vapor concentration.

It should be noted that these results are in contradiction to other theoretical and experimental results (e.g., Kulmala et al., 1998, Ball et al., 1999), which is possibly due to influences of  $\text{NH}_3$ , which is to date impossible to measure in the concentration regime of interest, i.e.  $[\text{NH}_3] \approx 1$  ppt.

### $\text{O}_3$ - $\alpha$ -pinene-system

The experiments were conducted at a total pressure of 1000 mbar of synthetic air in the

absence of an OH radical scavenger using FT-IR (Fourier transform infrared) and GC-MS (gas chromatography-MS) measurements for the detection of the gaseous products and a differential mobility particle sizer (DMPS) for newly formed particles. The initial concentration of  $\alpha$ -pinene was  $(7.3 - 870) \times 10^{11}$  molecule  $\text{cm}^{-3}$  and for  $\text{O}_3$   $(3.0 - 46) \times 10^{12}$  molecule  $\text{cm}^{-3}$ . The average residence time was 140 s.

$\alpha$ -Pinene oxide and pinonaldehyde were identified as gaseous products and their formation yield was obtained in dependence on the amount of reacted  $\alpha$ -pinene.  $\alpha$ -Pinene oxide was found to be independent of experimental conditions with a formation yield of  $0.09 \pm 0.03$ . For the pinonaldehyde yield, a significant increase with decreasing amount of reacted  $\alpha$ -pinene was observed resulting in a maximum value of  $0.62 \pm 0.06$  for  $\Delta[\alpha\text{-pinene}] < 2 \times 10^{12}$  molecule  $\text{cm}^{-3}$ . Using a simple reaction scheme, from the observed formation yields of both gaseous products a maximum value for the OH radical yield of 0.41 was estimated:

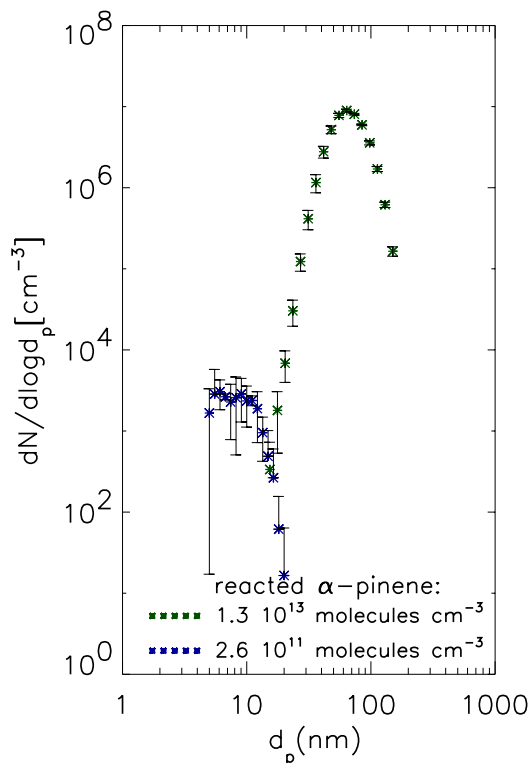
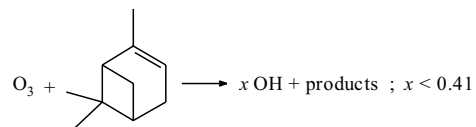


**Fig. 3:** Measured particle size distributions for different amounts of reacted  $\alpha$ -pinene.

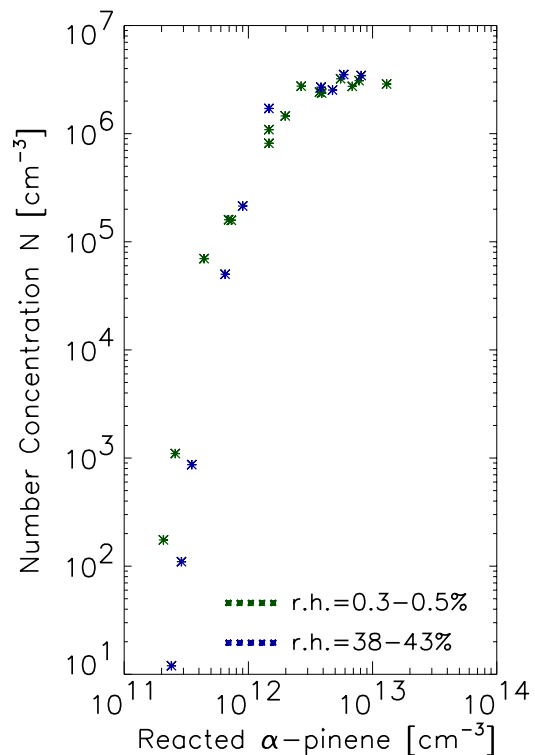


**Fig. 4:** Particle number as function of the amounts of reacted  $\alpha$ -pinene.



The reported OH radical yields for this reaction in the literature are significantly higher, 0.70 – 0.85 (Finlayson-Pitts and Pitts, 2000).

Simultaneously to the analysis of the gaseous products, newly formed particles were measured. Fig. 3 shows size distributions for the case of a low or high amount of reacted  $\alpha$ -pinene. It can be seen that the particle number concentration and volume increase with amount of reacted  $\alpha$ -pinene. In Fig. 4 for two ranges of the relative humidity (0.3 – 0.5 % and 38 – 43 %) the total number of newly formed particles as a function of reacted  $\alpha$ -pinene is plotted.

Below the saturation level (particle number  $< 10^6$   $\text{cm}^{-3}$ ), under "dry" conditions the number of newly formed particles was somewhat higher compared to the "wet" conditions. Generally, the particle number (also volume and surface) was found to

be strongly affected by the amount of reacted  $\alpha$ -pinene. Increasing the reacted  $\alpha$ -pinene from  $10^{11}$  to  $10^{12}$  molecule  $\text{cm}^{-3}$  the particle number increased by 5 – 6 orders of magnitude. The increase in both particle number and particle volume is anti-correlated with the formation yield of pinonaldehyde indicating that pinonaldehyde itself or a precursor represent particle components. The results for the reaction of  $\text{O}_3$  with  $\alpha$ -pinene indicate that under realistic atmospheric conditions a contribution to the formation of new particles is negligible.

Generally, the new flow tube reactor (IFT-LFT (laminar flow tube)) was found to be suitable to investigate particle formation processes from the  $\text{H}_2\text{SO}_4$ - $\text{H}_2\text{O}$  system as well as from the gas-phase ozonolysis of  $\alpha$ -pinene.

## References

- Ball, S.M. Hanson, D.R., Eisele, F.L., McMurry, P.H. 1999.** Laboratory studies of particle nucleation: Initial results for  $\text{H}_2\text{SO}_4$ ,  $\text{H}_2\text{O}$ , and  $\text{NH}_3$  vapors. *J. Geophys. Res.*, **104**, D19, 23709-23718.
- Finlayson-Pitts, B.J. and Pitts, Jr., J.N. 2000.** *Chemistry of the Upper and Lower Atmosphere*, Academic Press, San Diego.
- Kulmala, M., Laaksonen, A., Pirjola, L. 1998.** Parametrizations for sulfuric acid/Water nucleation rates. *J. Geophys. Res.*, **103**, 8301-8307.
- Patankar, S.V. 1980.** *Numerical Fluid Flow and Heat Transfer*, Mc-Graw-Hill Book Company, New York.
- Wilck, M. 1999.** *Modal Modelling of Multicomponent Aerosols*, VWF Verlag für Forschung GmbH, Berlin, 1999.



## The effect of subgrid scale turbulence on the formation of new particles

Olaf Hellmuth, Jürgen Helmert

### Introduction

Abundant sulfate particles in the atmosphere may have an important direct and indirect effect on Earth's climate. There are a large number of empirical findings from in situ measurements indicating that these particles are formed in various parts of the atmosphere, that is, in the free troposphere, in the marine boundary layer, in the vicinity of evaporating clouds, in Arctic areas etc.. Binary homogeneous nucleation of sulfuric acid and water vapor has been widely accepted to be the principal mechanism for new particle formation in the atmosphere. In this process two species form molecular clusters that grow sufficiently in size to form spontaneously stable particles corresponding to the Kelvin radius. An important feature of that mechanism is that, unlike homogeneous nucleation of a single species, binary homogeneous nucleation can occur when the concentrations of both species are below their respective saturations (Easter and Peters 1994).

There exist some obscurities in the thermodynamics of the formation process, such as the affinity of sulfuric acid to form hydrates in the gas phase and the participation of a third molecule (ammoniac) in the nucleation process. Also the influence of radiation, vertical transport processes and the related turbulent mixing processes are not yet understood.

Closely related to this is the question, how to deal with the scale dependency of the nucleation process in mesoscale and large scale models. Numerical models are designed in terms of "grid scale variables", that represents spatio-temporal averaged mean values over grid cell volume and model time step. The averaging procedure can be described by a filter operator. Subgrid scale processes cannot be resolved by the model grid, thus they must be parameterized. Assuming that the nucleation rate can be described by a process function (for instance a numerical process model, an analytical function, or a multidimensional parameter look-up-table), then the usual approach is to replace the grid scale value of the process function with the process function of their grid scale parameters. In the case of binary nucleation the grid scale parameters are temperature, partial pressure of water vapor and sulfuric acid. Such an approach is only valid for a linear process function. Unfortunately, this is not the case for condensation processes.

Easter and Peters (1994) evaluated the effect of turbulent-scale variations on the binary homogeneous nucleation rate for correlated and uncorrelated fluctuations of the temperature and water vapor. They found, that for the anticorrelation of temperature and humidity (top of the planetary boundary layer (PBL)) the turbulence induced nucleation rate (grid scale or mean process function) is up to seventy times larger than the bulk nucleation rate (function of grid scale parameters). They concluded, that as we try to measure these phenomena in the atmosphere, **it is not sufficient to consider only mean conditions in evaluating field data, but also concentration, temperature, and humidity fluctuations must be considered.**

### Model results

Here, we present first results of the influence of subgrid scale turbulence on the nucleation rate in a steady-state planetary boundary layer (PBL). The PBL model consists of a coupled system of diagnostic differential equations for the grid scale potential temperature, the water vapor mixing ratio, sulfuric acid concentration, the wind velocity as well as the turbulent kinetic energy and the variances of temperature, water vapor mixing ratio and sulfuric acid content. The model has been initialized using well-defined profile-gradient relations from the similarity theory, as well as length scale parameterizations from large-eddy simulations, whereas the vertical profile of sulfuric acid has been scaled assuming similarity theory arguments as for water vapor. The model boundary conditions are set up by scaling properties (friction velocity, scaling temperatures, Bowen ratio, mixing layer height, entrainment heat flux ratio etc.). The model is used to predict grid scale temperature, relative humidity, and acidity (ratio of partial pressure to saturation vapor pressure for sulfuric acid) as well as their second moments (Figs. 1-4) for the specification of the probability density function of the nucleation process, which is a part of the filter operator. The process function is calculated using the numerical nucleation model of Kulmala et al. (1998) for homogenous binary nucleation including hydration effects.

Fig. 5 shows the nucleation rate as a function of the grid scale temperature, humidity and acidity (bulk nucleation rate), and the nucleation rate as the function of grid scale parameters and their second order moments (mean nucleation rate). Both, the

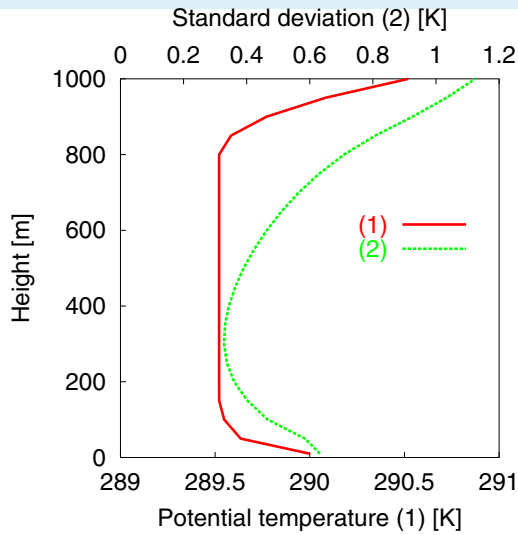


Fig. 1: Potential temperature (1) and standard deviation (2).

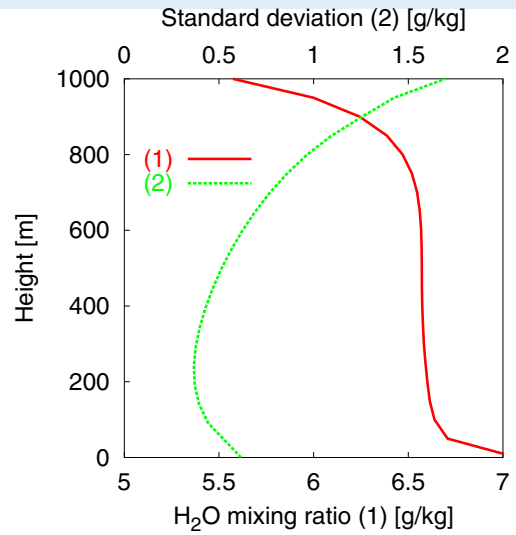


Fig. 2: Water vapor mixing ratio (1) and standard deviation (2).

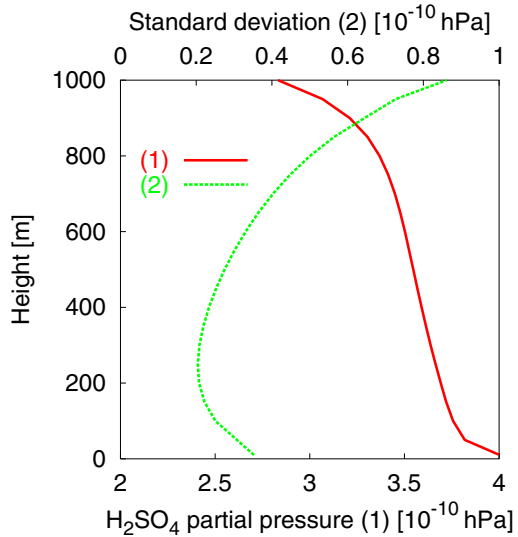


Fig. 3: Sulfuric acid partial pressure (1) and standard deviation (2).

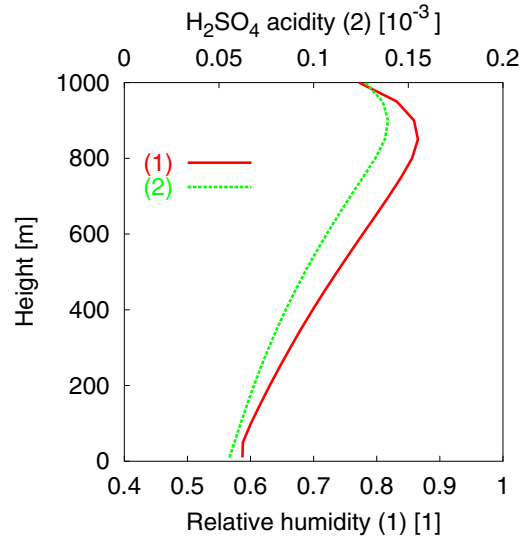


Fig. 4: Relative humidity (1) and acidity (2).

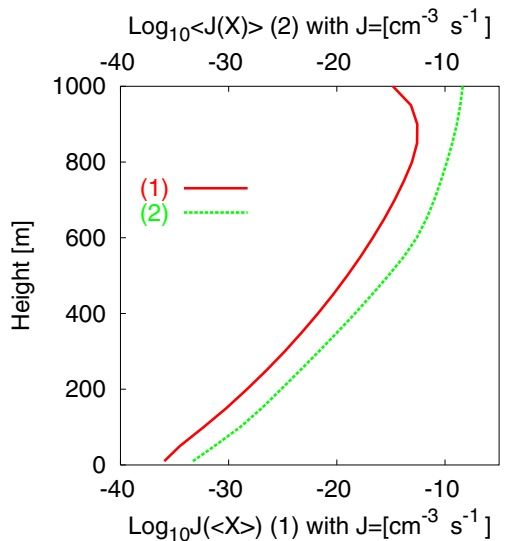


Fig. 5: Comparison of bulk nucleation rate (1) and gridscale nucleation rate (2).

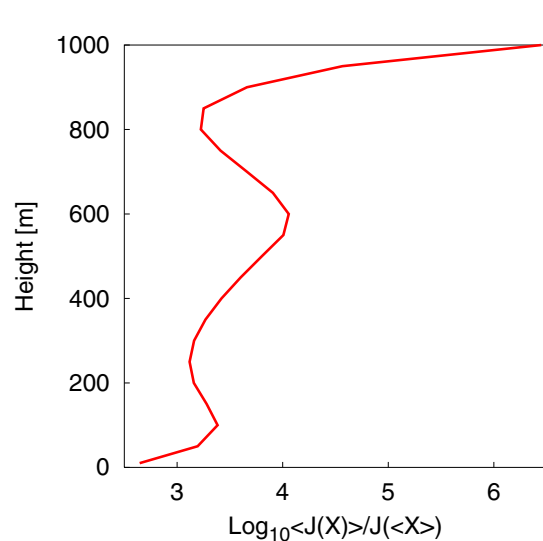


Fig. 6: Orders of magnitude of the ratio of gridscale to bulk nucleation rate.



bulk nucleation rate as well as the mean nucleation rate increases by several orders of magnitude with height. The bulk nucleation rate assumes its maximum below, the mean nucleation rate at the PBL top. While Easter and Peters (1994) reported a difference between mean and bulk nucleation rate of maximal two orders of magnitude (factor  $\sim 70$ ), we find in Fig. 6 a difference of up to six orders of magnitude for the present PBL setup (factor  $\sim 10^6$ ). However, it can be shown that the differences can very easily assume much higher orders of magnitude.

### Conclusions

The effect of subgrid turbulence can exceed orders of magnitude that are comparable to the

effect of hydration of sulfuric acid as well as ternary nucleation including ammoniac (Korhonen et al., 1999). Thus, the subgridscale effect is not negligible, and the gridscale nucleation rate should be applied in mesoscale and climate models rather than its bulk property. For application in the chemistry-transport model MUSCAT we are going to parameterize the gridscale nucleation rate in terms of gridscale parameters and their second order moments. The present approach can be applied also to other, highly nonlinear subgridscale processes, such as coagulation and cloud condensation processes.

Our findings support the importance of second order moments for treatment of aerosol and cloud physics in dynamical models.

### References

- Easter, R., and Peters, L. K. 1994. Binary homogeneous nucleation: temperature and relative humidity fluctuations, nonlinearity, and aspects of new particle production in the atmosphere. *J. Appl. Met.*, **33**, 775-784.
- Kulmala, M., Laaksonen, A., and Pirjola, L. 1998. Parameterization for sulfuric acid/ water nucleation rates. *J. Geophys. Res.*, **103**, D7, 8301-8307.
- Korhonen, P., Kulmala, M., Laaksonen, A., Viisanen, Y., McGraw, R., and Seinfeld, J.H., 1999. Ternary nucleation of sulfuric acid, ammoniac and water vapor in the atmosphere. *J. Geophys. Res.*, **104**, D21, 26349-26353.

#### Cooperation

- Department of Physics, University of Helsinki, Helsinki, Finland
- Deutscher Wetterdienst (DWD), Abteilung Forschung und Entwicklung, Offenbach

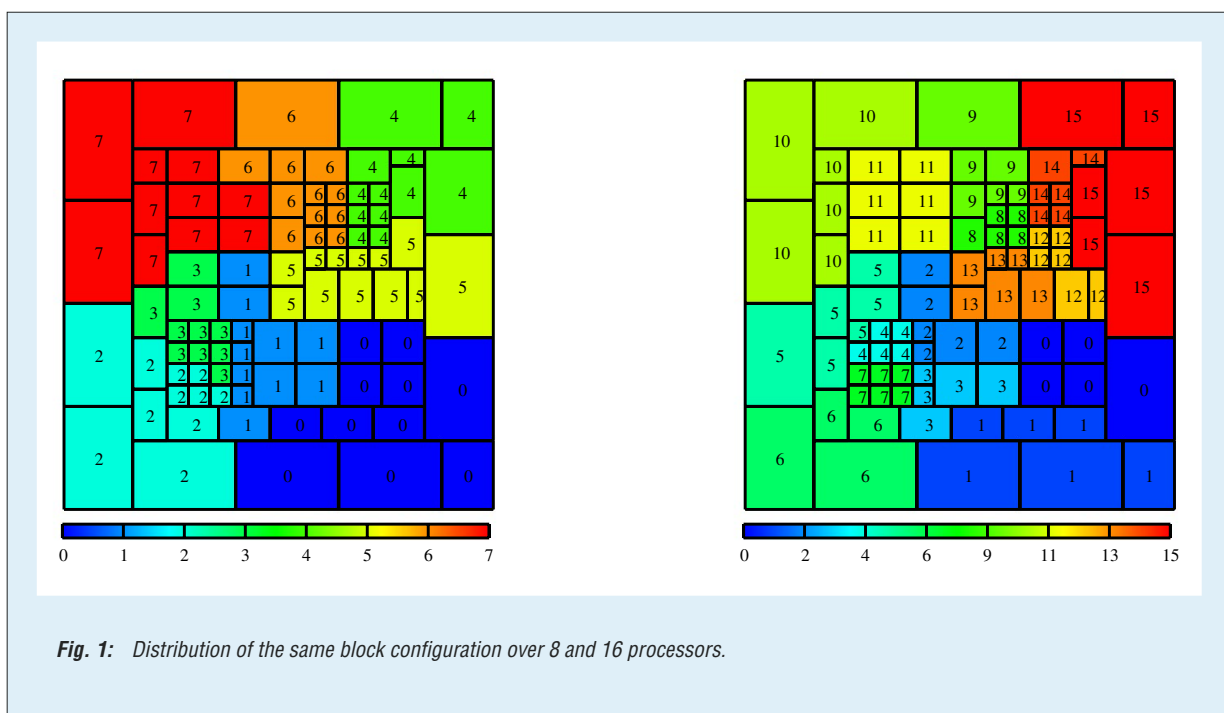


## Parallelization of Chemistry-Transport Models

Oswald Knoth, Ralf Wolke, Jörg Weickert

In chemical transport models, chemical reactions and the transport of species are described by very large and stiff systems of differential equations. To date, one limitation of schemes has been their inability to solve equations both quickly and with a high accuracy in multiple grid cell models. This requires the use of fast parallel computers. Multiblock grid techniques and implicit-explicit (IMEX) time integration schemes are suited

of columns) as measure of the work load of the respective block. Therefore, the total number of horizontal cells of each processor is to be balanced. This is achieved by the grid-partitioning tool ParMETIS (Karypis et. al., 1998). It optimizes both the balance of columns and in addition the "edge cut", i.e., it takes care of short inter-processor border lines. A distribution of 90 blocks to eight and 16 processors is shown in Fig. 1.



to benefit from the parallel architecture (Wolke and Knoth, 2000). A parallel version of the multiscale chemistry-transport code MUSCAT is presented which is based on these techniques. The special grid structure of the model originates from dividing an equidistant horizontal grid into rectangular blocks of different size. Each block can be coarsened or refined separately. This is done on condition that the grid size of neighbouring blocks differ by one level at the most. The maximum size of the already refined or coarsened blocks is limited by a given maximum number of columns.

Our parallelization approach is based on the distribution of blocks among the processors. We consider a static partitioning where the blocks are distributed between the processors only once at the beginning of the execution of the program. Here, we use the number of horizontal cells (i.e.,

Inter-processor communication is realized by means of the message passing interface language MPI. An exchange of data over block boundaries is necessary only once during each horizontal advection step. Each block needs the concentration values in one or two cell rows of its neighbours, according to the order of the advection scheme. The implementation of the boundary exchange is not straightforward because of the different resolutions of the blocks. The possibilities of one cell being assigned to two neighbouring cells or of two cells receiving the same value must be taken into account. We apply the technique of "extended arrays" where the blocks use additional boundary stripes on which incoming data of neighbouring blocks can be stored. Hence, each processor only needs memory for the data of blocks that are assigned to it.



Unfortunately the size of each block is only a crude estimate of the necessary work in the course of the integration of the chemistry-transport equations in time. These load imbalances are due to the sophisticated error control inside the used numerical algorithms. In order to improve the load balance, techniques allowing for redistribution of blocks have been implemented (Wolke et al. 2000). The workload of a block work is estimated using the numbers of Jacobian  $N_J$  and function evaluations  $N_F$  applied during a past time period. They represent measures of the expense of factorizing the system matrix and solving the resulting systems. The work load of processor  $P$  is defined by

$$a_P = \sum_{B \in P} (N_{FB} + 1.4 * N_{JB}) * N_{CB},$$

where the factor 1.4 balances the workload of the two parts.  $B \in P$  stands for the blocks currently located on this processor,  $N_{CB}$  is the number of columns of block  $B$ . For repartitioning, we again

use ParMETIS which is called if the ratio

$$\frac{\min_P a_P}{\max_P a_P}$$

falls below a certain critical value. According to the work loads of the blocks, ParMETIS searches for a better distribution, besides minimizing the movements of blocks. The communication required for the exchange of block data can be done by means of similar strategies as for the boundary exchange.

Fig. 2c and 2d show the partitions in the beginning and the end of a twelve hour simulation using four processors. The test is performed for an ozone scenario for the Saxony area (Fig. 2a) using a multiscale grid. Judging the work load, we compare the estimated work loads and the actual CPU times for runs with and without dynamic load balancing. Both values are the sum of all time steps, where in each step the "slowest" processor is considered. The results are given for two different relative tolerances  $RTOL$  of the implicit integrator (Tab. 1) and have been determined on a SGI Origin 2000.

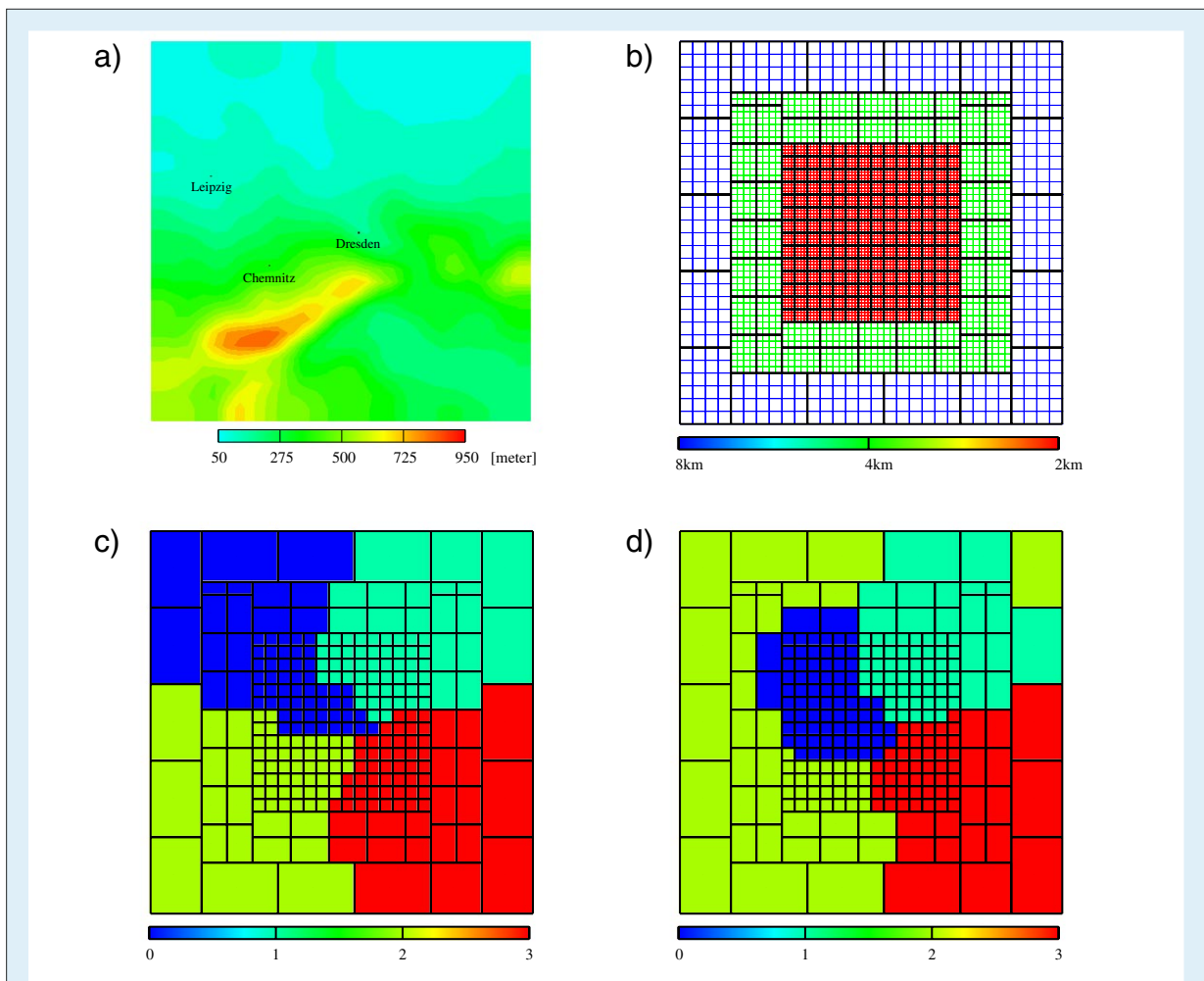


**Fig. 2:** "Ozone in Saxony": Orography of the simulation area (a), multiscale 2km-4km-8km grid (b), block distribution for 4 processors in the beginning (c) and the end of a 12 hours simulation (d).



The estimated improvement in execution time through the above model is in good agreement with the actual improvement measured by the reduced CPU time. This means that the cost function is a good measure for the workload of a single block. Furthermore, Tab. 1 shows that for tighter

tolerances RTOL dynamic load balancing leads to a larger reduction in the CPU time. The results of the 8 and 16 processors run on the CRAY T3E demonstrate the almost linear speedup of the parallel transport code MUSCAT.

RTOL	CPU time		improvement	
	static	dynamic	CPU	estimated
SGI (4 processors)				
1.e-2	4:17 hours	4:04 hours	94,9 %	94,2 %
1.e-3	6:57 hours	6:02 hours	86,4 %	93,6 %
T3E (8 processors)				
1.e-2	1:18 hours	1:16 hours	98,3 %	98,7 %
1.e-3	1:48 hours	1:27 hours	80,4 %	83,3 %
T3E (16 processors)				
1.e-2	0:45 hours	0:44 hours	97,0 %	96,9 %
1.e-3	0:58 hours	0:52 hours	89,8 %	88,7 %

Tab. 1: CPU times for the ozone scenario in Saxony for different number of processors.

### References

**Karypis, G., Schloegel, K., and Kumar, V. 1998.** ParMETIS. Parallel graph partitioning and sparse matrix ordering library. Version 2.0. University of Minnesota.

**Wolke, R., and Knoth, O. 2000.** Implicit-explicit Runge-Kutta methods applied to atmospheric chemistry-transport modelling. Environ. Model. Software, **15**, 711-719.

**Wolke, R., Knoth, O., and Weickert, J. 2000.** Load balancing in the parallelization of the multiscale atmospheric chemistry-transport model MUSCAT. 16<sup>th</sup> IMACS World Congress, Lausanne, Switzerland, 21-25. August, 2000, CD-ROM, 7 p.

#### Funding

- Deutsche Forschungsgemeinschaft

#### Cooperation

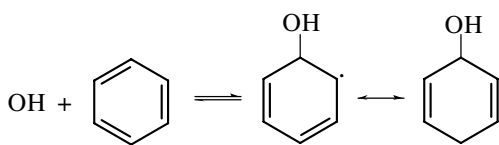
- Meteorologisches Institut und Institut für Informatik der Universität Leipzig
- John von Neumann Institut für Computing, Forschungszentrum Jülich
- Zentrum für Hochleistungsrechnen der Technische Universität Dresden



## The gas-phase reaction of OH radicals with benzene

Torsten Berndt, Olaf Böge

Benzene and a series of alkylated derivatives (toluene, xylenes, etc.) are predominantly emitted into the atmosphere by human activities (car traffic, solvent use). In urban areas, atmospheric mixing ratios up to 30 ppb have been measured (Finlayson-Pitts and Pitts, 2000). Under atmospheric conditions, the degradation process of benzene is exclusively initiated by the addition of OH radicals forming the OH-adduct radical (Atkinson, 1994).



The atmospheric fate of the resonance stabilized OH-adduct radical is governed by the reaction with  $O_2$  (Knispel *et al.*, 1990; Bohn and Zetzsch,

1999). The products of the reaction of  $O_2$  with the OH-adduct radical are still uncertain. Klotz *et al.*, 1997 proposed the formation of benzene oxide / oxepin as the primary products of the reaction of  $O_2$  with the OH-adduct radical. As a result of an experimental study from this laboratory, the formation of benzene oxide / oxepin was found to be negligible (Berndt *et al.*, 1999). The aim of the present work is to determine the first stable reaction products under different experimental conditions.

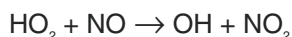
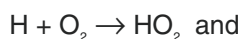
The experiments have been performed in a flow tube (2.0 cm i.d. quartz glass, 45 cm long) at  $T = 295 \pm 2$  K in different He/ $O_2$  mixtures at a total pressure of 100 mbar and a bulk velocity of  $1.45$  m  $s^{-1}$ . For product identification on-line GC-MS (gas chromatography-mass spectrometry) (HP 5890 with HP-MSD 5971) as well as Fourier transform infrared (FTIR) measurements (Nicolet Magna 750) were used.



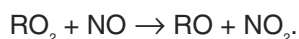
Fig. 1: Experimental set-up for studies of the reaction of OH radicals with aromatics.

**Experiments for the reaction of the OH-adduct with O<sub>2</sub> in the presence of NO:**

The experimental conditions were chosen so that the OH-adduct radicals reacted predominantly with O<sub>2</sub> producing peroxy radicals and after the consecutive reaction with NO the corresponding oxy radicals. OH radicals were produced from the sequence:

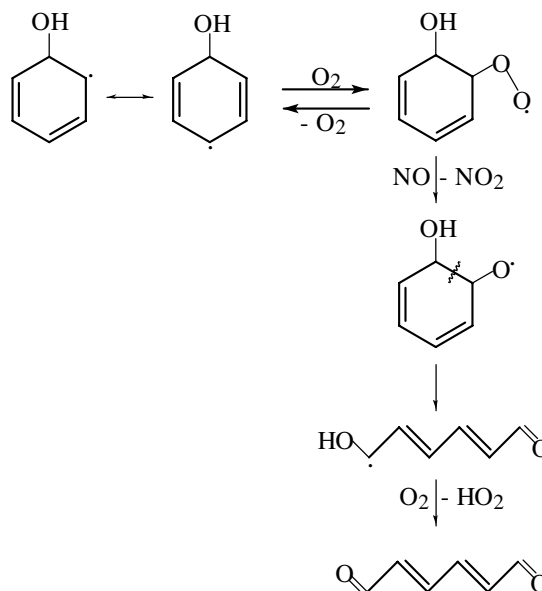


By means of GC-MS analysis *p*-benzoquinone, phenol, *cis,trans*- and *trans,trans*-2,4-hexadienedial and nitrobenzene were identified using authentic samples of reference substances in each case. Also in the FT-IR spectra, absorptions arising from these substances were observed. With increasing NO concentration an increase of produced NO<sub>2</sub> was found resulting in a saturation level for a large excess of NO. This fact can be explained by a more important reaction of peroxy radicals with NO with increasing NO concentration *via*



Stable products of the corresponding oxy radicals are the observed 2,4-hexadienedials with a maximum formation yield of 0.44. For phenol a noticeable decrease of the product yield was found for [NO] > 10<sup>14</sup> molecule cm<sup>-3</sup> (phenol yield for low NO concentrations: 0.20). *p*-Benzoquinone was found to be produced independent of the NO concentration with a yield of 0.08. The yield of nitrobenzene increased with increasing

NO concentration up to a value of *ca.* 0.09. The following reaction scheme explains possible pathways for the generation of 2,4-hexadienedial. For simplification the *trans,trans*-species is shown only.



The 2,4-hexadienedials, often discussed in the literature to be products of the atmospheric benzene oxidation, were detected for the first time as a result of this study. Further experiments are in progress under more realistic conditions (*p* = 500 mbar, [O<sub>2</sub>] = 9 × 10<sup>18</sup> molecule cm<sup>-3</sup>). Subject of these studies is the product formation in the presence of low NO<sub>x</sub> concentrations with special attention to phenol and carbonylic substances.

**References**

- Atkinson, R., 1994:** Gas-Phase Tropospheric Chemistry of Organic Compounds, J. Phys. Chem. Ref. Data Monograph No. 2, 47.
- Berndt, T., Böge, O., and H. Herrmann, 1999:** On the formation of benzene oxide / oxepine in the gas-phase reaction of OH radicals with benzene, Chem. Phys. Lett. 314, 435.
- Bohn, B. and C. Zetzsch, 1999:** Gas-phase reaction of the OH-benzene adduct with O<sub>2</sub>: reversibility and secondary formation of HO<sub>2</sub>, Phys. Chem. Chem. Phys. 1, 5097.
- Klotz, B., Barnes, I., Becker, K.H., and B.T. Golding, 1997:** Atmospheric chemistry of benzene oxide / oxepine, J. Chem. Soc. Faraday Trans. 93, 1507.
- Knispel, R., Koch, R., Siese, M., and C. Zetzsch, 1990:** Adduct Formation of OH Radicals with Benzene, Toluene, and Phenol and Consecutive Reactions of the Adducts with NO<sub>x</sub> and O<sub>2</sub>, Ber. Bunsenges. Phys. Chem. 94, 1375.
- Finlayson-Pitts, B.J. and J.N. Pitts, Jr., 2000:** Chemistry of the Upper and Lower Atmosphere, Academic Press, San Diego.

**Cooperation:**

- Fraunhofer Institut für Toxikologie und Aerosolforschung Hannover



## Direct investigations of OH reactions in aqueous solution

Johannes Hesper, Hartmut Herrmann

### Introduction

Free radicals play an important role in the chemistry of the aqueous tropospheric particle phase (Zellner and Herrmann, 1995). In order to assess the importance of the OH-radical kinetic data for reactions with relevant organic compounds are needed. The rate constants and the activation energies of reactions of the OH-radical with some organic compounds have been investigated for different temperatures and high ionic strengths.

### Experimental Methods

Up to now most kinetic investigations of the OH-radical in aqueous solution have been performed by competition kinetics, i.e. by competition of two reactions, one with a known and one with an unknown rate constant. One of the standard competition kinetics methods for OH reactions in solution makes use of thiocyanate (Chin and Wine, 1994).

The problem of this method is the possible side reaction of  $\text{HO}^-\text{SCN}^-$  and/or  $\text{SCN}^-$  which possibly could also react with the substrate. As a consequence, the obtained rate constant would be overestimated. For this method a good knowledge of the competitor kinetics (rate constants at different temperatures, ionic strengths, pH-values and the exact reaction pathway) is necessary.

A direct method was developed to determine the time dependence of OH-radical concentrations in the aqueous phase. An OH source was developed and with the help of a CCD-Camera spectroscopically investigated. In Fig. 1 the instrumental setup for spectroscopic investigations is shown.

The OH-radical is formed by excimer laser flash photolysis of water at 193 nm (active medium ArF):

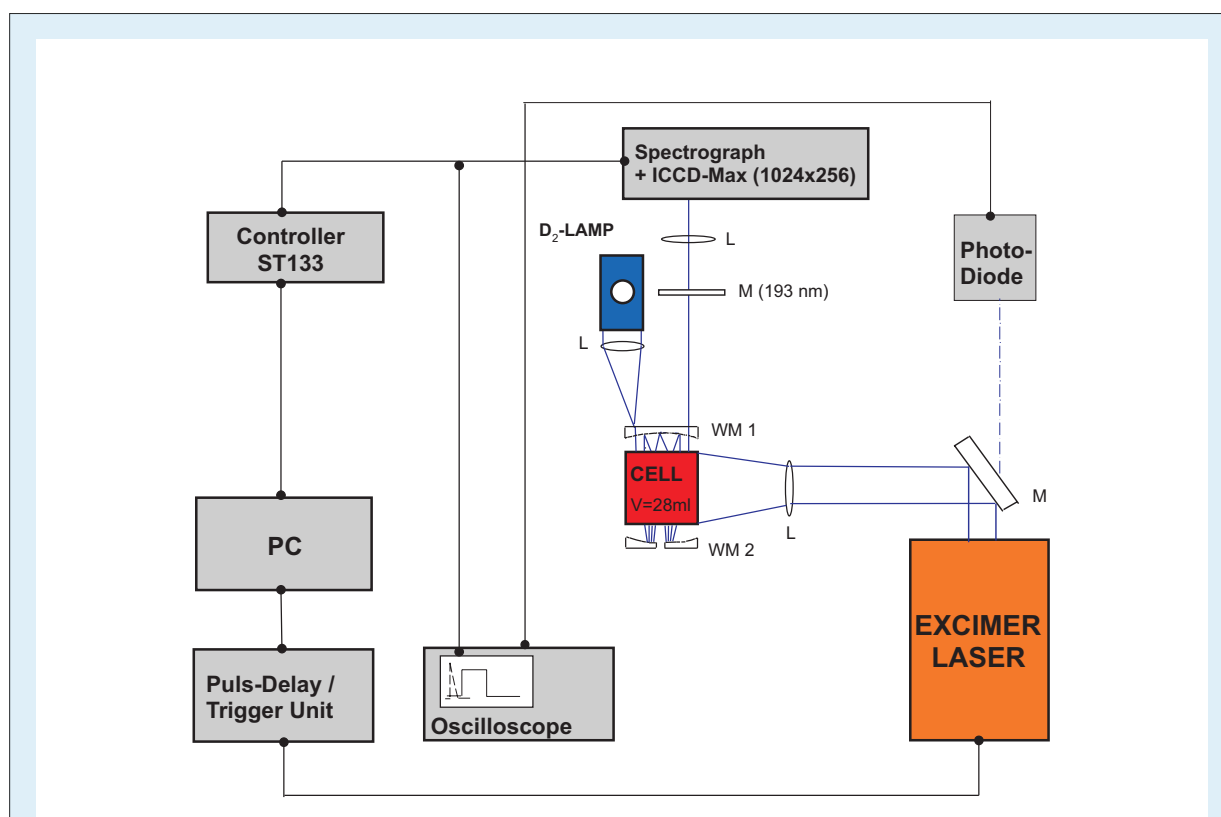
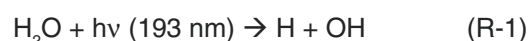


Fig. 1: Laser-photolysis-long-path-absorption (LP-LPA) apparatus for the study of radical reactions in aqueous solution.



The analyzing light source is a water cooled Deuterium lamp (UV-light) folded 8 times through the cell (28 ml) by the help of mirrors (WM1 and WM2) in White configuration to increase the sensitivity of the system. A combination of CCD-Camera (exposure time down to 2 ns) and grating (3 different gratings) was used to measure the absorption spectra of the radicals in the range of 200 nm to 400 nm.

The obtained absorption spectrum of the OH-radical (black line) is shown in Fig. 2. It is in reasonable agreement with the known literature.

temperatures and ionic strengths via  $\text{RO}_2$  product build-up kinetics.

### Kinetic results

The first investigations were performed to evaluate the kinetic setup. At first the reaction of OH with ethanol was investigated.

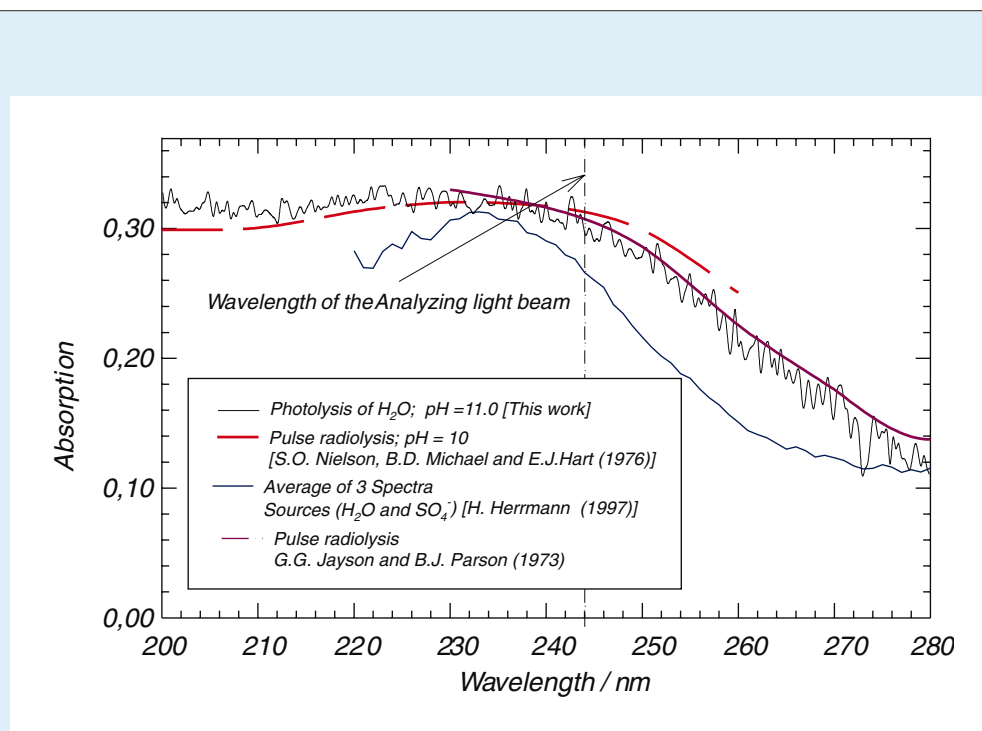


Fig. 2: Absorption spectra of the OH-radical in aqueous solution (this work - average of 4800 spectra).

Using these data (extinction coefficient  $\epsilon_{(\text{OH})244,10} = 500 \text{ l}\cdot\text{mol}^{-1}\text{cm}^{-1}$ ) the experimental setup was modified to observe the formation of  $\text{RO}_2$ -radicals (R-4). In the kinetic investigations of the  $\text{RO}_2$ -formation the interference by  $\text{HO}_2$ -radicals and OH-decay were taken into account. The  $\text{HO}_2$ -radical is absorbing at 244 nm ( $\epsilon_{244,10} = 1080 \text{ l}\cdot\text{mol}^{-1}\text{cm}^{-1}$ ).



The analyzing light source is now a frequency doubled Argon-ion-laser with an output wavelength of 244 nm (near the absorption maximum of the OH-radical). The detector unit used is a sensitive photodiode connected to a digital oscilloscope. With this setup it is possible to measure rate constants of OH-radicals with organic substances of relevance for tropospheric chemistry at different

The hydroxy-alkyl-radical ( $\text{CH}_3\text{CHOH}$ ) quickly reacts with oxygen:



The hydroxyethylperoxyl radical  $\text{CH}_3\text{C}(\text{O}_2)\text{HOH}$  has an absorption maximum at 244 nm ( $\epsilon_{244,10} = 1180 \text{ l}\cdot\text{mol}^{-1}\text{cm}^{-1}$ ). After the correction following results shown in Fig. 3 were obtained.

The observed rate constant  $k_{2\text{nd}} = (2.0 \pm 0.3) \cdot 10^9 \text{ l}\cdot\text{mol}^{-1}\text{s}^{-1}$  is in good agreement with the known literature values (e.g., Park and Getoff (1992);  $k_{2\text{nd}} = 1.9 \cdot 10^9 \text{ l}\cdot\text{mol}^{-1}\text{s}^{-1}$ ). This reaction was also investigated in the present study in the temperature interval from 288 K to 328 K to obtain the activation energy  $E_A$   
 $E_A(\text{OH} + \text{Ethanol}) = 14 \pm 4 \text{ kJ/mol}$ .

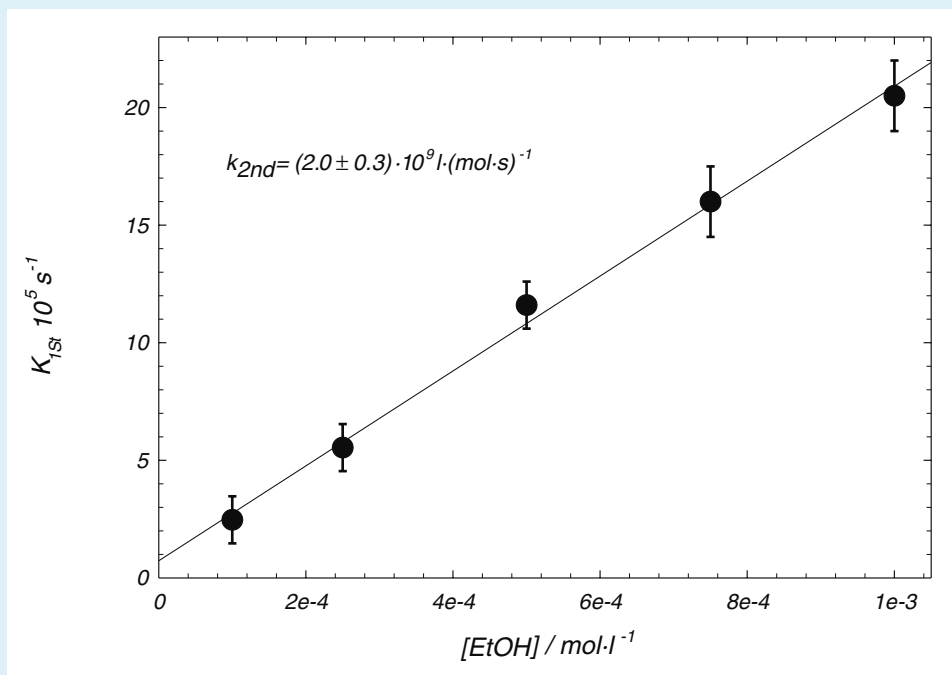


Fig. 3:  $k_{1st} = f([CH_3CH_2OH])$  for the reaction of  $\cdot OH$ -radical with ethanol;  $T = 298$  K;  $pH = 2.0$ .

No data on the T-dependence are available from literature. The system was also investigated for the first time at different ionic strengths ( $NaClO_4$  as an inert salt).

The reaction of  $OH + 2$ -Propanol including its temperature dependence in the range of 288 – 328 K was investigated next. The obtained values

at 298 K are in good agreement with available literature data.

The next step will be the investigation of substances more atmospherically relevant at different temperatures and ionic strengths, where no or only few literature values exist.

## References

- Zellner, R., and Herrmann, H. 1995. Free Radical Chemistry of the Aqueous Atmospheric Phase, R.J.H. Clark and R.E. Hester (Ed.). In *Spectroscopy in Environmental Science*. Wiley and Sons Ltd. **24**, 381-451.
- Chin, M., and Wine, P.H. 1992. A temperature-dependent kinetic study of the aqueous phase reactions  $OH + SCN^- \rightarrow SCNOH$  and  $SCN + SCN^- \rightarrow (SCN)_2^-$ . *J. Photochem. Photobiol.* **69**, 17-25.
- Nielson, S.O., Michael, B. D., and Hart E. J. 1976. Ultraviolet Absorption Spectra of  $e_{aq}^-$ , H, OH, D, and OD from Pulse Radiolysis of Aqueous Solutions. *J. Phys. Chem.* **80**, 152-161.
- Herrmann, H. 1997. Photochemische Bildung, Spektroskopie und Kinetik freier Radikale in wässriger Lösung. Habilitation, Universität Essen, 459.
- Jayson, G. G., and Parson, B. J. 1973. Some simple, highly reactive, inorganic chlorine derivatives in aqueous solution. Their formation using pulses of radiation and their role in the mechanism of the Fricke dosimeter. *J. Chem. Soc.* **69**, 1597-1607.
- Park, H.-R., and Getoff, N. 1992. Radiolysis of aqueous ethanol in the presence of CO. *A. Phys. Science.* **47A**, 985-991.



## Dry deposition of ammonia over grassland - micrometeorological flux gradient measurements and bidirectional flux calculations using an inferential model

Gerald Spindler

Atmospheric ammonia ( $\text{NH}_3$ ) is recognized as a major atmospheric pollutant emitted from agricultural (Misselbrook et al. 2000) and other sources (Sutton et al. 2000). This follows both from its role in regional-scale tropospheric chemistry and from its effects when deposited together with ammonium ( $\text{NH}_4^+$ ) to ecosystems. Ammonia is the dominant gaseous base in the troposphere; it neutralizes the acidic products of sulfur dioxide ( $\text{SO}_2$ ) and nitrogen oxides sulfuric acid ( $\text{H}_2\text{SO}_4$ ) and nitric acid ( $\text{HNO}_3$ ) to form ammonium sulfates

were measured and modelled. The measurements were carried out at the Melpitz field research station near Torgau (Fig. 1), Germany (86 m asl,  $51^\circ 31' \text{N}$ ,  $12^\circ 56' \text{E}$ ). For the calculation of fluxes the micrometeorological flux-gradient technique was applied using measurements of the horizontal wind velocity, temperature and wet-bulb temperature at eight levels ( $z$ ) with a continuous flow wet annular denuder gradient-system (AMANDA)  $\text{NH}_3$  concentration was detected in three levels (Fig. 2).



**Fig. 1:** View of the measurement field of the IFT-Research station near Torgau.



**Fig. 2:** Two gradient systems (AMANDA), both for  $\text{NH}_3$  measurements at three levels above ground, side by side during an intercomparison experiment in summer 2000 at the Bundesanstalt für Landwirtschaft, Braunschweig.

and nitrates in particulate matter. To assess the impacts of atmospheric nitrogen deposition, it is essential to quantify the exchange of  $\text{NH}_3$  between the atmosphere and vegetation. This process is complicated since both  $\text{NH}_3$  emission and deposition may occur. Because of the large area of arable land in Europe it is important to quantify the net fluxes in calculating atmospheric budgets.

For a 17 day period in late summer 1995 ammonia fluxes over a extensive area of short grassland

Both, downward fluxes to the canopy and upward fluxes from the grassland to the atmosphere were found. The ammonia canopy compensation point ( $\chi_c$ ) was estimated in the range from 0.6 to  $2.8 \mu\text{gm}^{-3}$ . Because the simple "canopy/surface resistance" or "big leaf" model assumed a surface concentration of zero for the observed trace gas (Wesely and Hicks 1977; Wesely 1989), the results of the measurements were compared with a "canopy compensation point-cuticular resistance model" (Sutton and Fowler 1993), which is able



to quantify the stomata compensation point ( $\chi_s$ ) and allows bidirectional fluxes. This model is able to describe situations where parallel deposition occurs onto leaf surfaces. This situation has been observed in many field studies (Sutton et al. 1995a). The model allows the interpretation of measured net fluxes and the inferential net flux under given conditions accounting for both bidirectional stomatal exchange and deposition to leaf cuticles. For the calculation the modeled total flux  $F_t$  must be conserved in its component fluxes to the cuticle/water and wax layers ( $F_w$ ) and with stomata ( $F_s$ ).

$$F_t = F_w + F_s \quad (1)$$

$$F_w = -\chi_c / R_w \quad ; \quad F_s = (\chi_s - \chi_c) / R_s \quad (2)$$

Substitution of Eq. (2) into Eq. (1) and a rearrangement provides:

$$F_t = \frac{(\chi_s - \chi_c)}{R_s} - \frac{\chi_c}{R_w} \quad (3)$$

In combination with Eq. (4) (Sutton et al. 1995b) it is possible to eliminate  $F_t$  and to obtain  $\chi_c$ .

$$\chi_c = \chi(z-d) + F_t \{R_a(z-d) + R_b\} \quad (4)$$

$R_a$  and  $R_b$  are the atmospheric resistance (Garland 1978) and the boundary-layer resistance (Hicks et al. 1987), respectively  $d$  is the displacement height. These parameters can be calculated from micrometeorological measurements. The canopy stomatal resistance  $R_s$  and the external leaf resistance  $R_w$  for surface water films or waxes can be estimated from parametrisations (Sutton et al. 1993, Hicks et al. 1987). The stomatal compensation point ( $\chi_s$ ) can be calculated based on the temperature dependent Henry equilibrium using realistic pH, e.g., 6 - 7 and a concentration in the leaf intercellular fluid, e.g. 100  $\mu\text{mol NH}_4^+\text{l}^{-1}$  (Farquhar et al. 1980). Equation 5 shows the calculation of  $\chi_s$  (in  $\mu\text{g m}^{-3}$ ),  $\text{NH}_4^+$  (in  $\mu\text{mol l}^{-1}$ ).  $T_s$  is the surface temperature :

$$\chi_s = \frac{161512}{T_s} * 10^{-4507.11/T_s} * [\text{NH}_4^+] / [\text{H}^+] * 17000 \quad (5)$$

For flux modeling with the described model measurements are necessary only at one height above ground. Fig. 3 shows an example of nine days from the whole period with a comparison between the measured flux,  $F_{tg}$ , the modeled flux,  $F_t$  for a given realistic ratio of  $\Gamma = [\text{NH}_4^+] / [\text{H}^+] = 1000$ , and the maximum possible modeled flux,  $F_{tmax}$ , the latter calculated with the assumption that the canopy resistance  $R_c$  is zero.

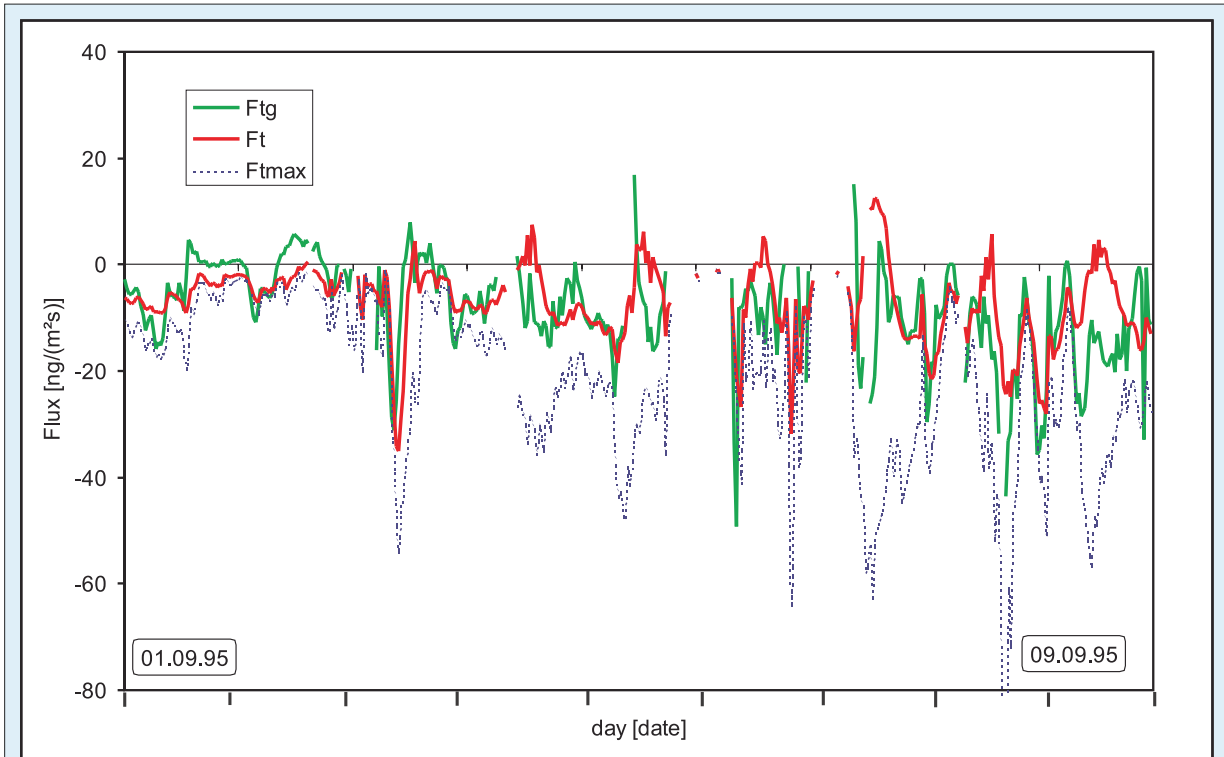


Fig. 3: Measured ( $F_{tg}$ ), modeled ( $F_t$ ) for  $\Gamma = 1000$ , and maximal possible modeled ammonia Flux ( $F_{tmax}$ ), for 1-9 September 1995.



For the whole period the agreement of the model and the measured fluxes was tested in dependence of  $\Gamma$ . The best agreement was found for  $\Gamma=1000$  with a difference  $F_{tg} - F_t$  of only  $0.06 \text{ ng m}^{-2} \text{ s}^{-1}$ . The model also shows bidirectional fluxes. There is a high diel variability but a basic pattern emerges and  $F_t$  never exceeds  $F_{tmax}$ . Some morning emission peaks are recognizable in the measurements, possibly due to emissions from cuticular desorption

or some litter  $\text{NH}_3$  emissions, which were not considered in the model. The highest emission situations generally occur during daytime. This surface atmosphere transport model is a useful tool for a further integration of the bidirectional flux of gaseous ammonia in larger scale chemistry-transport-modells. For further information see G. Spindler et al. 2001.

### References

- Misselbrook, T.H., Van der weerden, T.J., Pain, B.F., Jarvis, S.C., Chambers, B.J., Smith, K.A., Phillips, V.R. and Demmers, T.G.M. 2000** Ammonia emission factors for UK agriculture. *Atmos. Environ.* **34**, 871-880.
- Sutton, M.A., Dragosits, U., Tang, Y.S. and Fowler, D. 2000** Ammonia emissions from non-agricultural sources in the UK. *Atmos. Environ.*, **34**, 855-869
- Wesely, M.L. and Hicks, B.B. 1977.** Some factors that affect the deposition rates of Sulfur Dioxide and similar gases on vegetation. *J. Air pollut. Contr. Assoc.* **27**, 1110-1116.
- Wesely, M.L. 1989.** Parametrization of surface resistances to gaseous dry deposition in regional-scale numerical models. *Atmos. Environ.*, **23**, 1293-1304.
- Sutton, M.A. and Fowler, D. 1993.** A model for inferring bi-directional fluxes of ammonia over plant canopies. In: Proceedings of the WMO conference on the measurement and modelling of atmospheric composition changes including pollutant transport. WMO/GAW-91. (Sofia 4-8 October 1993). WMO, Geneva. 179-182.
- Sutton, M.A., Fowler, D., Burkhardt, J.K. , and Milford, C. 1995a.** Vegetation atmospheric exchange of Ammonia: Canopy cycling and the impacts of elevated nitrogen inputs. *Water Air Soil Pollut.* **85**, 2057-2063.
- Sutton, M.A., Schjørring, J.K., and Wyers, G.P. 1995b.** Plant - atmosphere exchange of ammonia. *Philos. trans. Roy. Soc. London.* **A 351**, 261-278.
- Garland J.A. 1978.** Dry and wet removal of sulfur from the atmosphere. *Atmos. Environ.*, **12**, 349-362.
- Hicks, B.B., Baldocchi, D.D., Meyers, T.P., Hosker R.P. Jr., and Matt, D.R. 1987.** A preliminary multiple resistance routine for deriving dry deposition velocities from measured quantities. *Water Air Soil Pollut.*, **36**, 311-330.
- Sutton, M.A., Pitcairn, C.E.R., and Fowler, D., 1993.** The exchange of ammonia between the atmosphere and plant communities. *Adv. Ecol. Research.* **24**, 301-393.
- Farquhar, G.D., Firth, P.M., Wetselaar R. , and Wier, B., 1980.** On the gaseous exchange of ammonia between leaves and the environment: determination of the ammonia compensation point. *Plant Physiol.* **66**, 710-714.
- G. Spindler, Teichmann, U., and Sutton, M.A., 2001.** Ammonia dry deposition over grassland - micrometeorological flux gradient measurements and bidirectional flux calculations using an inferential model. *Q.J.Roy.Meteor. Soc.* (in press).

#### Funding

- European Commission (DGXI, LIFE programme, 7221010)

#### Cooperation

- Institute of Terrestrial Ecology, Edinburgh, UK



*Appendix*

---





## Physics section

### Book Section

#### 2000

Wiedensohler, A., Stratmann, F., und Tegen, I. 2000. *Environmental Particles*. P. Gehr and J. Hyder (Ed.), In *Particle-lung interactions*. marcel dekker inc, p.67-88.

### Publications, peer-reviewed

#### 1999

Birmili, W., Stratmann, F., und Wiedensohler, A. 1999. Design of a DMA-based size spectrometer for a large particle size range and stable operation. *J. Aerosol Sci.* **30**, 549-553.

Birmili, W., Yuskiewicz, B., Wiedensohler, A., Stratmann, F., Choularton, T. W., und Bower, K. N. 1999. Climate-relevant modification of the aerosol size distribution by processes associated with orographic clouds. *Atmos. Res.* **50**, 241-263.

Bond, T. C., Bussemer, M., Wehner, B., Keller, S., Charlson, R. J., und Heintzenberg, J. 1999. Light absorption by primary particle emissions from a lignite burning plant. *Environ. Sci. Technol.* **33**, 3887-3891.

Bower, K. N., Choularton, T. W., Gallagher, M. W., Colvile, R. N., Beswick, K. M., Inglis, D. W. F., Bradbury, C., Martinsson, B. G., Swietlicki, E., Berg, O. H., Cederfeldt, S.-I., Frank, G., Zhou, J., Cape, J. N., Sutton, M. A., McFayden, G. G., Milford, C., Birmili, W., Yuskiewicz, B. A., Wiedensohler, A., Stratmann, F., Wendisch, M., Berner, A., Ctyroky, P., Galambos, Z., Mesfin, S. H., Dusek, U., Dore, C. J., Lee, D. S., Pepler, S. A., Bizjak, M., und Divjak, B. 1999. The Great Dun Fell Experiment 1995: An overview. *Atmos. Res.* **50**, 151-184.

Bradbury, C., Bower, K. N., Choularton, T. W., Swietlicki, E., Birmili, W., Wiedensohler, A., Yuskiewicz, B., Berner, A., Dusek, U., Dore, C. J., und McFadyen, G. G. 1999. Modelling of aerosol modification resulting from passage through a Hill Cap cloud. *Atmos. Res.* **50**, 185-204.

Brenninkmeijer, C. A. M., Crutzen, P. J., Fischer, H., Güsten, H., Hans, W., Heinrich, G., Heintzenberg, J., Hermann, M., Immelmann, T., Kersting, D., Maiss, M., Nolle, M., Pitscheider, A., Pohlkamp, H., Scharffe, D., Specht, K., und Wiedensohler, A. 1999. CARIBIC - Civil Aircraft for Global Measurements of Trace Gases and Aerosols in the Tropopause Region. *J. Atmos. Oceanic Technol.* **16**, 1373-1383.

Dippel, B., Jander, H., und Heintzenberg, J. 1999. NIR FT Raman spectroscopic study of flame soot. *Phys. Chem. Chem. Phys.* **1**, 4707-4712.

Heintzenberg, J., Wiedensohler, A., und Kütz, S. 1999. Modification of a commercial condensation particle counter for boundary layer balloon-borne aerosol studies. *J. Atmos. Ocean. Technol.* **16**, 597-601.

Laubach, J., und Teichmann, U. 1999. Surface energy budget variability: A case study over grass with special regard to minor inhomogeneities in the source area. *Theor. Appl. Climatol.* **62**, 9-24.

Martinsson, B. G., Frank, G., Cederfeldt, S. I., Swietlicki, E., Berg, O. H., Zhou, J., Bower, K. N., Bradbury, C., Birmili, W., Stratmann, F., Wendisch, M., Wiedensohler, A., und Yuskiewicz, B. 1999. Droplet nucleation and growth in orographic clouds in relation to the aerosol population. *Atmos. Res.* **50**, 289-315.

Müller, D., Wandinger, U., und Ansmann, A. 1999. Microphysical particle parameters from extinction and backscatter lidar data by inversion with regularization: Simulation. *Appl. Opt.* **38**, 2358-2368.

Müller, D., Wandinger, U., und Ansmann, A. 1999. Microphysical particle parameters from extinction and backscatter lidar data by inversion with regularization: Theory. *Appl. Opt.* **38**, 2346-2357.

Orsini, D. A., Wiedensohler, A., Stratmann, F., und Covert, D. S. 1999. A new volatility Tandem Differential Mobility Analyzer to measure the volatile sulfuric acid aerosol fraction. *J. Atmos. Oceanic Technol.* **16**, 760-772.

Pirjola, L., Kulmala, M., Wilck, M., Bischoff, A., Stratmann, F., und Otto, E. 1999. Formation of sulfuric acid aerosols and cloud condensation nuclei: An expression for significant nucleation and model comparison. *J. Aerosol Sci.* **30**, 1079-1094.

Swietlicki, E., Zhou, J., Berg, O. H., Martinsson, B. G., Frank, G., Cederfeldt, S. I., Dusek, U., Berner, A., Birmili, W., Wiedensohler, A., Yuskiewicz, B., und Bower, K. N. 1999. A closure study of sub-micrometer aerosol particle hygroscopic behaviour. *Atmos. Res.* **50**, 205-240.



- Wehner, B., Bond, T. C., Birmili, W., Bussemer, M., Heintzenberg, J., Wiedensohler, A., and Charlson, R. J. 1999. Climate-relevant particulate emission characteristics of a coal fired heating plant. *Environ. Sci. Technol.* **33**, 3881-3886.
- Wendisch, M. 1999. Review of: Microphysics of clouds and precipitation by Pruppacher, H. R. and Klett, J. D. J. *Atmos. Chem.* **32**, 420-422.
- Wendisch, M., und Keil, A. 1999. Discrepancies between measured and modeled solar and UV radiation within polluted boundary layer clouds. *J. Geophys. Res.* **104**, 27373-27385.
- Yuskiewicz, B. A., Stratmann, F., Birmili, W., Wiedensohler, A., Swietlicki, E., Berg, O., und Zhou, J. 1999. The effects of in-cloud mass production on atmospheric light scatter. *Atmos. Res.* **50**, 265-288.

## 2000

- Althausen, D., Müller, D., Ansmann, A., Wandinger, U., Hube, H., Clauder, E., und Zörner, S. 2000. Scanning 6-wavelength 11-channel aerosol lidar. *J. Atmos. Oceanic Technol.* **17**, 1469-1482.
- Ansmann, A., Althausen, D., Wandinger, U., Franke, K., Müller, D., Wagner, F., und Heintzenberg, J. 2000. Vertical profiling of the Indian aerosol plume with six-wavelength lidar during INDOEX: A first case study. *Geophys. Res. Lett.* **27**, 963-966.
- Banse, D. F., Esfeld, K., Hermann, M., Sierau, B., und Wiedensohler, A. 2000. Particle counting efficiency of the TSI CPC 3762 for different operating parameters. *Journal of Aerosol Science* **32**, 157-161.
- Bates, T. S., Quinn, P. K., Covert, D. S., Coffman, D. J., Johnson, J. E., und Wiedensohler, A. 2000. Aerosol physical properties and processes in the lower marine boundary layer: a comparison of shipboard sub-micron data from ACE-1 and ACE-2. *Tellus* **52B**, 258-272.
- Birmili, W., und Wiedensohler, A. 2000. New particle formation in the continental boundary layer: Meteorological and gas phase parameter influence. *Geophys. Res. Lett.* **27**, 3325-3328.
- Birmili, W., Wiedensohler, A., Plass-Dülmer, C., und Berresheim, H. 2000. Evolution of newly formed aerosol particles in the continental boundary layer: A case study including OH and H<sub>2</sub>SO<sub>4</sub> measurements. *Geophys. Res. Lett.* **27**, 2205-2209.
- Dingenen Van, R., Virkkula, A. O., Raes, F., Bates, T. S., und Wiedensohler, A. 2000. A simple non-linear analytical relationship between aerosol accumulation number and sub-micron volume, explaining their observed ratio in the clean and polluted marine boundary layer. *Tellus* **52B**, 439-451.
- Früh, B., Trautmann, T., und Wendisch, M. 2000. Measurement-based J(NO<sub>2</sub>) sensitivity in a cloudless atmosphere under low aerosol loading and high solar zenith angle conditions. *Atmos. Environ.* **34**, 5249-5254.
- Früh, B., Trautmann, T., Wendisch, M., und Keil, A. 2000. Comparison of observed and simulated NO<sub>2</sub> photodissociation frequencies in a cloudless atmosphere and in continental boundary layer clouds. *J. Geophys. Res.* **105**, 9843-9857.
- Gérémy, G., Wobrock, W., Flossmann, A. I., Schwarzenböck, A., und Mertes, S. 2000. A modelling study on the activation of small Aitken-mode particles during CIME 97. *Tellus* **52B**, 959-979.
- Heintzenberg, J., und Bussemer, M. 2000. Development and application of a spectral light absorption photometer for aerosol and hydrosol samples. *J. Aerosol Sci.* **31**, 801-812.
- Heintzenberg, J., Covert, D. S., und Van Dingenen, R. 2000. Size distribution and chemical composition of marine aerosols: A compilation and review. *Tellus* **52B**, 1104-1122.
- Heintzenberg, J., und Erfurt, G. 2000. Modification of a commercial integrating nephelometer for outdoor measurements. *J. Atmos. Oceanic Technol.* **17**, 1645-1650.
- Johnson, D. W., Osborne, S., Wood, R., Suhre, K., Johnson, R., Businger, S., Quinn, P. K., Wiedensohler, A., Durkee, P. A., Russell, L. M., Andreae, M. O., O'Dowd, C., Noone, K., Bandy, B., Rudolph, J., und Rapsomanikis, S. 2000. An overview of the Lagrangian experiments undertaken during the North Atlantic regional Aerosol Characterisation Experiment (ACE-2). *Tellus* **52B**, 290-320.
- Müller, D., Wagner, F., Althausen, D., Wandinger, U., und Ansmann, A. 2000. Physical properties of the Indian aerosol plume derived from 6-wavelength lidar observations on 25 March 1999 of the Indian Ocean Experiment. *Geophys. Res. Lett.* **27**, 1403-1406.
- Müller, D., Wagner, F., Wandinger, U., Ansmann, A., Wendisch, M., Althausen, D., und Hoyningen-Huene von, W. 2000. Microphysical particle parameters from extinction and backscatter lidar data by inversion with regularization: Experiment. *Appl. Opt.* **39**, 1879-1892.
- Russell, P. B., und Heintzenberg, J. 2000. An overview of the ACE-2 Clear Sky Column Closure Experiment (CLEARCOLUMN). *Tellus* **52 B**, 463-483.
- Schwarzenböck, A., und Heintzenberg, J. 2000. Cut size minimization and cloud element break-up in a ground-based CVI. *J. Aerosol Sci.* **31**, 477-489.



- Schwarzenböck, A., Heintzenberg, J., und Mertes, S. 2000. Incorporation of aerosol particles between 25 and 850 nanometers into cloud elements: Measurement with a new complementary sampling system. *Atmos. Res.* **52**, 241-260.
- Swietlicki, E., Zhou, J., Covert, D. S., Hämeri, K., Busch, B., Väkevä, M., Dusek, U., Berg, O. H., Wiedensohler, A., Aalto, P., Mäkelä, J., Martinsson, B. G., Papaspiropoulos, G., Mentes, B., Frank, G., und Stratmann, F. 2000. Hygroscopic properties of aerosol particles in the north-eastern Atlantic during ACE-2. *Tellus* **52B**, 201-227.
- Tomasi, C., Marani, S., Vitale, V., Wagner, F., Cacciari, A., und Lupi, A. 2000. Precipitable water evaluations from infrared sun-photometric measurements analyzed using the atmospheric hygrometry technique. *Tellus* **52B**, 734-749.
- Voutilainen, A., Stratmann, F., und Kaipio, J. P. 2000. Hierarchical non-homogeneous regularization method for estimation of narrow aerosol size distributions. *J. Aerosol Sci.* **31**, 1433-1445.
- Wehner, B., Wiedensohler, A., und Heintzenberg, J. 2000. Submicrometer aerosol size distributions and mass concentration of the Millennium fireworks 2000 in Leipzig, Germany. *J. Aerosol Sci.* **31**, 1489-1493.
- Zahn, A., Brenninkmeijer, C. A. M., Maiss, M., Scharffe, D., Crutzen, P. J., Hermann, M., Heintzenberg, J., Güsten, H., Heinrich, G., Fischer, H., Cuijpers, J. W. M., und Velthoven van, P. F. J. 2000. Identification of extratropical 2-way troposphere-stratosphere mixing based on CARIBIC measurements of O<sub>3</sub>, CO, and ultrafine particles. *J. Geophys. Res.* **105**, 1527-1535.

## Conference Proceedings

### 1999

- Althausen, D., Müller, D., Wagner, F., Wandinger, U., und Ansmann, A. 1999. *Measurements with a multiwavelength lidar during LACE 98*. European Aerosol Conference, Prag, 6.-10. September, 433-434.
- Ansmann, A. 1999. *Lindenberg Aerosol Characterization Experiment LACE 98*. European Aerosol Conference, Prag, 6.-10. September, 219-220.
- Bates, T., Quinn, P., Coffman, D., Covert, D., Hamilton, D., Johnson, J., Miller, T., Massling, A., Neusüß, C., Nowak, A., Leinert, S., Wiedensohler, A., Perry, K., Durkee, P., und Nielson, K. 1999. *Aerosol physical and chemical properties in the Atlantic ocean lower marine boundary layer: preliminary results from the aerosols 99 cruise*. International Global Atmospheric Chemistry (IGAC) Conference, Bologna, Italy, 13.-17. September.
- Berresheim, H., Birmili, W., Elste, T., Plass-Dülmer, C., und Wiedensohler, A. 1999. *Atmospheric sulfuric, OH, and aerosol particle measurements at Hohenpeissenberg, South Germany*. EGS XIV General Assembly, Den Haag,
- Berresheim, H., Plass-Dülmer, C., Elste, T., Birmili, W., und Wiedensohler, A. 1999. *Atmospheric particle nucleation, H<sub>2</sub>SO<sub>4</sub>, and OH measurements at Hohenpeissenberg, South Germany*. International Global Atmospheric Chemistry (IGAC) Conference, Bologna, Italy, 13.-17. September.
- Birmili, W., Heintzenberg, J., und Wiedensohler, A. 1999. *Parameterization of the continental submicron particle size distribution on the basis of number concentration*. 12th International Congress International Society for Aerosols in Medicine (ISAM), Wien,
- Birmili, W., Heintzenberg, J., und Wiedensohler, A. 1999. *Representative measurement and parameterization of the submicron continental particle size distribution*. European Aerosol Conference, Prag, 6.-10. September, 229-230.
- Birmili, W., Wiedensohler, A., Plass-Dülmer, C., und Berresheim, H. 1999. *Long-term studies of new particle formation at Hohenpeissenberg, a rural mountain site in South Germany*. European Aerosol Conference, Prag, 6.-10. September, 839-840.
- Böckmann, C., Sarközi, J., und Althausen, D. 1999. *Collocation methods for ill-posed inverse problems of multiwavelength lidar measurements and applications on LACE98-data*. European Aerosol Conference, Prag, 6.-10. September, 485-486.
- Böckmann, C., Wandinger, U., und Müller, D. 1999. *Inversion of aerosol particle properties from multiwavelength lidar measurements*. 10th International Workshop on Multiple Scattering Experiments (MUSCLE 10), Florence, Italy, 19. - 22. April, 218-226.
- Bruckbach, U., Nowak, A., Neusüß, C., Massling, A., Leinert, S., Busch, B., Wiedensohler, A., Coffmann, D., Bates, T., und Covert, D. 1999. *Size-segregated mass closure study of the clean marine and continentally polluted aerosol in the marine boundary layer during INDOEX*. 1999 AGU Fall Meeting, San Francisco, USA, F185.



- Bundke, U., Hänel, G., Horvath, H., Kaller, W., Seidel, S., Wex, H., und Wiedensohler, A. 1999. *Measurements of dry aerosol optical properties during LACE 98*. European Aerosol Conference, Prag, 6.-10. September, 435-436.
- Dippel, B., und Heintzenberg, J. 1999. *Soot characterization in atmospheric particles from different sources by NIR Raman spectroscopy*. European Aerosol Conference, Prag, 6.-10. September, 907-908.
- Dippel, B., Philippin, S., Wehner, B., und Wiedensohler, A. 1999. *Measurements of particulate emissions of a directly injected gasoline-driven automobile*. European Aerosol Conference, Prag, 6.-10. September, 647-648.
- Flossmann, A., Wobrock, W., Gérémy, G., Schwarzenböck, A., und Mertes, S. 1999. *A modelling study of cloud ice mountain experiment (CIME)*. International Global Atmospheric Chemistry (IGAC) Conference, Bologna, Italy, 13.-17. September.
- Früh, B., Trautmann, T., Wendisch, M., und Keil, A. 1999. *Comparison of observed and simulated NO<sub>2</sub> photodissociation rates using detailed in-situ measurements*. International Global Atmospheric Chemistry (IGAC) Conference, Bologna, Italy, 13.-17. September.
- Früh, B., Trautmann, T., Wendisch, M., und Keil, A. 1999. *Comparison of observed and simulated NO<sub>2</sub> photodissociation rates using measured aerosol and drop size distribution*. European Aerosol Conference, Prag, 6.-10. September, 165-166.
- Heintzenberg, J. 1999. *Das troposphärische Aerosol: Chemie, Physik und Klimawirksamkeit*. Bunsentagung, Dortmund, 13.-15. Mai,
- Hermann, M., Heintzenberg, J., und Wiedensohler, A. 1999. *Aerosol particle number concentrations in the upper troposphere and lower stratosphere measured by CARIBIC*. European Aerosol Conference, Prag, 6.-10. September, 205-206.
- Hermann, M., Stratmann, F., und Wiedensohler, A. 1999. *Calibration of an aircraft-borne aerosol inlet system for fine particle measurements*. European Aerosol Conference, Prag, 6.-10. September, 153-154.
- Hoyningen-Huene, W. v., Silva, A. M., Bugalho, M. L., Heintzenberg, J., Henning, S., und Philippin, S. 1999. *Comparison of volumetric physico-chemical properties between two different sites during ACE 2 CLEARCOLUMN*. International Global Atmospheric Chemistry (IGAC) Conference, Bologna, Italy, 13.-17. September, P2.14.
- Jaenisch, V., Wilck, M., und Stratmann, F. 1999. *Parameterization of particle formation and condensational growth during turbulent mixing processes*. European Aerosol Conference, Prag, 6.-10. September, 507-508.
- Kaden, H., Zosel, J., Heintzenberg, J., und Richter, K. 1999. *Untersuchungen zu einem miniaturisierten Psychrometer für die Troposphärenforschung (in German)*. 4. Dresdner Sensor-Symposium, Dresden, Germany, 95-96.
- Kaller, W., Wex, H., Seidl, S., und Horvath, H. 1999. *Horizontal extinction of ambient aerosol and scattering of dried aerosol during the LACE 98 Experiment - A comparison*. European Aerosol Conference, Prag, 6.-10. September, 521-522.
- Laj, P., Fuzzi, S., Orsi, G., Ricci, L., TenBrink, H., Jongejan, P., Mertes, S., und Schwarzenböck, A. 1999. *Phase partitioning of NH<sub>3</sub> and H<sub>2</sub>O<sub>2</sub> in mixed clouds*. International Global Atmospheric Chemistry (IGAC) Conference, Bologna, Italy, 13.-17. September.
- Massling, A., Wiedensohler, A., und Busch, B. 1999. *Concept of an advanced Hygroscopic Tandem Differential Mobility Analyzer with a great operation stability*. European Aerosol Conference, Prag, 6.-10. September, 395-396.
- Massling, A., Wiedensohler, A., und Busch, B. 1999. *Hygroscopic growth of aerosol particles in the Southern Atlantic Ocean and Indian Ocean*. European Aerosol Conference, Prag, 6.-10. September, 837-838.
- Mertes, S., Schwarzenböck, A., Heintzenberg, J., und Wobrock, W. 1999. *Changes of the phase partitioning of atmospheric aerosol particles during ice formation in supercooled clouds due to the Bergeron Findeisen process*. European Aerosol Conference, Prag, 6.-10. September.
- Müller, D., Franke, K., Wandinger, U., Wagner, F., Althausen, D., und Ansmann, A. 1999. *Radiative impact of pollution outbreaks from India and comparison to southern-hemispheric conditions based on measurements with a 6-wavelength lidar at the Maldives*. 1999 AGU Fall Meeting, San Francisco, F161-F162.
- Müller, D., Wendisch, M., und Keil, A. 1999. *Comparison of ground-based measured and model-derived spectral irradiances*. European Aerosol Conference, Prag, 6.-10. September, 835-836.



- Nowak, A., Leinert, S., Covert, D., Wiedensohler, A., und Bates, T. 1999. *Submicrometer particle size distribution of biomass aerosols observed during the aerosol and Indoex field studies*. European Aerosol Conference, Prag, 6.-10. September, 179-180.
- Philippin, S., Neusüß, C., Stratmann, F., und Wiedensohler, A. 1999. *Determination of non-volatile carbon fractions in fine aerosol particles: A comparison of methods*. European Aerosol Conference, Prag, 6.-10. September, 217-218.
- Philippin, S., Stratmann, F., und Wiedensohler, A. 1999. *Quantification of non-volatile number and volume fractions of atmospheric aerosols in different environments*. European Aerosol Conference, Prag, 6.-10. September, 117-118.
- Schwarzenböck, A., Heintzenberg, J., Mertes, S., und Wieprecht, W. 1999. *Size dependency of 25-850 nm aerosol particles incorporated in cloud droplets*. European Aerosol Conference, Prag, 6.-10. September, 241-242.
- Schwarzenböck, A., Mertes, S., Heintzenberg, J., und Wobrock, W. 1999. *First in situ evidence for Bergeron-Findeisen process*. European Aerosol Conference, Prag, 6.-10. September, 131-132.
- Seidl, S., Wex, H., Kaller, W., und Horvath, H. 1999. *Extinction, absorption and scattering coefficients measured with three different instruments during LACE 98 - A comparison*. European Aerosol Conference, Prag, 6.-10. September, 479-480.
- Stratmann, F., Zdimal, V., Wilck, M., und Smolik, J. 1999. *New 2-D coupled fluid flow, heat and mass transfer model for the description of thermal diffusion cloud chambers*. European Aerosol Conference, Prag, 6.-10. September, 75-76.
- Voutilainen, A., Stratmann, F., und Kaipio, J. P. 1999. *A new data inversion algorithm for DMPS and TDMA measurements*. European Aerosol Conference, Prag, 6.-10. September, 775-776.
- Wandinger, U. 1999. *Multiwavelength lidar measurements of spectral extinction and backscatter coefficients for the inversion of particle properties*. MUSCLE 10, 10th International Workshop on Multiple Scattering Experiments, Florence, Italy, 19. - 22. April, 31.
- Wandinger, U. 1999. *Recent aerosol characterization studies of European and Asian aerosols with a multiwavelength aerosol Raman lidar*. Optical Remote Sensing of the Atmosphere, Santa Barbara, 21.-25. Juni, 154-156.
- Wehner, B., und Wiedensohler, A. 1999. *Aerosol characterization of a natural gas and oil-fired heating plant*. European Aerosol Conference, Prag, 6.-10. September, 113-114.
- Wehner, B., und Wiedensohler, A. 1999. *Statistical analysis on a long term study of number size distributions in the urban area*. European Aerosol Conference, Prag, 6.-10. September, 645-646.
- Weitkamp, C., Reichardt, J., Behrendt, A., Ansmann, A., Riebesell, M., und Wandinger, U. 1999. *Capabilities of a multipurpose Raman lidar*. International Laser Sensing Symposium ILSS'99, Fukui-City, Japan, 6. - 8. September,
- Wendisch, M., und Keil, A. 1999. *Measured aerosol absorption profiles and their influence on clear-sky aerosol forcing*. IUGG 99, Birmingham,
- Wendisch, M., Keil, A., Wandinger, U., Althausen, D., Wex, H., Müller, D., und Armbruster, W. 1999. *Measured and calculated clear-sky radiation using detailed aircraft and Lidar aerosol data*. IUGG 99, Birmingham,
- Wex, H., Koziar, C., Neusüß, C., und Wiedensohler, A. 1999. *In-situ closure studies on scattering and backscattering coefficients and their sensitivity*. European Aerosol Conference 1999, Prag, 6.-10. September, 481-482.
- Wex, H., Wendisch, M., Keil, A., und Wiedensohler, A. 1999. *Closure studies on optical relevant aerosol properties using aircraft and ground-based measurements*. European Aerosol Conference, Prag, 6.-10. September, 439-440.
- Wiedensohler, A., Massling, A., Busch, B., Neusüß, C., Miller, T., Coffmann, D., Bates, T., Quinn, P., und Covert, D. 1999. *Closure study between hygroscopic growth and solubility of the clean marine and continentally polluted aerosol during INDOEX. 1999 AGU Fall Meeting*, San Francisco, USA, F187.
- Wiegner, M., Bösenberg, J., Böckmann, C., Eixmann, R., Freudenthaler, V., Mattis, I., und Trickl, T. 1999. *Lidar network to establish an aerosol climatology*. European Aerosol Conference, Prag, 6.-10. September, 429-430.
- Wilck, M., Hermann, M., Bräsel, S., und Stratmann, F. 1999. *Evaporation of sulfuric acid-water particles in an aircraft-borne aerosol sampling system*. European Aerosol Conference, Prag, 6.-10. September, 155-156.
- Wilck, M., Nowacki, P., Müller, F., und Stratmann, F. 1999. *Modelling of haze and cloud chemistry: Comparison of different model approaches*. European Aerosol Conference, Prag, 6.-10. September, 461-462.



### 2000

- Althausen, D., Arshinov, Y., Bobrovnikov, S., Serikov, I., Ansmann, A., Mattis, I., und Wandinger, U. 2000. *Temperature profiling in the troposphere using a pure rotational Raman lidar*. 5th International Symposium on Tropospheric Profiling: Needs and Technology, Adelaide, Australia, 4. - 8. Dezember, 31-33.
- Althausen, D., Franke, K., und Verver, G. 2000. *Correlation between particle backscatter measured over the Tropical Indian Ocean and residence time of the observed aerosols in the boundary layer over the Asian continent*. 20th International Laser Radar Conference (ILRC), Vichy, France, 10. - 14. July.
- Althausen, D., Müller, D., Wagner, F., Franke, K., Wandinger, U., und Ansmann, A. 2000. *Aerosol characterization with advanced aerosol lidar for climate studies*. 7. International Symposium on Atmospheric and Ocean Optics, Tomsk, 390-397.
- Ansmann, A., Franke, K., Althausen, D., Müller, D., Wagner, F., und Wandinger, U. 2000. *Extinction-to-backscatter ratios of clean marine aerosols and European and Asian pollution plumes observed with Raman lidar*. 20th International Laser Radar Conference (ILRC), Vichy, France, 10. - 14. July.
- Arshinov, Y., Bobrovnikov, S., Serikov, I., Althausen, D., Mattis, I., Wandinger, U., und Ansmann, A. 2000. *Spectrally absolute instrumental approach to isolate pure rotational Raman lidar returns from nitrogen molecules of the atmosphere*. 20th International Laser Radar Conference (ILRC), Vichy, France, 10. - 14. July.
- Berresheim, H., Elste, T., Plass-Dülmer, C., Birmili, W., Wiedensohler, A., O'Dowd, C. D., Hansson, H. C., und Mäkelä, J. M. 2000. *Observed  $H_2SO_4$  and OH concentrations and their relation to particle nucleation events in marine and rural continental air*. ICNAA Conference, Missouri-Rolla.
- Birmili, W., Wiedensohler, A., Plass-Dülmer, C., und Berresheim, H. 2000. *Long-term measurements of events of new particle formation at Hohenpeissenberg: Methods of analysis and climatology*. ICNAA Conference, Missouri-Rolla.
- Boonjawat, J., Heintzenberg, J., und Carmichael, G. 2000. *Capacity building in atmospheric aerosol measurements in Southeast Asia*. Synthesis Workshop on Greenhouse Gas Emissions; Aerosols, Land Use and Cover Changes in Southeast Asia, Chungli, Taipei.
- Bower, K. N., Flynn, M. J., Choularton, T. W., Burgess, R. A., Coe, H., Swietlicki, E., Martinsson, B., Zhou, J., Wiedensohler, A., Birmili, W., Müller, K., und Berner, A. 2000. *Observations of the evolution of particulate in an urban plume and following interaction with cloud*. Nucleation and atmospheric aerosols 2000, 15th International Conference, Rolla, Missouri, 631-634.
- Bower, K. N., Flynn, M. J., Choularton, T. W., Coe, H., Burgess, R., Birmili, W., Müller, K., Berner, A., Swietlicki, E., und Martinsson, B. G. 2000. *A field study of the evolution of an urban plume and its interaction with cloud*. EUROTRAC II Symposium „Transport and Chemical Transformation of Pollutants in the Troposphere“, Garmisch-Partenkirchen, 27.-31. März.
- Bräsel, S., Wilck, M., und Stratmann, F. 2000. *New particle formation and growth in a  $H_2O/H_2SO_4$  system - first results from a flow-tube-2-D model*. European Aerosol Conference, Dublin, 3.-8. September, 556-557.
- Bruckbach, U., Nowak, A., Neusüß, C., Massling, A., Leinert, S., Busch, B., Wiedensohler, A., Coffmann, D., Bates, T., Miller, T., und Covert, D. 2000. *Size-segregated mass closure study of the clean marine and continentally polluted aerosol in the marine boundary layer during INDOEX*. 25th EGS General Assembly, Nice, 25. - 29. April.
- Bugalho, M. L., Hoyningen-Huene, W. v., Silva, A. M., Heintzenberg, J., Henning, S., und Philippin, S. 2000. *Comparação de Propriedades Físico/Químicas Volumétricas de aerossóis captados em dois locais diferentes da Costa Sudoeste Portuguesa durante CLEARCOLUMN*. 2ª Assembleia Luso-Espanhola de Geodesia e Geofísica, Lagos, Portugal, 449-450.
- Franck, U., Wehner, B., Herbarth, O., und Wiedensohler, A. 2000. *Indoor size distributions of fine particles compared with outdoor distributions in the absence and presence of significant indoor sources*. Aerosols and Health, Karlsruhe.
- Grabowski, J., Papayannis, A., Galani, E., Wendisch, M., und Blaszczak, Z. 2000. *Nonconstraint solution of a differential backscattering lidar equation and an inversion algorithm*. 20th International Lidar Radar Conference (ILRC 2000), Vichy, France.
- Haman, J., Malinowski, S. P., Stru, B. D., Busen, R., Stefko, A., und Siebert, H. 2000. *A family of ultrafast aircraft thermometers for warm and supercooled clouds and various types of aircraft*. 13th International Conference on Clouds and Precipitation, Reno/Nevada.
- Heintzenberg, J. 2000. *Aerosol influence on the radiation budget: Where do we stand?* 20th International Laser Radar Conference, Vichy, 10.-14. Juli.



- Heintzenberg, J. 2000. *Airborne aerosol measurements: State of the art, future need and directions*. GORDON Research Conference, Boston, 24.-28. Juni.
- Heintzenberg, J. 2000. *Atmospheric aerosols, or understanding the haze we are living in*. MIT Global Change Forum, 21.-23. Juni.
- Kaden, H., Zosel, J., Heintzenberg, J., und Hartig, T. 2000. *Untersuchungen zu einem miniaturisierten Psychrometer für die Troposphärenforschung (in German)*. 4. Dresdner Sensor-Symposium, Dresden, 169-172.
- Keil, A., und Wendisch, M. 2000. *Solar radiative forcing by particles containing Black Carbon - measurement-based case studies*. International Radiation Symposium (IRS 2000), St. Petersburg, Russia.
- Keil, A., Wendisch, M., und Heintzenberg, J. 2000. *Twomey effect over land induced by power plant emissions*. International Radiation Symposium (IRS 2000), St. Petersburg, Russia.
- Klugmann, D. 2000. *Application of an explicit cloud microphysics algorithm in a non-hydrostatic mesoscale model*. 13<sup>th</sup> International Conference on Clouds and Precipitation, Reno, USA, 471-474.
- Klugmann, D. 2000. *A compact 94-GHz FM-CW Doppler cloud radar using semiconductor devices for power generation*. International Geoscience and Remote Sensing Symposium (IGARSS 2000), Honolulu, Hawaii, USA, 1801-1803.
- Klugmann, D. 2000. *A semiconductor based 94-GHz Doppler radar profiler*. 5th International Symposium on Tropospheric Profiling: Needs and Technology, Adelaide, Australia, 247-249.
- Klugmann, D., und Wendisch, M. 2000. *Design and sensitivity estimation of a new airborne cloud radar*. 13<sup>th</sup> International Conference on Clouds and Precipitation, Reno, USA, 318-321.
- Laj, P., Flossmann, A. I., Wobrock, W., Fuzzi, S., Orsi, G., Ricci, L., Mertes, S., Schwarzenböck, A., Heintzenberg, J., Jongejan, P., und Ten Brink, H. 2000. *Behaviour of H<sub>2</sub>O<sub>2</sub>, NH<sub>3</sub> and black carbon in mixed phase clouds during CIME*. EUROTRAC-2 Symposium, Garmisch-Partenkirchen, 27. - 31. März.
- Leinert, S., und Wiedensohler, A. 2000. *APS counting efficiency calibration for submicrometer particles*. European Aerosol Conference, Dublin, 3.-8. September, 404-405.
- Massling, A., Wiedensohler, A., Busch, B., Miller, T., Coffman, D., Quinn, P., Bates, T., und Covert, D. 2000. *Soluble particle volume fractions derived from hygroscopic growth and chemical composition measurements during INDOEX*. European Aerosol Conference, Dublin, 3.-8. September, 991-992.
- Massling, A., Wiedensohler, A., Busch, B., Neusüß, C., Miller, T., Coffman, D., Quinn, P., Bates, T., und Covert, D. 2000. *Comparison between hygroscopic properties and elemental carbon for aerosols originated from the Indian subcontinent*. 25th EGS General Assembly, Nice, 25. - 29. April.
- Mattis, I., Jaenisch, V., Müller, D., Franke, K., und Ansmann, A. 2000. *Classification of particle extinction profiles derived within the framework of the German lidar network by the use of cluster analysis of backtrajectories*. 20th International Laser Radar Conference (ILRC), Vichy, France, 10. - 14. Juli.
- Müller, D., Althausen, D., Wagner, F., Franke, K., Wandinger, U., und Ansmann, A. 2000. *Comprehensive particle characterization with advanced aerosol lidar for climate-impact studies*. 20th International Laser Radar Conference (ILRC), Vichy, France, 10. - 14. Juli.
- Müller, D., Balis, D., Böckmann, C., Bösenberg, J., Calpini, B., Chaikovskiy, A. P., Comeron, A., Flamant, P., Freudenthaler, V., Hågård, A., Mattis, I., Mitev, V., Papayannis, A., Pappalardo, G., Pelon, J., Perrone, M. R., Resendes, D. P., Schneider, J., Spinelli, W., Trickl, T., Vaughan, G., und Visconti, G. 2000. *EARLINET: A European Aerosol Research Lidar Network to Establish an Aerosol Climatology*. Conference on Research Infrastructures, Strasbourg, France, 18. - 20. September.
- Müller, D., Franke, K., Ansmann, A., Wagner, F., und Althausen, D. 2000. *Seasonal cycle of optical and physical particle properties over the Indian Ocean from 6-wavelength lidar observations in the Maldives*. International Workshop on „Tropical Environmental Problems in the light of INDOEX Program“, Palampur, India, 9. - 13. Oktober.
- Müller, D., Franke, K., Ansmann, A., Wagner, F., und Althausen, D. 2000. *Seasonal cycle of optical and physical properties over the Indian Ocean from 6-wavelength lidar observations*. AGU Fall Meeting, San Francisco, California, 15. - 19. Dezember, F 152.
- Müller, D., Wendisch, M., Heintzenberg, J., und Schell, D. 2000. *Concept and first tests of a new airborne spectrometer system for solar radiation measurements*. 13<sup>th</sup> International Conference on Clouds and Precipitation, Reno, USA.
- Müller, D., Wendisch, M., Schell, D., und Heintzenberg, J. 2000. *Development and first application of a new solar irradiance spectrometer system with horizontally stabilized optics*. International Radiation Symposium (IRS 2000), St. Petersburg, Russia.



- Schmidt, S., Wendisch, M., und Brenguier, J.-L. 2000. *Comparison of Fast FSSP, PVM and King probe microphysical measurements during ACE 2*. 13<sup>th</sup> International Conference on Precipitation, Reno, USA.
- Schneider, J., Balis, D., Böckmann, C., Bösenberg, J., Calpini, B., Chaikovsky, A. P., Comeron, A., Flamant, P., Freudenthaler, V., Hågård, A., Mattis, I., Mitev, V., Papayannis, A., Pappalardo, G., Pelon, J., Perrone, M. R., Resendes, D. P., Spinelli, N., Trickl, T., Vaughan, G., und Visconti, G. 2000. *A European Aerosol Research Lidar Network to establish an aerosol climatology (EARLINET)*. European Aerosol Conference, Dublin, 3.-8. September, 592-593.
- Siebert, H., und Muschinski, A. 2000. *Performances of a three-dimensional ultrasonic anemometer/thermometer for turbulence measurements*. 14th Symposium on Boundary Layers and Turbulence, Aspen, Colorado.
- Siebert, H., und Teichmann, U. 2000. *Concept and design of a new airship-borne cloud turbulence measurement system*. 13th International Conference on Clouds and Precipitation, Reno, Nevada.
- Sierau, B., Hofmann, D., Pelzing, M., Stratmann, F., und Wilck, M. 2000. *Analysis of submicrometer organic aerosol particles - A new method and first laboratory results*. European Aerosol Conference, Dublin, 3.-8. September, 973-974.
- Stratmann, F., Wilck, M., Zdimal, V., und Smolik, J. 2000. *First results of a new 2-D model for the description of thermal diffusion cloud chambers*. European Aerosol Conference, Dublin, 3.-8. September, 98-99.
- Teichmann, U., und Siebert, H. 2000. *Concept and first results of an airship-borne cloud turbulence system*. 14th Symposium on Boundary Layers and Turbulence, Aspen, Colorado.
- Uhrner, U., Birmili, W., Wilck, M., Berresheim, H., Plass-Dülmer, C., Wiedensohler, A., Ackermann, I. J., und Stratmann, F. 2000. *Particle formation and loss processes for a remote hill site. Comparison of model results with observations*. European Aerosol Conference, Dublin, 3.-8. September, 144-145.
- Wandinger, U. 2000. *Characterization of tropospheric aerosol particles from multiwavelength lidar measurements*. 5th Symposium on Tropospheric Profiling: Needs and Technologies, Adelaide, Australia, 4. - 8. Dezember, 205-207.
- Wandinger, U., und Ansmann, A. 2000. *Experimental determination of the laser-beam-receiver-field-of-view overlap function*. 20th International Laser Radar Conference (ILRC), Vichy, France, 10. - 14. Juli.
- Wandinger, U., Turner, D., Whiteman, D., und Wulfmeyer, V. 2000. *Raman lidar studies of water vapor: A joint review*. 5th Symposium on Tropospheric Profiling: Needs and Technologies, Adelaide, Australia, 4. - 8. Dezember, 21.
- Wehner, B. 2000. *Temporal and spatial variation of nanoparticle number concentration in the urban area*. 4. ETH Conference on Nanoparticle Measurement, Zürich.
- Wehner, B., und Wiedensohler, A. 2000. *Seasonal and diurnal variability of the PM1 mass concentration in the urban area of Leipzig, Germany*. European Aerosol Conference, Dublin, 3.-8. September, 566-567.
- Wendisch, M., Garrett, T., Hobbs, P. V., und Strapp, J. W. 2000. *PVM-100A performance tests in the IRT and NRC wind tunnels*. 13th International Conference on Clouds and Precipitation, Reno, USA.
- Wex, H., Koziar, C., Neusüß, C., Wiedensohler, A., und Heintzenberg, J. 2000. *Sensitivity studies for closure studies on scattering and absorption coefficients*. European Aerosol Conference, Dublin, 3.-8. September, 981-982.
- Whitby, E. R., Stratmann, F., und Wilck, M. 2000. *Dynamic mode manager for modal aerosol dynamics models*. European Aerosol Conference, Dublin, 3.-8. September, 843-844.
- Wiedensohler, A., und Heintzenberg, J. 2000. *Overview of the ground-based aerosol measurements during the intensive field phase of INDOEX. EGS 2000*, Nizza.
- Wiedensohler, A., Wehner, B., Massling, A., und Philippin, S. 2000. *Physical properties of the urban aerosol*. Aerosol and Health, Karlsruhe.
- Wilck, M., Müller, F., und Stratmann, F. 2000. *Parameterization of cloud chemical and microphysical processes by means of a moving-monodisperse model with low fraction number*. European Aerosol Conference, Dublin, 3.-8. September, 993-994.



## Lectures

### 1999

- Althausen, D., Ansmann, A., Franke, K., Hube, H., Müller, D., Wagner, F., und Wandinger, U. 1999. Overview about the measurements of the multiwavelength aerosol lidar, sunphotometer and radiosonde at Hulule. INDOEX-Workshop, Utrecht.
- Franke, K. 1999. Die räumliche und zeitliche Korrelation der Solarstrahlung auf unterschiedlich orientierten Flächen in Sachsen. Umweltforschungszentrum Leipzig Arbeitsgruppe Stadtklima.
- Heintzenberg, J. 1999. Advanced measurement techniques. EMEP/WMO Workshop on Fine Particles - Emissions, Modelling and Measurements, Interlaken, Switzerland. \*)
- Heintzenberg, J. 1999. Klimarelevante Wechselwirkung von Aerosolen, Wolken und Strahlung. GKSS-Forschungszentrum Geesthacht GmbH, Institut für Atmosphärenphysik. \*)
- Heintzenberg, J. 1999. Klimawirksamkeit von Aerosolen. DECHEMA-Jahrestagung ,99, Sonderveranstaltung „Aerosole und Umwelt“. \*)
- Siebert, H., und Hoff, A. 1999. Airship-borne cloud turbulence measurement system. University of Bremen, DGLR Workshop III - Flight Systems Lighter-than-Air.
- Wehner, B. 1999. Größenaufgelöste Partikelmessungen in der urbanen Atmosphäre von Leipzig. Gastvortrag, Sächsisches Landesamt für Umwelt und Geologie, Abteilung Luft, Lärm, Strahlen.
- Wendisch, M. 1999. PVM measurements during the wind tunnel tests at Nasa Lewis. Workshop on cloud microphysical measurement techniques. \*)
- Wendisch, M., und Wex, H. 1999. Vertical profiles of microphysical and optical properties of aerosol particles over the Eastern Mediterranean area. Meteorological Research Flight (MRF), Farnborough. \*)
- Wex, H. 1999. Aerosole in der Klimaforschung - Meßtechniken und Qualitätssicherung. FU Berlin. \*)
- Wiedensohler, A. 1999. Messungen von ultrafeinen und feinen Aerosolen und ihre Anwendung und Bedeutung auf Schweißrauch. Bundesanstalt für Arbeitsschutz und Arbeitsmedizin. \*)
- Wiedensohler, A. 1999. New results from the aerosol and cloud group of the Institute for Tropospheric Research. NILU Lilleström. \*)
- Wiedensohler, A. 1999. Studies and observations of the clean marine and polluted atmospheric aerosol in the marine boundary layer during ACE-2. Brookhaven National Laboratory. \*)
- Wiedensohler, A. 1999. Studies and observations of the clean marine and polluted atmospheric aerosol in the marine boundary layer during ACE-2. Oak Ridge National Laboratory. \*)

### 2000

- Heintzenberg, J. 2000. 100 years of marine aerosol research: A review. University of Tokyo, Center for Climate System Research. \*)
- Heintzenberg, J. 2000. Aerosol influence on the radiation budget: Where do we stand? Meteorological Research Institute, Tsukuba, Japan. \*)
- Heintzenberg, J. 2000. Aerosol measurements in the tropopause region from a commercial aircraft: The CARIBIC project. Meteorological Research Institute, Tsukuba, Japan. \*)
- Heintzenberg, J. 2000. Atmospheric aerosols, 10 years of IGAC research. IGAC Community Review Meeting, Aspen, Colorado.
- Heintzenberg, J. 2000. Present status and remaining challenges concerning aerosol effects on climate. University of Hiroshima, Dept. of Chemical Engineering. \*)
- Heintzenberg, J. 2000. What is wrong with today's climate models? University of Alaska. \*)
- Keil, A., Wendisch, M., Brüggemann, E., und Heintzenberg, J. 2000. Solar radiative forcing by particles containing black carbon-measurement-based case studies. Hadley Centre for Climate Prediction and Research, Bracknell, U.K.
- Klugmann, D. 2000. Cloud microphysics at IFT: Measurement and model. NOAA, Boulder, Colorado. \*)
- Klugmann, D. 2000. A semiconductor cloud radar for airborne/ground based. NCAR, Boulder, Colorado. \*)
- Klugmann, D. 2000. Wolken-Mikrophysik am IFT: Modell und Messung. Universität Mainz, Institut für Physik der Atmosphäre. \*)
- Mertes, S., Schwarzenböck, A., Brüggemann, E., Gnauk, T., Dippel, B., und Plewka, A. 2000. Reservoiraufteilung von Ruß, organischen Bestandteilen, Gesamtkohlenstoff, löslichen Substanzen und Aerosolpartikeln (Anzahl und Masse) in der Tropfen- und Zwischenraumphase von Wolken. Workshop Atmosphärische Aerosolforschung, Schierke.



- Müller, D. 2000. Seasonal cycle of optical and physical particle properties over the Indian Ocean from 6-wavelength lidar observations. NASA, Moffett Field, California.
- Teichmann, U., und Siebert, H. 2000. Concept and first results of an airship-borne cloud turbulence system. ATDD/NOAA, Oak Ridge. \*)
- Wendisch, M. 2000. Einfluss des Menschen auf das Klima. Evangelische Mittelschule Großrückerswalde. \*)
- Wendisch, M., Müller, D., Schell, D., und Heintzenberg, J. 2000. The new spectral albedometer of IfT. METEO FRANCE (CNRM), Toulouse. \*)
- Wiedensohler, A. 2000. Ergebnisse zu Aerosol-Feldexperimenten: In-situ Schließungsexperiment, Größenverteilungen des urbanen Aerosols und Partikelneubildung in der verschmutzten Grenzschicht. PSI Villingen. \*)

### Patent

#### 1999

- Stratmann, F., Sierau, B., Heintzenberg, J., und Pelzing, M. 1999. Verfahren und Vorrichtung zur größen aufgelösten chemischen und physikalischen Bestimmung von Aerosolpartikeln (patent application).

\*) invited lectures



## Chemistry section

### Publications, peer-reviewed

#### 1999

- Berndt, T., Böge, O., und Herrmann, H. 1999. On the formation of benzene oxide/oxepin in the gas-phase reaction of OH radicals with benzene. *Chem. Phys. Lett.* **314**, 435-442.
- Berndt, T., Picht, R., und Stratmann, F. 1999. An approximate method for numerically solving PDEs in chemical kinetics using Laplace transformation. *Z. Phys. Chem.* **209**, 259-270.
- Brüggemann, E., und Spindler, G. 1999. Wet and dry deposition of sulfur at the site Melpitz in East Germany. *Water Air Soil Pollut.* **109**, 81-99.
- Herrmann, H., Ervens, B., Nowacki, P., Wolke, R., und Zellner, R. 1999. A chemical aqueous phase radical mechanism for tropospheric chemistry. *Chemosphere* **38**, 1223-1232.
- Herrmann, H., Reese, A., Ervens, B., Wicktor, F., und Zellner, R. 1999. Laboratory and modelling studies of tropospheric multiphase conversions involving some C<sub>1</sub> and C<sub>2</sub> peroxy radicals. *Phys. Chem. Earth, Part B.* **24**, 287-290.
- Jacobi, H.-W., Wicktor, F., Herrmann, H., und Zellner, R. 1999. A laser flash photolysis kinetic study of reaction of the Cl<sub>2</sub>-radical anion with oxygenated hydrocarbons in aqueous solution. *Int. J. Chem. Kinet.* **31**, 169-181.
- Müller, K. 1999. A 3-year study of the aerosol in northwest saxonía (Germany). *Atmos. Environ.* **33**, 1679-1685.
- Spindler, G., Müller, K., und Herrmann, H. 1999. Main particulate matter components in Saxony (Germany) - trends and sampling aspects. *Environ. Sci. Pollut. Res.* **6**, 89-94.
- Umschlag, T., und Herrmann, H. 1999. The carbonate radical (HCO<sub>3</sub><sup>•</sup>/CO<sub>3</sub><sup>•-</sup>) as a reactive intermediate in Water chemistry: kinetics and modelling. *Acta hydrochim. hydrobiol.* **27**, 214-222.

#### 2000

- Benkelberg, H.-J., Böge, O., Seuwen, R., und Warneck, P. 2000. Product distributions from the OH radical-induced oxidation of but-1-ene, methyl-substituted but-1-enes and isoprene in NO<sub>x</sub>-free air. *Phys. Chem. Chem. Phys.* **2**, 4029-4039.
- Ervens, B., und Herrmann, H. 2000. Reply to „comment on „A chemical aqueous phase radical mechanism for tropospheric chemistry“ by R. Sander and P. Crutzen. *Chemosphere* **41**, 633-634.
- Herrmann, H., Ervens, B., Jacobi, H. W., Wolke, R., Nowacki, P., und Zellner, R. 2000. CAPRAM2.3: A chemical aqueous phase radical mechanism for tropospheric chemistry. *Journal of Atmospheric Chemistry* **36**, 231-284.
- Hofmann, D., und Herrmann, H. 2000. Method development to characterization of polar VOC-oxidations products in cloud water and aerosol. *J. High Resol. Chromatogr.* **23**, 285.
- Neusüß, C., Pelzing, M., Plewka, A., und Herrmann, H. 2000. A new analytical approach for size-resolved speciation of organic compounds in atmospheric aerosol particles: Methods and first results. *J. Geophys. Res.* **105**, 4513-4527.
- Neusüß, C., Weise, D., Birmili, W., Wex, H., Wiedensohler, A., und Covert, D. 2000. Size-segregated chemical, gravimetric and number distribution-derived mass closure of the aerosol in Sagres, Portugal during ACE-2. *Tellus* **52B**, 169-184.
- Quinn, P. K., Bates, T. S., Coffman, D. J., Miller, T. L., Johnson, J. E., Covert, D. S., Putaud, J.-P., Neusüß, C., und Novakov, T. 2000. A comparison of aerosol chemical and optical properties from the first and second Aerosol Characterization Experiments. *Tellus* **52B**, 239-257.



## Conference Proceedings

### 1999

- Berndt, T., Böge, O., und Herrmann, M. 1999. *Gas-phase reaction of NO<sub>3</sub> radicals with b-pinene.* EUROTRAC II Symposium „Transport and Chemical Transformation in the Troposphere“, Garmisch-Partenkirchen 23. - 27. März, 79-83.
- Berndt, T., Böge, O., und Herrmann, H. 1999. *Gas-phase products from the reaction of OH radicals with benzene.* EC/EUROTRAC-2 Joint Workshop „Chemical Mechanism Development (CMD)“, Aachen, 20. - 22. September, 36-39.
- Berndt, T., Böge, O., und Herrmann, H. 1999. *Produktstudien zur Gasphasenreaktion von OH Radikalen mit Benzol.* Bunsentagung 1999, Dortmund, 13.-15. Mai.
- Bolzacchini, E., Meinardi, S., Rindone, B., Hjorth, J., Umschlag, T., Weise, D., Walter, A., Herrmann, H., Palm, H., Zetzsch, C., Whitacker, B., und Pilling, M. J. 1999. *EC-Project UNARO „uptake and nitration of aromatics“.* EC/EUROTRAC-2 Joint Workshop „Chemical Mechanism Development (CMD)“, Aachen, 20.-22. September, 154-157.
- Brüggemann, E., Spindler, G., Grüner, A., Thomas, A., und Herrmann, H. 1999. *Artefacts in aerosol filterpack collection.* European Aerosol Conference, Prag, 6.-10. September, 591-592.
- Ervens, B., Böge, O., Wolke, R., und Herrmann, H. 1999. *Modellrechnungen zur troposphärischen Multiphasenchemie mittels CAPRAM2.4.* Bunsentagung 1999, Dortmund, 13.-15. Mai.
- Ervens, B., Herrmann, H., und Wolke, R. 1999. *Model calculations of tropospheric multiphase chemistry.* EGS annual meeting, Den Haag, 19.-23. April.
- Ervens, B., Wolke, R., und Herrmann, H. 1999. *Modelling calculations with CAPRAM2.4 and RACM describing tropospheric multiphase chemistry.* EC/EUROTRAC-2 Joint Workshop „Chemical Mechanism Development (CMD)“, Aachen, 20.-22. September, 324-327.
- Herrmann, H. 1999. *Current issues in tropospheric aqueous particle chemistry.* 2nd Gentener Symposium on Geoscience, Nazareth, Israel, 22.-24. Oktober.
- Herrmann, H. 1999. *Model development for atmospheric aqueous phase chemistry.* EC Cluster 2 Meeting, Brüssel, 25. November.
- Herrmann, H., Ervens, B., Hesper, J., und Wicktor, F. 1999. *Radical-induced tropospheric multiphase formation and degradation of atmospheric reactive substances (ARS).* First International Symposium on Atmospheric Reactive Substances (ARS), Bayreuth, 14.-16. April.
- Herrmann, H., Ervens, B., Hesper, J., und Wicktor, F. 1999. *Tropospheric aqueous phase chemistry laboratory and modelling studies.* Fine Particle Science and Environmental Chamber Workshop, Riverside, Oktober.
- Neusüß, C., Brüggemann, E., Gnauk, T., Wex, H., Herrmann, H., und Wiedensohler, A. 1999. *Chemical composition and mass closure of the size-segregated atmospheric aerosol in Falkenberg during LACE.* European Aerosol Conference 1999, Prag, 6.-10. September, 913-914.
- Plewka, A., Pelzing, M., Müller, K., und Herrmann, H. 1999. *Characterisation of organic substances in particulate Matter.* EGS annual meeting, Den Haag, 19.-23. April.
- Spindler, G., Brüggemann, E., Müller, K., und Herrmann, H. 1999. *Variations of nitric acid (HNO<sub>3</sub>) concentration at a rural site in saxony.* First International Symposium on Atmospheric Reactive Substances (ARS), Bayreuth, 14. - 16. April.
- Spindler, G., Müller, K., und Herrmann, H. 1999. *PM 10 and PM 2.5 particle concentration measurements with filterpacks - a four year study in Saxony (Germany).* European Aerosol Conference, Prag, 6.-10. September, 895-896.
- Umschlag, T., Herrmann, H., und Zellner, R. 1999. *Kinetic study of the reaction of NO<sub>3</sub>· radicals with different aromatic compounds in pH dependent measurements in aqueous solution.* EC/EUROTRAC-2 Joint Workshop „Chemical Mechanism Development (CMD)“, Aachen, 20. - 22. September, 175-178.
- Wicktor, F., und Herrmann, H. 1999. *Direct Laser-based kinetic and spectroscopic investigations of the Cl-atom in aqueous solution.* EC/EUROTRAC-2 Joint Workshop „Chemical Mechanism Development (CMD)“, Aachen, 20. - 22. September, 183-186.

### 2000

- Barzaghi, P., und Herrmann, H. 2000. *Oxidation process of phenol by Nitrate radical in aqueous phase: A product study.* EUROTRAC-2 Joint Workshop, Lausanne, 10.-13. September.
- Berndt, T., und Böge, O. 2000. *Gas-phase reaction of OH radicals with Benzene: products and mechanism.* EUROTRAC-2 Joint Workshop, Lausanne, 10.-13. September.



- Berndt, T., Böge, O., Conrath, T., Stratmann, F., und Heintzenberg, J. 2000. *Formation of new particles in the system  $H_2SO_4(SO_3)/H_2O/(NH_3)$  - first results from a flow-tube study.* European Aerosol Conference, Dublin, 3.-8. September, 554-555.
- Brüggemann, E., Gnauk, T., Müller, K., Neusüß, C., Plewka, A., Spindler, G., und Herrmann, H. 2000. *Recent results from different aerosol chemical characterisation field experiments: budgets and processes.* Fourth German-Italien-Workshop on Atmospheric Chemistry, Kloster Marienthal, 2. Juni.
- Donati, A., und Herrmann, H. 2000. *Laser-based laboratory studies of Cl atom reactions in aqueous solution.* EUROTRAC-2 Joint Workshop, Lausanne, 10.-13. September.
- Engelhardt, T., Lammel, G., Neusüß, C., Röhrli, A., und Wieser, P. 2000. *Changes of the aerosol chemical composition during transport over a metropolitan area.* European Aerosol Conference, Dublin, 3.-8. September, 751-752.
- Ervens, B., Donati, A., Barzagli, P., Hesper, J., und Herrmann, H. 2000. *Laboratory and modelling studies of radical (OH,  $NO_3$ )-initiated tropospheric organic aqueous phase conversion processes.* AGU-Meeting, San Francisco, 14.-15. Dezember.
- Ervens, B., und Herrmann, H. 2000. *CAPRAM2.4 - Ein Multiphasenmechanismus zur Beschreibung troposphärischer Wolkenchemie.* Bunsentagung, Würzburg, 1.-3. Juni.
- Ervens, B., und Herrmann, H. 2000. *Experimental determination of OH-reaction rates with organics ( $^3C_2$ ) and their importance to tropospheric multiphase chemistry.* EUROTRAC-2 Joint Workshop, Lausanne, 10.-13. September.
- Ervens, B., Hesper, J., Neusüß, C., und Herrmann, H. 2000. *Field, laboratory and modelling studies of tropospheric aerosol and cloud chemistry.* 25th EGS General Assembly, Nice, 25. - 29. April.
- Ervens, B., Wolke, R., und Herrmann, H. 2000. *CAPRAM2.4: An updated and revised chemical aqueous phase radical mechanism describing tropospheric cloud chemistry.* EUROTRAC II Symposium „Transport and Chemical Transformation of Pollutants in the Troposphere“, Garmisch-Partenkirchen, 27.-31. März.
- Herrmann, H. 2000. *Connected laboratory studies and mechanism development in CMD: tropospheric aqueous phase chemistry as an exemple.* 4th Gloream Workshop, Cottbus, 20.-22. September.
- Herrmann, H. 2000. *Laboratory studies and mechanism development for tropospheric aqueous particle chemistry.* EUROTRAC II Symposium „Transport and Chemical Transformation of Pollutants in the Troposphere“, Garmisch-Partenkirchen, 27-31 März.
- Herrmann, H., Ervens, B., Weise, D., Wicktor, F., Donati, A., und Barzagli, P. 2000. *Abbau- und Konversionsreaktionen organischer Verbindungen in troposphärischen wässrigen Partikeln.* Jahrestagung der GDCh-Fachgruppe Umweltchemie und ...kotoxikologie, Bayreuth, 7.-10. Oktober.
- Hesper, J., und Herrmann, H. 2000. *A T-dependent study of the reaction of the superoxide radical anion ( $O_2^-$ ) with ozone in aqueous solution.* EUROTRAC II Symposium „Transport and Chemical Transformation of Pollutants in the Troposphere“, Garmisch-Partenkirchen, 27.-31. März.
- Hofmann, D., und Herrmann, H. 2000. *Method development for the characterization of polar VOC-oxidations products in cloud water and aerosol.* EUROTRAC II Symposium „Transport and Chemical Transformation of Pollutants in the Troposphere“, Garmisch-Partenkirchen, 27. - 31. März.
- Müller, K., Brüggemann, E., Gnauk, T., Plewka, A., Herrmann, H., Franck, U., Wennrich, R., und Stärk, H.-J. 2000. *Chemical and structural characterization of size segregated winter time aerosol from two urban and a rural sampling site in NW Saxony (Germany).* European Aerosol Conference, Dublin, 3. - 8. September.
- Müller, K., Pelzing, M., Gnauk, T., Spindler, G., Teichmann, U., Siebert, H., Herrmann, H., Kuhn, U., Kesselmeier, J., und Wolf, A. 2000. *Biogenic emissions of rape (*Brassica napus*) during blooming period.* EUROTRAC II Symposium „Transport and Chemical Transformation of Pollutants in the Troposphere“, Garmisch-Partenkirchen, 27.-31. März.
- Neusüß, C., Brüggemann, E., und Herrmann, H. 2000. *Organic acids in atmospheric particles: Results from different field campaigns in Europe.* European Aerosol Conference, Dublin, 3.-8. September, 238-239.
- Plewka, A., Müller, K., und Herrmann, H. 2000. *Size-resolved sampling and analysis of organics in urban airborne particles by means of Curie-Point-Pyrolysis-GC/MS.* EUROTRAC II Symposium „Transport and Chemical Transformation of Pollutants in the Troposphere“, Garmisch-Partenkirchen, 27.-31. März.
- Spindler, G., Gnauk, T., und Herrmann, H. 2000. *PM 10, PM 2.5 and PM 1 particle Ion and soot concentration measurements with Filterpacks 1999 in saxony (Germany).* EUROTRAC II Symposium „Transport and Chemical Transformation of Pollutants in the Troposphere“, Garmisch-Partenkirchen, 27.-31. März.



- Spindler, G., Gnauk, T., Herrmann, H., Müller, K., und Teichmann, U. 2000. *Size dependent particle concentration and deposition measurements with filterpakcs - a five year study in Germany*. The Sixth International Conference on Air-Surface Exchange of Gases and Particles, Edinburgh, 3.-7. Juli.
- Weise, D., Ervens, B., Wolke, R., und Herrmann, H. 2000. *Modeling of multiphase chemistry in clouds under marine boundary layer conditions*. EUROTRAC-2 Joint Workshop, Lausanne, 10.-13. September.
- Wicktor, F., Herrmann, H., und Zellner, R. 2000. *Laser-based laboratory studies of Cl-reactions in aqueous solution*. 4th-Italien-German Workshop on Tropospheric Chemistry, St. Marienthal, 2. - 4. Juni.
- Wolke, R., Knoth, O., und Herrmann, H. 2000. *Numerical treatment of aqueous-phase chemistry in atmospheric chemistry transport modelling*. 24th Internat. Meeting on Air Pollution and its Applications, Boulder, USA.

### Lectures

#### 1999

- Herrmann, H. 1999. Vorstellung der Arbeiten der Abteilung Chemie des IfT. Sitzung der Sektion E der WGL Potsdam.
- Neusüß, C., Plewka, A., Pelzing, M., und Herrmann, H. 1999. Bestimmung des organischen Anteils von Partikeln verschiedener Größen in der Atmosphäre. Dresden, Juli.
- Neusüß, C., Plewka, A., Pelzing, M., und Herrmann, H. 1999. Die chemische Zusammensetzung von Partikeln verschiedener Größen in der Atmosphäre. Tag der offenen Tür der Universität Leipzig, Juli.

#### 2000

- Herrmann, H. 2000. Laboruntersuchungen und Modellrechnungen zur troposphärischen Multiphasenchemie. Seminar über aktuelle Forschungsthemen der Meteorologie, Institut für Meteorologie und Klimaforschung Karlsruhe. \*)
- Herrmann, H. 2000. Mechanismenentwicklung zur heterogenen Chemie. DWD Offenbach. \*)
- Herrmann, H. 2000. Troposphärische Mehrphasenchemie in Feld- und Laborexperimenten sowie Modellierung. Institutskolloquium, FH Magdeburg. \*)
- Herrmann, H. 2000. Troposphärische Multiphasenchemie in Feld, Labor und Modellierung. Institutskolloquium, TU München. \*)
- Spindler, G., Brüggemann, E., Gnauk, T., Müller, K., Neusüß, C., Plewka, A., und Herrmann, H. 2000. Partikel in der Troposphäre. Kolloquium „Fassadenverschmutzungen“, Deutsches Amphibolin-Werk von Robert Murjahn GmbH & Co.KG. \*)
- Spindler, G., Brüggemann, E., Gnauk, T., Müller, K., Neusüß, C., Plewka, A., und Herrmann, H. 2000. Depositionen aus der Troposphäre. Symposium „Denkmal 2000“, Leipzig, 26.-28. Oktober. \*)

\*) invited lectures



## Modeling section

### Book Section

#### 2000

Hellmuth, O. 2000. *Erfassung des Geländeklimas*. H. Barsch, K. Billwitz, and H.-R. Bork (Ed.), In *Arbeitsmethoden in Physiogeographie und Geoökologie*. Klett-Perthes, Gotha und Stuttgart, p.230-253.

### Publications, peer-reviewed

#### 1999

Münzenberg-St. Denis, A., und Renner, E. 1999. Numerical investigation of the influence of biogenic emissions on ozone over Saxony (Germany). *Physics and Chemistry of the Earth (C)* **24**, 487-490.

#### 2000

Göldner, R., Theiss, D., und Renner, E. 2000. Dynamisiertes Emissionskataster für den Freistaat Sachsen. *Umweltwiss. Schadstoff-Forsch.* **12**, 83-87.

Hellmuth, O., und Renner, E. 2000. Diagnostic determination of mixing layer height and entrainment layer thickness in the convective boundary-layer using a spectral entraining jet model. *Meteor. Zeitschr.* **9**, 283-298.

Krämer, M., Beltz, N., Schell, D., Elbert, W., Schütz, L., Sprengart-Eichel, und Wurzler, S. 2000. Cloud processing of continental aerosol particles: Experimental investigations for different drop sizes. *J. Geophys. Res.* **105**, 11739-11752.

Wolke, R., und Knuth, O. 2000. Implicit-explicit Runge-Kutta methods applied to atmospheric chemistry-transport modelling. *Environ. Model. Software* **15**, 711-719.

Wurzler, S., Reisin, T. G., und Levin, Z. 2000. Modification of mineral dust particles by cloud processing and subsequent effects on drop size distributions. *J. Geophys. Res.* **105**, 4501-4545.

### Conference Proceedings

#### 1999

Holke, H., und Knuth, O. 1999. *Atmospheric flows on locally refined grids. Numerical treatment of multi-scale problems*, 13. Internationales GAMM-Seminar, Kiel, 46-57.

Knuth, O., und Wolke, R. 1999. *Source splitting versus operator splitting in air chemistry models*. 5th SIAM-Conference on „Mathematical and Computational Issues in the Geoscience“, San Antonio, 24.-27. März.

Knuth, O., und Wolke, R. 1999. *Strang splitting versus implicit-explicit methods in solving chemistry-transport-models*. EUROTRAC Symposium ,98, Garmisch-Partenkirchen, 23.-27. März, 524-528.

Münzenberg-St. Denis, A., Renner, E., und Wolke, R. 1999. *The role of biogenic emissions on ozone production over Saxony investigated with the Model System METRAS-MUSCAT-Euro-RADM*. 2nd GLOREAM Workshop, Madrid, 16.-18. September, 26-35.

#### 2000

Albrecht, T., Notholt, J., Wolke, R., und Malberg, H. 2000. *Variations of CH<sub>2</sub>O: FTIR measurements and model studies*. AGU Fall Meeting, San Francisco.

Albrecht, T., Notholt, J., Wolke, R., Solberg, S., Dye, C., und Malberg, H. 2000. *Variations of CH<sub>2</sub>O and C<sub>2</sub>H<sub>2</sub> determined from groundbased FTIR measurements*. OSPAR (Committee on Space Research) - Assembly, Warsaw, Poland, 16.-23. Juli, CD-ROM.



- Hellmuth, O., und Renner, E. 2000. *Influence of turbulence parameterization on the mixing layer height prediction with a mesoscale model*. NATO/CCMS International Technical Meeting on Air Pollution Modeling and its Application, Boulder, USA, 15.-19. Mai, 387-396.
- Hinneburg, D., Knoth, O., Mölders, N., Münzenberg, A., und Wolke, R. 2000. *Subgrid-modelling of dry deposition*. Symposium EUROTRAC-2, Garmisch-Partenkirchen, 26.-31. März 2000.
- Münzenberg, A., Göldner, R., Heinrich, B., Knoth, O., Renner, E., Schröder, W., Theiss, D., und Wolke, R. 2000. *Numerical air quality studies for Saxony/Germany and the black triangle area*. Symposium EUROTRAC-2, Garmisch-Partenkirchen, 26.-31. März 2000.
- Münzenberg, A., Göldner, R., Renner, E., Theiss, D., und Wolke, R. 2000. *The influence of different emission source types on ozone formation over Saxony (Germany), investigated with the model system METRAS-MUSCAT-RACM*. GLOREAM-Workshop ,99, Ischia, 22.-24. September, 217.
- Vohl, O., Mitra, S., Wurzler, S., Pruppacher, H., Pinsky, M., und Khain, A. 2000. *Laboratory and theoretical studies of the collision efficiencies of cloud droplets and small rain drops*. 13th International Conference on Clouds and Precipitation (ICCP), Reno, USA, 102-104.
- Wolke, R., Knoth, O., und Herrmann, H. 2000. *Numerical treatment of aqueous-phase chemistry in atmospheric chemistry transport modelling*. 24th Internat. Meeting on Air Pollution and its Applications, Boulder, USA.
- Wolke, R., Knoth, O., Münzenberg, A., Renner, E., und Schröder, W. 2000. *Numerical modelling of urban and regional scale interactions*. SIMPAQ-2000 Symposium: Scale Interactions in Models and Policies for Air Quality Management, Antwerpen, Belgien, 13. und 14. April, 64-68.
- Wolke, R., Knoth, O., Münzenberg-St. Denis, A., und Schröder, W. 2000. *Online coupling of multiscale chemistry-transport models with non-hydrostatic meteorological models*. 23th Internat. Meeting on Air Pollution Modeling and its Application, Varna, 28. Sept. - 2. Oktober, 769-770.
- Wolke, R., Knoth, O., und Weickert, J. 2000. *Load-balancing in the parallelization of the multiscale atmospheric chemistry-transport model MUSCAT*. 16th IMACS World Congress 2000, Lausanne, Schweiz, 21.-25. Aug. 2000, 7.
- Wurzler, S. 2000. *The interactions between clouds, aerosol particles and gases*. 5th International WMO cloud modeling workshop, Glenwood Springs, Colorado.
- Wurzler, S., und Bott, A. 2000. *Numerical simulations of cloud microphysics and drop freezing as function of drop contamination*. 13th International Conference on Clouds and Precipitation, Reno, USA, 469-470.
- Wurzler, S., und Bott, A. 2000. *Numerical simulations of cloud microphysics and drop freezing as function of drop contamination*. European Aerosol Conference, Dublin, 3.-8. September, 152-153.
- Yin, Y., Wurzler, S., Reisin, T., und Levin, Z. 2000. *Modification of the size and composition of CCN by cloud processing of mineral dust particles and the effects on cloud microphysics*. 13th International Conference on clouds and precipitation, Reno, USA, 936-939.

### Lectures

#### 1999

- Knoth, O. 1999. Parallele Iterationsverfahren zur Lösung der 3D Laplace-Gleichung. 2. Halle-Leipzig-Seminar zur Parallelverarbeitung, Halle/Saale, 11. Januar.
- Münzenberg, A. 1999. Modellstudien zur Luftreinhaltung im Gebiet des Schwarzen Dreiecks. Kepler-Gymnasium Leipzig.
- Münzenberg, A., Göldner, R., Renner, E., Theiss, D., und Wolke, R. 1999. The influence of different emission source types on ozone formation over Saxony (Germany), investigated with the model system METRAS-MUSCAT-RACM,. GLOREAM-Workshop ,99.
- Renner, E. 1999. Modellsimulation zur SO<sub>2</sub>-Ausbreitung in der Erzgebirgsregion. Institut für Energetik und Umwelt, Leipzig.
- Weickert, J., und Wolke, R. 1999. Parallelisierung eines 3D Chemie-Transport-Modells. 2. Halle-Leipzig-Seminar zur Parallelverarbeitung, Halle/Saale, 11. Januar.
- Weickert, J., und Wolke, R. 1999. Load imbalances in the parallel implementation of the Multiscale Atmospheric Model MUSCAT. Sozopol, Bulgaria, 2.-6. Juni.
- Wolke, R., und Knoth, O. 1999. The efficiency of different time integration schemes in relation to the used horizontal resolution. Sozopol, Bulgaria.

**2000**

- Hellmuth, O. 2000. Parametrization of turbulent mixing processes in the mesoscale. University of Warsaw, Poland, Interdisciplinary Center of Modelling. \*)
- Hellmuth, O. 2000. Zum Einfluss turbulenter Austauschgrößen auf die mesoskalige Vorhersage meteorologischer Felder. Alfred-Wegener-Institut Potsdam.
- Hellmuth, O., Eger, R., und Helmert, J. 2000. Sensitivitätsstudien zur Parametrisierung des Vertikalaustausches zwischen planetarer Grenzschicht und freier Troposphäre mit einem mesoskaligen Modell. Freie Universität Berlin, Meteor. Institut.
- Hellmuth, O., und Helmert, J. 2000. On the influence of turbulence parametrization on the mixing layer height prediction using a mesoscale model. LINEX-Workshop, Meteor. Observatorium Lindenberg. \*)
- Knoth, O. 2000. Integrationsverfahren für kinetische Gleichungen in Produktform. Institut für Numerische Mathematik, Martin-Luther-Universität, Halle. \*)
- Knoth, O. 2000. Kopplung von meteorologischen und Ausbreitungsmodellen: Die Berechnung divergenzfreier Windfelder. Oberseminar Numerische Mathematik/Scientific Computing, FU Berlin und ZIB, Berlin. \*)
- Knoth, O., und Wolke, R. 2000. Coupled integration of chemistry and transport in microscale air quality modelling. 9th Seminar NUMDIFF on Numerical Solution of Differential and Differential-Algebraic Equations, Halle. \*)
- Münzenberg, A., Göldner, R., Heinrich, B., Renner, E., Schröder, W., Theiss, D., und Wolke, R. 2000. Szenarienrechnungen zur Immissionsbelastung mit SO<sub>2</sub>, Ozon und Feinstaub: Analyse und Prognose. OMKAS-Tagung, Dresden.
- Weickert, J., und Wolke, R. 2000. Parallele Modelle zur Berechnung der Schadstoffausbreitung. 6. Südostdeutsches Kolloquium zur Numerischen Mathematik, Chemnitz.
- Wolke, R. 2000. Mesoskalige Chemie-Transport-Modellierung am IfT Leipzig. AWI Potsdam. \*)
- Wolke, R. 2000. Time-Integration of multiphase chemistry in size-resolved cloud models. 9th Seminar NUMDIFF on Numerical Solution of Differential and Differential-Algebraic Equations, Halle. \*)
- Wurzler, S. 2000. Laboratory investigations of possible turbulence effects in clouds. University of Warsaw, Poland, Interdisciplinary Center of Modelling. \*)

\*) invited lectures



**University courses**

**University Leipzig  
Faculty for Physics  
and Geosciences**

<b>Winter Semester</b>		<b>1998/1999</b>
<u>Ansmann, A.</u> <u>Heintzenberg, J.</u> <u>Klugmann, D.</u> <u>Teichmann, U.</u>	<i>Modern Meteorological Instruments I</i>	1 HPW*)
<u>Heintzenberg, J.</u>	<i>Radiation in the Atmosphere</i>	1 HPW
<u>Heintzenberg, J.</u> <u>Stratmann, F.</u> <u>Wiedensohler, A.</u>	<i>Atmospheric Aerosols I</i>	2 HPW
<u>Herrmann, H.</u>	<i>Atmospheric Chemistry I</i>	2 HPW
<u>Renner, E.</u>	<i>Modeling of transport and chemical transformation of air pollutants</i>	2 HPW
<u>Wendisch, M.</u>	<i>Airborne Physical Measurement Methods</i>	1 HPW

<b>Summer Semester</b>		<b>1999</b>
<u>Herrmann, H.</u>	<i>Atmospheric Chemistry II</i> <i>Atmospheric Chemistry Seminar</i>	2 HPW 2 HPW
<u>Renner, E.</u> <u>Hellmuth, O.</u> <u>Knoth, O.</u> <u>Wolke, R.</u>	<i>Introduction to Mesoscale Models</i>	2 HPW
<u>Stratmann, F.</u> <u>Wiedensohler, A.</u>	<i>Atmospheric Aerosols II</i>	2 HPW
<u>Wendisch, M.</u>	<i>Airborne Physical Measurement Methods</i>	1 HPW



Winter Semester		1999/2000
<u>Heintzenberg, J.</u>	<i>Radiation in the Atmosphere</i>	1 HPW
<u>Heintzenberg, J.</u> <u>Stratmann, F.</u> <u>Wiedensohler, A.</u>	<i>Atmospheric Aerosols I</i>	2 HPW
<u>Heintzenberg, J.</u>	<i>Modern Meteorological Instruments I</i>	1 HPW
<u>Herrmann, H.</u>	<i>Atmospheric Chemistry I</i> <i>Atmospheric Chemistry Seminar</i> <i>Atmospheric Chemistry Lab</i>	2 HPW 2 HPW block course
<u>Renner, E.</u>	<i>Modeling of transport and chemical transformation of air pollutants</i>	2 HPW
<u>Wandinger, U.</u>	<i>Atmospheric Optics</i>	2 HPW
<u>Wendisch, M.</u>	<i>Airborne Physical Measurement Methods</i>	1 HPW

**Friedrich-Schiller-University Jena  
Faculty for Chemistry  
and Geosciences**

<u>Renner, E.</u> <u>Hellmuth, O.</u>	<i>Environmental Meteorology</i> <i>Modeling of transport and chemical transformation of air pollutants</i>
--	--

**University Leipzig  
Faculty for Physics  
and Geosciences**

Summer Semester		2000
<u>Heintzenberg, J.</u> <u>Stratmann, F.</u> <u>Wiedensohler, A.</u>	<i>Atmospheric Aerosols II</i>	2 HPW
<u>Heintzenberg, J.</u>	<i>Modern Meteorological Instruments</i>	1 HPW
<u>Herrmann, H.</u>	<i>Atmospheric Chemistry II</i> <i>Atmospheric Chemistry Exercises</i> <i>Atmospheric Chemistry Seminar</i>	2 HPW 1 HPW 2 HPW
<u>Renner, E.</u> <u>Hellmuth, O.</u> <u>Knoth, O.</u> <u>Wolke, R.</u>	<i>Mesoscale Meteorological Modeling</i>	2 HPW
<u>Wendisch, M.</u>	<i>Airborne Physical Measurement Methods</i>	1 HPW

\*) hours per week



**Doctoral theses 1999**

**University Leipzig  
Faculty for Physics and  
Geosciences**

Holke, Henrik Numerische Untersuchungen zur Verwendung lokal verfeinerter Gitter in nichthydrostatischen mesoskaligen Atmosphärenmodellen

**University Leipzig  
Faculty for Chemistry and  
Mineralogy**

Kind, Ina Kinetische Untersuchungen atmosphärisch relevanter Gasphasenreaktionen des  $\text{NO}_3$ -Radikals

**Doctoral theses 2000**

**University Leipzig  
Faculty for Physics  
and Geosciences**

Hermann, Markus Development and application of an aerosol measurement system for use on commercial aircraft

Keil, Andreas Einfluß absorbierender Aerosolpartikel und verschmutzter Wolken auf den solaren Strahlungshaushalt der Atmosphäre

Philippin, Sabine Development and applications of an analyser for airborne non-volatile aerosol compounds

Wagner, Frank Kombinierte Mehrwellenlängen-Lidar-Photometermessungen von optischen und physikalischen Partikelparametern während ACE-2

Wehner, Birgit Particle formation in the urban atmosphere

**University Leipzig  
Faculty for Chemistry  
and Mineralogy**

Neusüß, Christian Größenaufgelöste Zusammensetzung atmosphärischer Aerosolpartikel: Chemische Massenbilanz und organische Säuren

**Master theses 1999****University Leipzig  
Faculty for Physics  
and Geosciences**

- Helmert, Jürgen                      Zur Parametrisierung der Mächtigkeit der Entrainmentschicht unter Verwendung von Large-Eddy-Simulations- und LIDAR-Daten
- Schmidt, Sebastian                Das Fast FSSP: Charakterisierung und Messbeispiele
- Weise, Diana                        Aerosolgrößenverteilung in der planetaren Grenzschicht bei Sagres/ Portugal (ACE-2-Experiment)

**Fachhochschule Aachen  
Fachbereich Maschinenbau**

- Cohrt, Carsten                      Quantitative Analyse des graphitischen Kohlenstoff-Anteils im atmosphärischen Aerosol mittels NIR-FT-Raman-Spektroskopie

**Westsächsische Hochschule Zwickau  
Fachbereich Physikalische Technik/Informatik**

- Rockmann, Alexander            Modifikation und Kalibrierung eines Rußphotometers für die Messung von Rußproben eines automatischen Aerosolprobensammlers auf einem kommerziellen Flugzeug

**Master theses 2000****University Leipzig  
Faculty for Physics  
and Geosciences**

- Eger, Reinhard                      3D-Simulationen mit einem mesoskaligen Modell zum Einfluß der Turbulenzparametrisierung auf die Entwicklung der Mischungsschicht-höhe
- Koziar, Christian                    Ursachen und Auswirkungen von Partikelnukleation - Eine Analyse im Rahmen des Lindenberger Aerosol-Charakterisierungs-Experimentes
- Nowak, Andreas                      Aerosolgrößenverteilungen in diversen Klimazonen
- Walter, Arno                        Modifikation und Anwendung eines troposphärenchemischen Mehrphasenmodells

**Fachhochschule Magdeburg  
Fachbereich Chemie/Pharmatechnik**

- Witter, Markus                      Ozonolyse ausgewählter Terpene in der Gasphase



## Guest scientists

### 1999

Dr. Evan Whitby	23./26. März 99	Cimera Tech Minneapolis, USA
Prof. Dr. Robert J. Charlson	19./30. April 99	University of Washington, Seattle, USA Dept. of Atmospheric Sciences
Scot T. Martin	2./6. Sept. 99	University of North Carolina at Chapel Hill, USA
Dr. S. Bobrovnikov Dr. Y. Arshinov I. Serikov	11.Okt./8. Dez.99	Russ. Academy of Sciences Inst.f. Atmosph. Optics Tomsk

### 2000

Dr. Maring	17./18. Febr. 00	University of Miami, Florida, USA
Dr. Maria K. Facchini	23./25. Febr. 00	Inst. of Atmospheric and Oceanic Sciences National Research Council, Bologna, Italy
Dr. Yinon Rudich	3./5. April 00	Weizmann Institute Rehovot, Israel Dept. of Environmental Sciences
Dr. Y. Arshinov I. Serikov	15.Juni/15.Juli 00	Russ. Academy of Sciences Inst.f. Atmosph. Optics Tomsk
Dr. Fred Brechtel	2./17. April 00	Brookhaven National Laboratory, Upton, USA
Prof. Michael R. Hoffmann	23./30. Mai 00	California Institute of Technology, Pasadena, USA
R. Kouznetsov	4./6. Juni 00	Russian Academy of Sciences Inst. of Atmospheric Physics
Prof. Dr. Robert J. Charlson	26.Okt./4.Nov.00	University of Washington, Seattle, USA Dept. of Atmospheric Sciences
Dr. Andreas Muschinski	19. –23. Juni 00	Cooperative Institute for Research in
	20. –24. Nov. 00	Environmental Sciences, University of Colorado/NOAA, Boulder, Colorado, USA
Assoc.Prof. Min Hu	1./31. Dez.00	Peking University, China Center for Environmental Sciences



## Scientific events

1999

Event	Place and Date	Participants
Workshop on Urban Aerosols	Leipzig, 25-26 January 1999	University of Lund, Sweden University of Helsinki, Finland University of Manchester, Inst.f.Science and Technology, UK Eidgenössische Material- und Prüfungsanstalt Dübendorf, Schweiz TSI GmbH Aachen ECN - Netherlands Energy Research Foundation, Petten, Netherlands GSF- Forschungszentrum für Gesundheit und Umwelt GmbH München/Erfurt Umweltforschungszentrum Leipzig/Halle GmbH

2000

Event	Place and Date	Participants
Project Meeting CARIBIC (Civil Aircraft for Regular Investigation of the atmosphere Based on an Instrument Container)	Leipzig, 16 May 2000	Max-Planck-Institut für Chemie, Mainz Kernforschungszentrum Karlsruhe, Inst. für Meteorologie und Klimaforschung Max-Planck-Institut f. Aeronomie, Katlenburg-Lindau Royal Dutch Meteorological Institute de Bilt, Netherland Lund University, Sweden University of East Anglia, Norwich, UK



## Memberships

### Ansmann, A.

Committee on Laser Atmospheric Studies (CLAS)

### Heintzenberg, Jost

Nationales Komitee für Forschung auf dem Gebiet globaler Umweltveränderungen der Deutschen Forschungsgemeinschaft  
Ordentliches Mitglied der Sächsischen Akademie der Wissenschaften  
Wissenschaftlicher Beirates des Deutschen Wetterdienstes  
VDI-Ausschuß Messen von Ruß  
Editor of Geophysical Research Letters  
Editorial Board Tellus B, Atmospheric Research  
Permanent Scientific Advisory Committee of the Centro de Geofisica de Evora, Portugal

### Herrmann, Hartmut

IUPAC Committee "Aqueous Solution Kinetics Data for Atmospheric Chemistry"  
Koordiniierungskomitee des EUROTRAC II-Projekts CMD  
Kordinator des CMD-Teilprojekts CMD-APP (Aqueous Phase Processes)  
CMD Data Evaluation Panel  
GdCh, Arbeitskreis "Atmosphärenchemie"

### Müller, Konrad

EUROTRAC Subprojekt AEROSOL Steering Committee

### Renner, Eberhard

TFS-Gutachtergremium des Bundesministeriums für Bildung und Forschung

### Stratmann, Frank

Stellv. Vorsitzender der Arbeitsgruppe "Aerosol Modelling" der European Aerosol Assembly (EAA)  
Vorstand der Gesellschaft für Aerosolforschung  
"Scientific Programm Committee" der Europäischen Aerosolkonferenz

### Wandinger, Ulla

International Commission on Lasers in Atmospheric Sciences (ICLAS)

### Wendisch, Manfred

Koordinierungskomitee "Direct Aerosol Radiative Forcing" (IGAC)

### Wiedensohler, Alfred

Vizepräsident und Mitglied des Vorstandes der Gesellschaft für Aerosolforschung  
Koordinierungskomitee "Aerosol Characterisation and Process Studies" (IGAC)  
"Scientific Advisory Group" für Aerosole innerhalb des "Global Watch"-Programmes der World Meteorological Organization



## National and international cooperation

1999/2000

Research Project	Cooperation Partners
<p>AEROSOL "The Aerosol Balance in Europe" EUROTRAC 2</p> <p>Characterization of aerosols in strong anthropogenically influenced industry and agrarregions</p> <p>Characterization of aerosols over the Indian Ocean Indian Ocean Experiment (INDOEX)</p> <p>New particle formation</p> <p>Multiwavelength lidar and aircraft observations during an aerosol closure experiment</p> <p>Characterization of the vertical aerosol distribution over an anthropogenically influenced region</p> <p>Optimization of methods for the reduction emissions in the black triangle</p>	<p>European Partners</p> <p>Max-Planck-Institut für Meteorologie, Hamburg Universität Hohenheim Umweltforschungszentrum Leipzig/Halle GmbH</p> <p>Center for Clouds, Chemistry and Climate, Scripps Institution of Oceanography, La Jolla, USA Florida State University, Tallahassee, USA Koninklijk Nederlands Meteorologisch Instituut, De Bilt, Netherlands Max Planck Institut für Chemie, Mainz Meterological Service of the Maldives National Center for Atmospheric Research (NCAR), Boulder, USA National Oceanographic and Atmospheric Administration (NOAA), Boulder, USA University of Washington, Seattle, USA NOAA-PMEL, Seattle, USA</p> <p>Deutscher Wetterdienst Met. Observatorium Hohenpeißenberg</p> <p>Max-Planck-Institut für Meteorologie, Hamburg Max-Planck-Institut für Chemie, Mainz GSF - Forschungszentrum für Umwelt und Gesundheit, München Met. Observatorium Lindenberg Deutsches Zentrum für Luft- und Raumfahrt, Oberpfaffenhofen / Neustrelitz Universitäten: Berlin, Darmstadt, Potsdam, Frankfurt, Bremen München, Mainz, Würzburg, Hohenheim, Wien</p> <p>Max-Planck-Institut für Meteorologie, Hamburg Leibniz-Institut für Atmosphärenphysik, Kühlungsborn Universität Potsdam Fraunhofer-Institut für Atmosphären- und Umweltforschung, Garmisch-Patenkirchen</p> <p>Hochschule Zittau/Görlitz Sächs. Landesamt für Umwelt und Geologie, Dresden</p>



Research Project	Cooperation Partners
Modelling of unimolecular reactions Model Development	Universität Halle, Institut für Physikalische Chemie
Reservoir distribution of atmospheric trace gases	Brandenburgische Technische Universität Cottbus Fraunhofer-Institut für Toxikol. und Aerosol- forschung Hannover
PROCLOUD "Laboratory studies of free radical aqueous phase cloud and aerosol processes"	European Partners
CMD-APP "Interactions of free radicals with organics within the tropospheric aqueous phase"	European Partners
CMD-MPM "Modelling calculations of tropospheric gasphase and aqueous phase chemistry"	European Partners
UNARO "Uptake and nitration of aromatics"	University of Milano, Italy University of Leeds, England Fraunhofer-Institut für Toxikologie und Aerosol- forschung, Hannover
MODAC "Model development for tropospheric cloud- and aerosol chemistry"	University of Utrecht, Netherlands University of Strasbourg, France
The influence of heterogeneous reactions In seasalt-aerosol on regional and global photooxidant chemistry	Max-Planck-Institut für Chemie, Mainz University of Utrecht, Netherlands
Atmospheric aerosol chemistry	Harvard University, Boston, USA
MITRAS, Development of a numerical scheme for high resolution models under consideration of transport and deposition of diesel soot	Universität Hamburg, Meteorologisches Institut Alfred-Wegener-Institut, Bremerhaven Fraunhofer Institut f. Atmosphären- und Umweltforschung, Garmisch-Partenkirchen
Modelling of mixing height and of entrainment processes	Universität Hamburg, Meteorologisches Institut Deutscher Wetterdienst, Offenbach Deutscher Wetterdienst, Met. Observatorium Lindenberg
Parallelization of meteorological and chemical transport models	Universität Leipzig, Inst. f. Meteorologie Universität Leipzig, Inst. f. Informatik Technische Universität Chemnitz, Fakultät für Mathematik
Modelling of micro-physical and chemical processes in cloud droplets	Brandenburgische Technische Universität Cottbus Universität Hamburg, Meteorologisches Institut



Research Project	Cooperation Partners
Implicit-explicit methods for integration of chemistry-transport-models	Universität Halle, Fachbereich Mathematik und Informatik Centrum for Wiskunde en Informatica, Amsterdam, Netherlands
GLOREAM, "Regional modelling of air pollution in Europe"	European Partners
SATURN, "Studying atmospheric pollution in urban areas"	European Partners
EARLINET (A European Aerosol Research Lidar Network to establish an aerosol climatology)	European Partners
Development of a dynamical high resolution emission inventory for Saxony	Technische Universität Dresden Hochschule Zittau/Görlitz
The role of cloud processing and of organic matter in the formation of soluble layers on mineral dust particles and the impact on cloud characteristics	Universität Bonn, Meteorologisches Institut Max-Planck-Institut für Chemie, Mainz, Tel Aviv University, Israel Dept. of Geophysics and Planetary Sciences Weizmann Institut Rehovot, Israel
Effects of aerosol particles on drop size distributions and drop freezing: A numerical investigation with detailed cloud microphysics and derivation of parameterizations	Universität Bonn, Institut für Meteorologie
Influence of anthropogenically polluted clouds on the radiation budget of the atmosphere and the formation of photochemical smog.	Universität Bonn, Meteorologisches Institut Universität Mainz, Institut für Physik der Atmosphäre Universität Leipzig, Institut für Meteorologie
Temperature lidar	Institute for Atmospheric Optics, Siberian Branch of the Russian Academy of Sciences, Tomsk, Russia



## Boards

### Scientific Advisory Board

1999/2000

Name	Institution
Chair Prof. Dr. E. Schaller	Brandenburgische Technische Universität Cottbus Lehrstuhl für Umweltmeteorologie
Dr. Ruth Baumann	Umweltbundesamt Wien, Österreich
Prof. Dr. H. W. Gäggeler	Paul-Scherrer-Institut Würenlingen/Villigen, Schweiz
Prof. Dr. O. Herbarth	Umweltforschungszentrum Leipzig/Halle GmbH
Prof. Dr. D. Kley	Forschungszentrum Jülich, Institut für Chemie 2
Prof. Dr. J. Lelieveld	Max-Planck-Institut für Chemie, Mainz
Prof Dr. P. Lemke	Universität Kiel, Institut für Meereskunde
Prof. Dr. U. Schurath	Forschungszentrum Karlsruhe GmbH Institut für Meteorologie und Klimaforschung
Prof. Dr. G. Tetzlaff	Universität Leipzig, Institut für Meteorologie
Dr. C. Weitkamp	GKSS Forschungszentrum Geesthacht GmbH

### Boards of Trustees

1999/2000

Name	Institution
RD J. Linek (until Sept. 2000)	Sächsisches Staatsministerium für Wissenschaft und Kunst, Dresden
MinR'in Dr. P. Karl (from Okt. 2000)	Sächsisches Staatsministerium für Wissenschaft und Kunst, Dresden
Dr. G. Hahn	Bundesministerium für Bildung und Forschung, Bonn
Prof. Dr. H. Graßl	Max-Planck-Institut für Meteorologie, Hamburg



**Member  
of the IfT-Association (e.V.)**      **1999**

Name	Institution
Chair Prof. Dr. H. Hinzpeter	Universität Hamburg, Meteorologisches Institut
RD J. Linek	Sächsisches Staatsministerium für Wissenschaft und Kunst, Dresden
MR C. Lammich	Bundesministerium für Bildung und Forschung, Bonn
Prof. Dr. B. Brümmer	Universität Hamburg, Meteorologisches Institut
Prof. Dr. P. Warneck	Max-Planck-Institut für Chemie, Mainz

**Member  
of the IfT-Association (e.V.)**      **2000**

Name	Institution
Chair Prof. Dr. P. Warneck	Max-Planck-Institut für Chemie, Mainz
RD J. Linek (until Sept. 2000)	Sächsisches Staatsministerium für Wissenschaft und Kunst, Dresden
MinR'in Dr. P. Karl (from Okt. 2000)	Sächsisches Staatsministerium für Wissenschaft und Kunst, Dresden
Dr. G. Hahn	Bundesministerium für Bildung und Forschung, Bonn
Prof. Dr. B. Brümmer	Universität Hamburg, Meteorologisches Institut
Prof. Dr. W. Engewald	Universität Leipzig, Fakultät für Chemie und Mineralogie
Dr. D. Koch	Bruker Saxonia Analytik GmbH, Leipzig



